NONDISPERSIVE WAVE PACKETS

by

Amr Mohamed Shaarawi

Dissertation submitted to the Faculty of the

Virginia Polytechnic Institute and State University

in partial fulfillment of the requirements for the degree of

DOCTOR OF PHILOSOPHY

in

Electrical Engineering

APPROVED:

I. M. Besieris, Chairman

G. S. Brown

D. A. de Wolf

W. E. Kohler

A. H. Nayfeh

May, 1989

Blacksburg, Virginia

NONDISPERSIVE WAVE PACKETS

by

Amr Mohamed Shaarawi

I. M. Besieris, Chairman

Electrical Engineering

(ABSTRACT)

In this work, nondispersive wavepacket solutions to linear partial differential equations are investigated. These solutions are characterized by infinite energy content; otherwise they are continuous, nonsingular and propagate in free space without spreading out. Examples of such solutions are Berry and Balazs' Airy packet, MacKinnon's wave packet and Brittingham's Focus Wave Mode (FWM). It is demonstrated in this thesis that the infinite energy content is not a basic problem *per se* and that it can be dealt with in two distinct ways. First these wave packets can be used as bases to construct highly localized, slowly decaying, time-limited pulsed solutions. In the case of the FWMs, this path leads to the formulation of the bidirectional representation, a technique that provides the most natural basis for synthesizing Brittingham-like solutions. This representation is used to derive new exact solutions to the 3-D scalar wave equation. It is also applied to problems involving boundaries, in particular to the propagation of a localized pulse in an infinite acoustic waveguide and to the launchability of such a pulse from the opening of a semi-infinite waveguide. The second approach in dealing with the infinite energy content utilizes the bump-like structure of nondispersive solutions. With an appropriate choice of parameters, these bump fields have very large amplitudes around the centers, in comparison to their tails. In particular, the FWM solutions are used to model massless particles and are capable of providing an interesting interpretation to the results of Young's two slit experiment and to the wave-paricle duality of light. The bidirectional representation provides, also, a systematic way of deriving packet solutions to the Klein-Gordon, the Schrodinger and the Dirac equations. Nondispersive solutions of the former two equations are compared to previously derived ones, e.g., the Airy packet and MacKinnon's wave packet.

Acknowledgements

I wish to express my gratitude to Professor I. M. Besieris for his advice, aid and guidance. I am especially grateful to him for the freedom he allowed to me to leisurely experience various areas of physics, mathematics and engineering without being limited to a narrow path of learning.

I am greatly indebted to Dr. R. W. Ziolkowski for the support, enthusiasm and encourgement he provided during the course of this work and for the technical discussions and valuable contributions concerning various aspects of this thesis.

I wish to thank Professors G. S. Brown, D. de Wolf, W. E. Kohler and A. H. Nayfeh for serving on my Ph.D. advisory committee and for their support and guidance throughtout my graduate studies.

I am deeply appreciative of my family's support. Without the patience and assistance of my mother and my brother , and the care of my wife ., I would not have had the opportunity to study for my Ph.D. degree.

I would like , finnally, to acknowledge my thanks to for the long interesting discussions about the nature of photons and for helping me in preparing the figures included in this thesis.

This work has been supported, in part, by Lawrence Livermore National Laboratory under contract No. 20812103.

Table of Contents

1.0 INTRODUCTION

A few years ago, Brittingham [1] proposed a search for packet-like solutions to the homogeneous Maxwell's equations with the properties that (1) they are continuous and non-singular, (2) they have a three-dimensional pulse structure, (3) they are nondispersive for all time, (4) they move at the velocity of light in straight lines, and (5) they carry finite electromagnetic energy. Such solutions have been termed focus wave modes (FWM).

Brittingham was successful in proving that the FWMs satisfy the homogeneous Maxwell's equations together with the first four of the aforementioned properties. The original FWM integrals were found to be of infinite energy. To remedy that shortcoming, Brittingham introduced two infinitely extended surfaces of discontinuities that travel along the direction of propagation of the FWMs and divide space into three regions. The fields in the central region between these two surfaces were chosen to be equal to the original FWM integrals, while the fields outside were identically set equal to zero.

The search for solutions of this kind goes back to the beginning of the century, ever since Einstein hypothesized that light beams are comprised of wave packets or light corpuscles, each having an energy proportional to the frequency. The mental picture associated with a corpuscle is that of a ball-like object travelling in free space without spreading out. Experimental evidence supports this point of view; a click in a photodetector or a dot on a photographic plate is a manifes-

tation of the localization of light particles. A more recent experiment that establishes the localization of photons has been carried out by Hong and Mandel [2].

It is well known that light is governed by Maxwell's equations or, in situations where polarization effects are unimportant, by the scalar wave equation. Nevertheless, exact, nondispersive, localized, finite energy solutions to these equations had not been reported prior to Brittingham's proposal. Part of the reason for this difficulty is due to the fact that a boost solution of the form $\Psi(x, y, z - ct)$ reduces the scalar wave equation $[\nabla^2 - c^{-2}\,\partial_t^2]\,\Psi(x, y, z - ct) = 0$ into a Laplace equation $\nabla^2\,\Psi(x, y, z - ct) = 0$, for which $\Psi(x, y, z - ct)$ is a harmonic function with no maxima or minima. This prevents the wave function from having a localized compact support. Other types of exact deterministic solutions were found inadequate to explain the corpuscular aspect of light. The only successful treatment is based on the second quantization of the electromagnetic field. Such a quantization follows in the spirit of the Copenhagen interpretation of the quantum theory [3] which abandons completely the notions of particle localization, causality and objective reality.

Difficulties arose immediately with Brittingham's FWMs, especially with respect to their energy content. Wu and King [4] showed that Maxwell's equations cannot be satisfied across the discontinuities introduced by Brittingham. Consequently, it was established that the FWMs are characterized by infinite total energy content. That assertion was corroborated by the work of Sezginer [5], followed by that of Wu and Lehman [6] who proved that any finite energy solution will involve the spreading of energy.

The work by Belanger [7,8], Sezginer [5] and Ziolkowski [9] showed that the original FWMs can be related to exact solutions of the three-dimensional scalar wave equation. Such solutions, which are expressed as products of a plane wave moving in the negative z-direction with velocity c and an envelope function depending on x, y and z-ct, will be termed the scalar FWMs in the sequel. All three authors indicated that the envelope function itself obeys exactly a complex parabolic Schrodinger-like equation and demonstrated the intimate relation of the FWMs to the solutions arising from the paraxial approximation to the wave equation. Belanger [7] and Sezginer [5] showed that the FWMs can easily be written in terms of Gaussian-Laguerre and Gaussian-Hermite

packet-like solutions. Later, Belanger [8] demonstrated that a Gaussian monochromatic beam can be observed as a Gaussian packet-like beam when the observer's inertial frame is moving at the same speed as the wave. Meanwhile, Ziolkowski [9] made the significant observation that the scalar FWMs describe fields that originate from moving complex sources. This observation linked the FWMs with earlier work by Deschamps [10] and Felsen [11] describing Gaussian beams as fields equivalent paraxially to spherical waves with centers at stationary complex locations.

At this stage, the main objection to the FWMs was their infinite energy content as established by Wu and Lehman [6]. It implied that any attempt to construct finite energy solutions would lead to pulses that would eventually spread out at infinity. The rate by which such pulses would disperse would differ from one case to another. It was pointed out by Ziolkowski [9] that plane waves share with the FWMs their infinite energy property, and it was demonstrated that a superposition of these modes can produce finite energy solutions. Ziolkowski pointed out, also, that since the central portions of these modes are localized in space, a superposition of the FWMs might have an advantage over plane waves when it comes to describing the transfer of directed pulses in free space. Such pulses, characterized by high directionality and slow energy decay, were called electromagnetic directed energy pulse trains (EDEPTs), and it was argued by Ziolkowski [16] that they could be launched from a finite size antenna array.

Ziolkowski's EDEPTs share their high directionality and slow energy decay properties with the electromagnetic missile solutions introduced by Wu [17], who argued that the electromagnetic energy density transmitted by a finite aperture under transient excitation does not have to decrease as R^{-2} when $R \to \infty$. The energy reaching the receiver has to decay eventually to zero. Wu demonstrated that one can make the product of the missile's cross-sectional area and the average energy per unit area approach zero as slowly as one wishes by choosing suitable frequency components of the exciting current. Wu deduced his results using the total received electromagnetic energy. Lee [18], on the other hand, used the Mellin transform to derive asymptotic expressions for the $\vec{E}$ and $\vec{H}$ field components of an instantaneously excited missile field. Later, Lee [19] rederived the field components for a source with a finite excitation time. An interesting account of the launchability of electromagnetic missiles from a point source embedded in a spherical dielectric lens

was given by Wu *et al.* [20]. They found that such electromagnetic missiles can be classified into strong and weak ones according to the corresponding critical points of differentiable maps in two dimensions. A more recent study of the launchability of electromagnetic missiles deals with a line source within a cylindrical dielectric lens [21].

The unusual finite energy pulse solutions introduced by Wu [17] and Ziolkowski [9,16] seem to have been predicted on the basis of theoretical investigations that differ substantially from each other. In both cases, however, the directionality aspects of the solutions depend greatly on the appropriate choice of their spectral components. An experiment investigating the feasibility of launching an acoustical directed energy pulse train (ADEPT) was performed by Ziolkowski *et al.* [22]. They established that an ADEPT pulse launched from a linear synthetic array holds itself and does not spread out to twice the Rayleigh length. They also demonstrated that an ADEPT field generated by a rectangular array spreads out at a slower rate than a more conventional field generated by a Gaussian-driven array. Preliminary experimental studies of the launchability of electromagnetic missiles were reported by Shen [23].

Ideas similar to those underlying the work on E(A)DEPTs and electromagnetic missiles were contemplated by Durnin [24] when he introduced the diffraction-free "Bessel beams" and he was able to demonstrate that such beams have a larger depth compared to Gaussian beams, even if their central spots have the same radii. The increase in the depth of the beam was achieved, however, at the expense of the power utilized [25]. This behavior, which has been verified experimentally by Durnin *et al.* [26], can be attributed mainly to differences in the energy distribution over identical apertures. Durnin's monochromatic beams are composed of different spatial spectral components. The depth of the monochromatic Bessel beams can be controlled by varying only their spatial spectral content or changing their energy distribution over the aperture. On the other hand, both temporal and spatial spectral components are required in synthesizing highly directional time-limited pulses, e.g., EDEPTs and electromagnetic missiles.

Another development along these lines is the use of Brittingham's modes by Hillion [12,13] to provide solutions to the homogeneous spinor wave equation and the massless Dirac equation. These solutions are called spinor focus wave modes. A weighted superposition of such modes re-

sults in finite energy pulses. Hillion studied in detail the particular case of Bessel weight functions. Hillion [14] was also able to find new solutions to the wave equation with boundary conditions on the hyperplane $z - ct = 0$. He made use of a Laplace transformation that relates solutions of the Laplace equation to those of the Schrodinger equation. Using such a method, he was able to derive several Brittingham-like solutions from known solutions of Laplace's equation. We mention, also, that a similarity reduction technique utilizing the Lorentz invariance of the scalar wave equation has been used by Sockell [15] to generate novel classes of Brittingham-like modes and to provide a group-theoretic explanation for the existence of the scalar FWMs.

It is clear that the various attempts to study and synthesize highly directional pulses and beams aim at the same goal. This leads one to wonder whether there is a deeper underlying reality. It is our aim in this work to uniformize some of these attempts and to address some of the unanswered questions concerning the physical realizability of such wave solutions. One major concern is the limited understanding of the energy decay patterns of pulses. This is highly reflected in the current literature which is mainly concerned with the propagation of monochromatic signals, or modulated CW signals. Such wave solutions, with a very narrow bandwidth, tend to obscure some of the physical properties of the propagation of pulses with finite time durations. Unlike narrow bandwidth signals, such pulses have infinite bandwidths which make a concept like the "far field region" totally ambiguous. This situation led Ziolkowski [9] to suggest that a superposition of Brittingham's FWMs is more appropriate for the synthesis of highly directional pulses, and that the nonlocality of plane waves contradicts the spirit of composing highly localized wave solutions.

The Brittingham-Ziolkowski formalism has been a more radical approach than any other, mainly because it calls upon a superposition method that differs significantly from a regular superposition of sinusoidal plane waves. This might prove to be very hard to handle mathematically, but at the same time it provides a fresh procedure with which new ideas might be introduced into the problem of propagation of nonsinusoidal pulses, and can point out some physical implications that may be concealed by formal procedures, e.g., the Fourier synthesis. Moreover, EDEPTs contain certain parameters that can be adjusted to increase their slow energy decaying range. If these parameters could be related to physically meaningful quantities, a systematic procedure could be es-

tablished to synthesize highly directional pulses that propagate in free space with very little spreading. In the spirit of this discussion, it seems worthwhile to pursue a better understanding of the Brittingham-Ziolkowski formalism and to study the physical realizability of highly directional wave solutions.

Another interesting prospect is related to the nondispersive character of the FWMs. This property can be quite valuable if the FWMs are used to represent light particles or photons. Even though a FWM has an infinite energy content, it is a bump-like field of relatively very large amplitude around the center. This central portion of very large energy density can be used to represent a light particle which is incorporated in an extended wave structure, thus combining the wave and the particle aspects of light in a single framework. This conjecture is motivated primarily by the fact that in Young's two slit interference experiment, a FWM pulse interferes with itself in such a way that it always imparts its energy onto one of the light fringes. It is well known that Young's experiment was the first to demonstrate the wave nature of light. According to the concept of wave-particle duality, a photon can behave both as a particle and a wave. The wave nature of light reveals itself in interference experiments, while its corpuscular nature manifests itself in the photoelectric and Compton effects. Bohr's complementarity principle regards these aspects of light as two manifestations of reality that cannot exist simultaneously, but can only reveal themselves in different situations. This is in sharp contrast with de Broglie's conception of the wave-particle duality, whereby the wave and the particle aspects of light exist simultaneously.

In a typical setting for a two slit interference experiment, light is shone on a screen containing two narrow slits and is observed on a photographic plate placed behind the screen. The wave nature of light is directly observed since waves going through either slit will interfere constructively or destructively upon reaching the photographic plate, thus forming interference fringes. The localized and compact nature of particles, on the other hand, makes it more difficult to explain the existence of the interference pattern. One way to circumvent such a difficulty is to assume that a large number of light particles or "photons" interact with each other, so that most of them end up on the light fringes. This was proved to be incorrect when very low intensity beams of light were used. In such a case, single photons go through the screen one at a time and always end up on one of the light

fringes. A single photon with transverse dimensions much less than the width of the slits, thus, interferes with itself. This raises the crucial question: how can a compact light particle, passing through one of the slits, feel the existence of the other one and interfere with itself? Several interpretations of the quantum theory attempted to answer this question. The most eminent among these is the probabilistic Copenhagen interpretation [3]. Other interesting, but less accepted, interpretations were introduced, including Bohm's causal interpretation [27,28], which makes use of the notion of a "quantum potential", the atemporal transactional interpretation [29] due to Cramer, and de Broglie's "double solution" theory [30]. These theories make use of a pilot or an advanced wave that guides the particle through the slits onto one of the light fringes of the interference pattern. The FWM pulse, with an appropriate choice of parameters, is a localized bump field with a large amplitude around the center buried in an extended nonlocal field of very low amplitude at the tails. Its precursor field fans out to cover relatively larger distances in the transverse direction as we go away from the center. It is this property that allows the field of the FWM to feel the two slits in Young's experiment, even though the central bump field is fairly localized. For such a field one can associate the corpuscular aspects of light with its central portion of large amplitude, while the wave character of light is an outcome of the nonlocal nature of the pulse's tails. Thus, extraneous notions like a "pilot wave" or a "quantum potential" of the aforementioned interpretations are replaced by the indigenous precursor field of the FWM pulse which guides the particle through the screen. In the same vein, it is of interest to investigate the possibility of deriving analogous solutions to partial differential equations representing massive particles; e.g., the Klein-Gordon, Dirac and Schrodinger equations.

It is our aim in this work to examine in detail these two prospects; namely, the synthesis of finite-energy, slowly decaying Brittingham-like solutions and the modelling of light and massive particles by bump-like fields that can accomodate simultaneously the corpuscular and wave aspects. Our work is based on a novel approach to the synthesis of wave signals. This method was introduced by Besieris and Shaarawi [31] in order to understand the salient features of the Brittingham-Ziolkowski formalism. Its scope is broader, however, and encompasses classes of problems altogether different from wave propagation *in vacuo* . Within the framework of this new approach,

exact solutions of the scalar wave equation are decomposed into bidirectional, backward and forward, plane waves travelling along a preferred direction z, viz., $\exp(-i\alpha(z-ct))\ \exp(i\beta(z+ct))$. These bilinear expressions can be elementary solutions to the Fourier-transformed (with respect to x and y) three-dimensional wave equation provided that a constraint relationship involving α, β and the Fourier variables dual to x and y is satisfied. Such elementary blocks constitute a natural basis for synthesizing Brittingham-like solutions, such as Ziolkowski's EDEPTs and splash pulses, Hillion's spinor modes and the Ziolkowski-Belanger-Sezginer scalar FWMs.

In Chapter 2, we shall provide a short introduction to the aforementioned new decomposition, together with a comparison to the well established Fourier method. For the sake of simplicity, the discussion will be restricted to the case of the three-dimensional scalar wave equation. It will be demonstrated, next, that all the known Brittingham-like solutions can be reproduced by choosing fairly simple spectra for this novel synthesis, in contradistinction to the more complicated spectra that would have to be utilized in the case of a Fourier synthesis. Other choices of spectra can result in other types of solutions that can be of some value. The necessary and sufficient conditions imposed on the spectra to ensure square integrability will be derived and the possibility of extending this analysis to other equations will be investigated.

In Chapter 3, a specific demonstration will be given in connection with an infinitely long circular cylinder excited by a localized initial pulse whose size is related directly to parameters similar to those arising in the EDEPT solutions. The case of a semi-infinite waveguide excited by the same initial pulse will be considered next. The radiation field from the open end of the waveguide is computed using Kirchhoff's integral formula with a time-retarded Green's function. An approximate evaluation of Kirchhoff's integral gives solutions that are causal, have finite energy and exhibit an unusual decay behavior. Like the EDEPTs, these approximate solutions contain certain parameters that can be adjusted in order to control the shape of the pulses as they propagate in free space. These parameters are related to meaningful physical quantities, e.g., the shape of the initial pulse, the cross sectional area of the waveguide and its cutoff frequencies. These aspects will be discussed in detail, together with the range of validity of the approximate solutions.

The possibility of using the FWM pulses as light particles or "photons" will be studied in Chapter 4. It will be demonstrated that, in a two slit interference experiment, a single FWM pulse can interfere with itself. It will also be shown that this behavior cannot be achieved for other localized pulses, e.g., a transverse Gaussian pulse. The energy and momentum of the central bump of the FWM pulse will be derived in connection to its possible interactions with other particles. The energy content can be related to the conventional photon energy relationship $E_\gamma = h\nu$.

The bidirectional representation will be used in Chapter 5 to derive nondispersive wavepacket solutions to the Klein-Gordon equation and the Dirac equation, Such wave packets have centers that move with velocities v less than the speed of light c. The possibility of using such solutions as de Broglie wave packets representing massive particles will be investigated.

In Chapter 6, wave packet solutions will be derived for the nonrelativistic Schrodinger equation. The centers of such solutions move with uniform velocities v_g which are equal to the velocities obtained through the action of a momentum operator on the phase of the wave function. These wave packets are compared to accelerating packet solutions and the latter will be used to derive a new class of solutions to the scalar wave equation. Finally, a summary and conclusion of this work will be provided in Chapter 7.

2.0 THE BIDIRECTIONAL REPRESENTATION

In this chapter, a new decomposition of exact solutions to the scalar wave equation into bidirectional, forward and backward, travelling plane wave solutions will be described. The resulting representation is a natural basis for synthesizing pulse solutions that can be tailored to give directed energy transfer in space. The derivation of this representation from a general operator embedding scheme will be given. The connection between this decomposition and various localized, slowly decaying pulses will be made explicit. Such pulse solutions include the focus wave modes, the electromagnetic directed energy pulse trains, the spinor splash pulses, and the Bessel beams. The efficacy of this representation in deriving new exact Brittingham-like solutions will be demonstrated. Finally, the new representation will be extended to other classes of equations, e.g., the Klein-Gordon and the dissipative scalar wave equations that model wave propagation in dispersive and dissipative media, respectively.

2.1 MOTIVATION AND PREVIOUS WORK

As mentioned in the introduction, the possibility of solutions of the wave equation that describe localized, slowly decaying transmission of energy in space-time has been suggested by several groups. These include efforts on "Focus Wave Modes" [1,5,7-9], "EDEPTs" [9,16,32], "Splash Modes" [9,12], "EM Missiles" [17-20,23,33], "Bessel Beams" [24-26], "EM bullets" [34,35] and "Transient Beams" [36-39]. Much of this work was actually motivated by the pioneering work of Brittingham [1]. It has been recently discovered that the original "Focus Wave Modes" represent Gaussian beams that translate through space with only local deformations and are the fundamental modes of a class of solutions that describe fields that originate from moving complex sources [9]. In particular, the scalar wave equation in real space, viz.,

$$\left[c^{-2}\partial_t^2 - \nabla^2 \right] \Psi(\vec{r}, t) = 0 , \tag{2.1.1}$$

has as an exact solution, the moving, modified Gaussian pulse

$$\Psi_\beta(\vec{r}, t) = \frac{1}{4\pi(a_1 + i\zeta)} e^{-\beta\rho^2/(a_1 + i\zeta)} e^{i\beta(z+ct)} . \tag{2.1.2}$$

The complex variance yields the beam spread $A = a_1 + \zeta^2/a_1$, the phase front curvature $R = \zeta + a_1^2/\zeta$, and beam waist $w = (A/\beta)^{1/2}$. Here, $\zeta = z - ct$ and ρ denotes the radial cylindrical coordinate. The fundamental pulse (2.1.2) describes a Gaussian beam that translates through space-time with only local variations. It represents a generalization of earlier work by Deschamps [10] and Felsen [11] describing Gaussian beams as fields radiated from stationary complex source points. From equation (2.1.2) it can be easily seen the the FWM solution has a magnitude $\sim 1/(4\pi a_1)$ around the center of the pulse, where $z < ct$ and $\rho < (a_1/\beta)^{1/2}$. Outside this portion of the field, the amplitude falls off as $1/(z - ct)$ along the direction of propagation. At the same time

the Gaussian pulse envelope stretches out in the transverse direction with a waist $(z-ct)/(\beta a_1)^{1/2}$ that increases as one moves away from the central part of the field.

It has been established [32] that the fundamental Gaussian pulse has either a plane wave or a particle-like character depending on whether β is small or large. Moreover, for all β it shares with the plane wave the property of having infinite energy. However, as with the plane waves, this is not to be considered as a drawback *per se*. The above solution procedure has introduced an added degree of freedom into the solution through the variable β that can be exploited. It has been shown by Ziolkowski [9,16] that fundamental Gaussian pulse fields, corresponding to different values of β, can be used as basis functions to represent new transient solutions of equation (2.1.1). In particular, the general EDEPT (electromagnetic directed energy pulse train) solution

$$\begin{aligned}\Psi(\vec{r}, t) &= \int_0^\infty d\beta\, \Psi_\beta(\vec{r}, t)\, F(\beta) \\ &= \frac{1}{4\pi[a_1 + i(z-ct)]} \int_0^\infty d\beta\, F(\beta)\, e^{-\beta s(\rho, z, t)}\,,\end{aligned} \tag{2.1.3}$$

where

$$s(\rho, z, t) = \frac{\rho^2}{a_1 + i(z-ct)} - i(z+ct)\,, \tag{2.1.4}$$

is an exact source-free solution of the wave equation. This representation, in contrast to a plane wave decomposition, utilizes basis functions that are more localized in space and hence, by their very nature, are better suited to describe the directed transfer of electromagnetic energy in space. The resulting pulses have finite energy if the spectrum $F(\beta)$ is square integrable [16].

It has been shown [9] that the superposition (2.1.3), with the "complex travelling center wave" basis functions, has an inverse. The functions

$$\Phi_\beta(\rho, \zeta, \eta) = 8\sqrt{\pi}\; e^{-(\zeta/4\beta a_1)^2}\, \Psi_\beta(\rho, \zeta, \eta)\,, \tag{2.1.5}$$

with $\eta = z + ct$, are orthogonal to the Ψ_β. This means these basis functions satisfy the completeness relation

$$\int_{-\infty}^{+\infty} d\eta \int_{-\infty}^{+\infty} d\zeta \int_0^{\infty} d\rho\, \rho\, \Phi_\beta^*(\rho, \zeta, \eta)\ \Psi_{\beta'}(\rho, \zeta, \eta) = \delta(\beta - \beta')\ , \tag{2.1.6}$$

where Φ_β^* is the complex conjugate of Φ_β. Hence, an inversion of the superposition (2.1.3) exists.

Clearly, different spectra $F(\beta)$ in equation (2.1.3) lead to different wave equation solutions, and hence, to different solutions of Maxwell's equations. Many interesting solutions of the wave equation can be created by simply referring to a Laplace transform table. One particularly interesting spectrum selection, recognized by Ziolkowski [40], is the "Modified Power Spectrum" (MPS)

$$\begin{aligned} F(\beta) &= \frac{p}{\Gamma(q)}\ (p\,\beta - b)^{q-1}\ e^{-[(p\beta - b)\,a_2]}\ , \qquad \beta > \frac{b}{p}\ , \\ &= 0\ , \qquad\qquad\qquad \frac{b}{p} > \beta \geq 0\ . \end{aligned} \tag{2.1.7}$$

It is so named because it is derived from the power spectrum $F(\beta) = \beta^{q-1}\ \exp(-\beta a_2)$ by a scaling and a truncation. This choice of spectrum leads to the "Modified Power Spectrum" (MPS) pulse

$$\Psi(\vec{r}\,, t) = \frac{1}{4\pi\,(a_1 + i\zeta)}\ \ \frac{e^{-bs/p}}{\left[\ a_2 + \frac{s}{p}\ \right]^q}\ . \tag{2.1.8}$$

Solutions to Maxwell's equations follow naturally from these scalar wave equation solutions using a Hertz potential formulation.

The behavior of the MPS pulse is determined primarily by the choice of the parameters a_1, a_2, p and q. This can be easily characterized along the direction of propagation. In particular, for $p >> 1$ and $q = 1$, it was pointed out [32] that

$$\Psi(\rho=0, z=ct) = \frac{[\cos(2bz/p) - (2z/pa_2)\ \sin(2bz/p)]}{4\pi\,[1+(2z/pa_2)^2]\,a_1 a_2}$$
$$\sim \frac{1}{4\pi a_1 a_2} \qquad \text{for } z << \frac{p}{2b} \text{ and } z < \frac{pa_2}{2}$$
$$\sim \frac{\cos(2bz/p)}{4\pi a_1 a_2} \qquad \text{for } z < \frac{pa_2}{2} \tag{2.1.9}$$
$$\sim -\frac{\sin(2bz/p)}{4\pi(2a_1/p)z} \qquad \text{for } z > \frac{pa_2}{2}\ .$$

As long as $z << p/2b$ and $z < pa_2/2$ the amplitude of the center of the MPS pulse stays constant. For the intermediate range $p/2b < z < pa_2/2$, the center of the pulse oscillates with an oscillation length equal to $\pi p/b$. Finally, when $z > pa_2/2$ the MPS pulse amplitude decreases as $1/z$. Along the transverse direction the pulse is essentially Gaussian with

$$\Psi(\rho, z=ct) = e^{-b\rho^2/pa_1}\,\Psi(\rho=0, z=ct)\ . \tag{2.1.10}$$

The MPS pulse can be optimized so that it is localized near the direction of propagation and its original amplitude can be recovered out to extremely large distances from its initial location. For the specific choice of parameters $a_1 = 10^{-3}$ m, $a_2 = 1.0$ m, q = 1.0 , $p = 6.0 \times 10^{15}$ and $b = 10^{12}$ m^{-1}, the amplitude of the pulse's center remains constant until $z \sim p/2b = 3 \times 10^3$ m , where it begins to oscillate recovering its initial amplitude every $\Delta z = \pi p/b = 1.88 \times 10^4$ m for $z < pa_2/2 = 3 \times 10^{15}$ m . Beyond this point the center of the pulse decays as $1/z$. Around the center of the pulse and for $z < 3 \times 10^{15}$ m, the transverse extent of the pulse equals $\rho = (pa_1/b)^{1/2} = 2.45$ m . This example definitively shows the localization of the field near the direction of propagation over very large distances.

It was recognized by Besieris and Shaarawi [31] that the representation (2.1.3) and its inverse has a generalization that can be exploited to explain the structure of localized, slowly decaying solutions in a single framework. This new representation is the main purpose of this chapter and will be introduced in the next section.

2.2 BIDIRECTIONAL PLANE WAVE DECOMPOSITION

The Cauchy problem

$$\left[c^{-2}\partial_t^2 + \hat{\Omega}(-i\nabla) \right] u(\vec{r}, t) = 0 , \qquad \vec{r} \in R^3 , t > 0 ; \tag{2.2.1a}$$

$$u(\vec{r}, 0) = u_0(\vec{r}) , \quad u_t(\vec{r}, 0) = u_1(\vec{r}) , \tag{2.2.1b}$$

where u is a real scalar-valued function and $\hat{\Omega}$ is a positive, self-adjoint, possibly pseudodifferential operator, can be used as a mathematical model for a large number of physical situations.

A Fourier synthesis of the solution to the Cauchy problem (2.2.1) can be effected as follows [41]:

$$u(\vec{r}, t) = 2\, Re\, \{ \Psi(\vec{r}, t) \} ; \tag{2.2.2a}$$

$$\Psi(\vec{r}, t) = \frac{1}{(2\pi)^3} \int_{R^3} d\vec{k}\ F(\vec{k}) e^{-i(\vec{k}\cdot\vec{r} - \Omega^{1/2}(-\vec{k})ct)} ; \tag{2.2.2b}$$

$$F(\vec{k}) = \frac{1}{2} \left[\tilde{u}_0(\vec{k}) - i \frac{\tilde{u}_1(\vec{k})}{c\,\Omega^{1/2}(-\vec{k})} \right] . \tag{2.2.2c}$$

The complex valued signal Ψ is generated via a linear superposition of plane waves propagating in the $\vec{k}$ direction with phase speeds $c\,\Omega^{1/2}(-\vec{k})/|\vec{k}|$. These plane waves are characterized by wave vectors $\vec{k}$ and they are weighted by the Fourier spectrum $F(\vec{k})$.

Equation (2.2.2) constitutes a mathematical solution to the Cauchy problem (2.2.1). However, for purposes of later comparison, the superposition (2.2.2b) can be recast in a more general form as follows:

$$\Psi(\vec{r}\,,t)=\frac{1}{(2\pi)^4}\int_{R^3}d\vec{k}\int_{R^1}d\omega\,\hat{F}(\vec{k}\,,\omega)\,e^{-i(\vec{k}\cdot\vec{r}\,-\omega t)}\;\delta[\frac{\omega^2}{c^2}-\Omega(-\vec{k})\,]\,. \tag{2.2.3}$$

The spectra entering into equations (2.2.2b) and (2.2.3) are linked through the relationship

$$F(\vec{k})=\frac{c\hat{F}(\vec{k}\,,\Omega(-\vec{k}))}{4\pi\,|\Omega^{1/2}(-\vec{k})|}\,. \tag{2.2.4}$$

Conditions can also be specified under which Ψ is square-integrable, or, even further, under which the solution $u(\vec{r}\,,t)$ of (2.2.1) is a finite energy signal. There is, however, a basic drawback associated with the Fourier method; namely, that in most cases the integral for Ψ can be computed only approximately by a variety of asymptotic approaches, such as the method of stationary phase/saddle point [42,43], ray-theoretic techniques [44,45] and phase space methods [46], or can be carried out numerically. Very few exact analytical solutions to (2.2.2b) are available, even for the simple, single mode dispersion relationship $\omega\equiv c\,\Omega^{1/2}(-\vec{k})=c\,(k^2+\mu^2)^{1/2}$ corresponding to the Klein-Gordon equation.

The Cauchy problem (2.2.1) will be used in the sequel as a vehicle for presenting a new principle of superposition that provides more freedom and flexibility when dealing with certain classes of solutions, e.g., the EDEPT solutions to the scalar wave equation.

Different types of superpositions are obtained by dividing the operator $L = [c^{-2}\,\partial_t^2 + \hat{\Omega}(-i\nabla)]$ into parts, each having its own eigenfunctions. A general solution can be constructed from the product of such eigenfunctions, together with a constraint relationship between their eigenvalues. The manner in which the operator L is partitioned determines the form of the final superposition. For example, the Fourier decomposition follows from partitioning L into two parts: $L_1 = c^{-2}\,\partial_t^2$ and $L_2 = \hat{\Omega}(-i\nabla)$. The superposition (2.2.3) contains the constraint $(\omega/c) = \Omega^{1/2}(-\vec{k})$ relating the eigenvalues of L_1 and L_2 corresponding to the eigenfunctions $\exp(i\omega t)$ and $\exp(-i\vec{k}\cdot\vec{r})$, respectively.

In general, the operator L can be partitioned in many different ways. Consider, for example, the preliminary splitting of the operator $\hat{\Omega}(-i\nabla)$ as follows:

$$\begin{aligned}\hat{\Omega}(-i\nabla) &= \hat{A}(-i\partial_z) + [\,\hat{\Omega}(-i\nabla) - \hat{A}(-i\partial_z)\,] \\ &\equiv \hat{A}(-i\partial_z) + \hat{B}(-i\nabla_T, -i\partial_z)\,.\end{aligned} \tag{2.2.5}$$

The operator $\hat{A}(-i\partial_z)$, which may or may not be a natural part of $\hat{\Omega}(-i\nabla)$, is assumed to be positive, self adjoint and the choice of the preferred variable z is arbitrary. Taking the Fourier transform with respect to the transverse components, the complex wave function $\Psi(\vec{r}, t)$ can be expressed as

$$\Psi(\vec{r}, t) = \frac{1}{(2\pi)^2} \int_{R^2} d\vec{\kappa}\ \tilde{\psi}(\vec{\kappa}, z, t)\ e^{-i\vec{\kappa}\cdot\vec{\rho}}\,, \tag{2.2.6}$$

with $\tilde{\psi}(\vec{\kappa}, z, t)$ governed by the equation

$$\left[\, c^{-2}\,\partial_t^2 + \hat{A}(-i\partial_z) + \hat{B}(-\vec{\kappa}, -i\partial_z)\,\right]\ \tilde{\psi}(\vec{\kappa}, z, t) = 0\,. \tag{2.2.7}$$

The operator $L \equiv c^{-2}\,\partial_t^2 + \hat{\Omega}(-\vec{\kappa}, -i\partial_z)$ can now be partitioned as follows:

$$L_1 = c^{-2}\,\partial_t^2 + \hat{A}(-i\partial_z)\,, \tag{2.2.8a}$$

$$L_2 = \hat{\mathrm{B}}(-\vec{\kappa}, -i\,\partial_z)\ . \tag{2.2.8b}$$

The most natural eigenfunctions of the operator L_1 are given by

$$\psi_e(z, t) = e^{-i\alpha\zeta}\ e^{i\beta\eta}\ , \tag{2.2.9}$$

where ζ and η are defined as follows:

$$\zeta = z - ct\ sgn(\alpha)\ \alpha^{-1}\ \mathrm{A}^{1/2}(\alpha)\ , \tag{2.2.10a}$$

$$\eta = z + ct\ sgn(\beta)\ \beta^{-1}\ \mathrm{A}^{1/2}(\beta)\ . \tag{2.2.10b}$$

The corresponding eigenvalues, denoted by $\lambda(\alpha, \beta)$, are given explicitly as follows:

$$\lambda(\alpha, \beta) = \mathrm{A}(\beta - \alpha) - \left[\ \mathrm{A}(\alpha) + \mathrm{A}(\beta) + 2\ sgn(\alpha)\ \mathrm{A}^{1/2}(\alpha)\ sgn(\beta)\ \mathrm{A}^{1/2}(\beta)\ \right]\ . \tag{2.2.11}$$

The elementary functions (2.2.9) consist of products of two plane waves travelling in opposite directions, with wavenumber-dependent phase speeds equal to $sgn(\alpha)\ \alpha^{-1}\ \mathrm{A}^{1/2}(\alpha)$ and $sgn(\beta)\ \beta^{-1}\ \mathrm{A}^{1/2}(\beta)$, respectively.

The bilinear functions (2.2.9) are also eigenfunctions of L_2 , with corresponding eigenvalues equal to $\mathrm{B}(-\vec{\kappa}, \beta - \alpha)$. As a consequence, a linear superposition of the bidirectional elementary solutions ψ_e results in a solution to equation (2.2.7), viz.,

$$\tilde{\psi}(\vec{\kappa}, z, t) = \int_{R^1} d\alpha \int_{R^1} d\beta\ C(\vec{\kappa}, \alpha, \beta)\ e^{-i\alpha\zeta}\ e^{i\beta\eta}\ \delta[\ \lambda(\alpha, \beta) + \mathrm{B}(-\vec{\kappa}, \beta - \alpha)\ ]\ , \tag{2.2.12}$$

where the constraint $\lambda(\alpha, \beta) + B(-\vec{\kappa}, \beta - \alpha) = 0$ is included in the integration. A general solution to equation (2.2.1) can be obtained by resorting to a transverse Fourier inversion [cf. equation (2.2.6)]; specifically,

$$\Psi(\vec{r}, t) = \frac{1}{(2\pi)^2} \int_{R^2} d\vec{\kappa}\, e^{i\vec{\kappa}\cdot\vec{\rho}} \int_{R^1} d\alpha \int_{R^1} d\beta\, C(\vec{\kappa}, \alpha, \beta)\, e^{-i\alpha\zeta}\, e^{i\beta\eta} \times \delta[\, \lambda(\alpha, \beta) + B(-\vec{\kappa}, \beta - \alpha)\,] \,. \tag{2.2.13}$$

This representation constitutes a generalization of the three-dimensional Fourier synthesis [cf. equation (2.2.3)]; in the latter, the operator $\hat{A}(-i\,\partial_z)$ was chosen to be a constant given by the relations

$$sgn(\alpha)\, A^{1/2}(\alpha) + sgn(\beta)\, A^{1/2}(\beta) = \frac{\omega}{c} \tag{2.2.14a}$$

and

$$\alpha - \beta = k_z \,. \tag{2.2.14b}$$

The main advantage of this decomposition is the introduction of the embedded operator $\hat{A}(-i\,\partial_z)$. This provides a fresh approach for addressing different classes of problems. At the same time the flexibility that one can enjoy through a clever choice of $\hat{A}(-i\,\partial_z)$ may open the way to approach some of the more impenetrable problems.

To clarify these ideas, consider specifically the case of the 3-D scalar wave equation for which $\hat{\Omega}(-i\nabla) = -\nabla^2$. The operator L, in this case, assumes the form $L = c^{-2}\partial_t^2 - \nabla^2$ and equation (2.2.1a) simplifies to

$$\left[\, c^{-2}\, \partial_t^2 - \nabla^2 \,\right]\, u(\vec{r}, t) = 0 \,. \tag{2.2.15}$$

In cylindrical coordinates, the Laplacian ∇^2 can be written as follows:

$$\nabla^2 = \partial_z^2 + \partial_\rho^2 + \rho^{-1}\,\partial_\rho + \rho^{-2}\,\partial_\phi^2 \,.$$

In the usual Fourier decomposition, the operator L is divided into two parts:

$$L_1 = -\left[\,\partial_z^2 + \partial_\rho^2 + \rho^{-1}\,\partial_\rho + \rho^{-2}\,\partial_\phi^2\,\right], \tag{2.2.16a}$$

$$L_2 = c^{-2}\,\partial_t^2 \,. \tag{2.2.16b}$$

The eigenfunctions of L_1 are $J_n(\kappa\rho)e^{\pm in\phi}e^{\pm ik_z z}$ and $N_n(\kappa\rho)e^{\pm in\phi}e^{\pm ik_z z}$, where $J_n(\kappa\rho)$ and $N_n(\kappa\rho)$ are Bessel functions of the first and second kind, respectively, and the eigenvalues equal $\kappa^2 + k_z^2$. The operator L_2 has eigenfunctions $e^{\pm i\omega t}$ with eigenvalues $-\omega^2/c^2$. An elementary solution to the scalar wave equation (2.2.15) can be written as

$$\Psi_e(\vec{r}\,,t) = \left[A_n\,J_n(\kappa\rho) + B_n\,N_n(\kappa\rho)\right]\; e^{\pm in\phi}\;\; e^{-i(k_z z \pm \omega t)}\,, \tag{2.2.17a}$$

with the constraint

$$\kappa^2 + k_z^2 - \frac{\omega^2}{c^2} = 0\,. \tag{2.2.17b}$$

Neglecting the terms $N_n(\kappa\rho)$ because of their infinite values at $\rho = 0$, one obtains a special case of the superposition (2.2.3), that gives the general Fourier synthesis solution to the scalar wave equation:

$$\Psi(\vec{r}\,,t) = \frac{1}{(2\pi)^2}\sum_{n=0}^{\infty}\int_0^{\infty} d\kappa \int_{-\infty}^{+\infty} d\omega \int_{-\infty}^{+\infty} dk_z\, A_n(\omega, k_z, \kappa)\,\kappa\, J_n(\kappa\rho)e^{\pm in\phi} \times e^{-ik_z z}\, e^{i\omega t}\,\delta\!\left[\frac{\omega^2}{c^2} - (\kappa^2 + k_z^2)\right]. \tag{2.2.18}$$

Consider next, the choice $\hat{A}(-i\,\partial_z) = -\,\partial_z^2$, which reduces equations (2.2.10) to

$$\zeta = z - ct \quad \text{and} \quad \eta = z + ct \,. \tag{2.2.19}$$

The operator L can be written , in this case, as

$$L = -\left[\, 4\partial^2_{\zeta\eta} + \partial^2_\rho + \rho^{-1}\,\partial_\rho + \rho^{-2}\,\partial^2_\phi \,\right],$$

and it can be partitioned as follows:

$$L_1 = -\left[\, \partial^2_\rho + \rho^{-1}\,\partial_\rho + \rho^{-2}\,\partial^2_\phi \,\right], \tag{2.2.20a}$$

$$L_2 = -\,4\,\partial^2_{\zeta\eta} \,. \tag{2.2.20b}$$

The eigenfunctions of L_1 are given now by $J_n(\kappa\rho)e^{\pm in\phi}$ and $N_n(\kappa\rho)e^{\pm in\phi}$, and its eigenvalues equal $+\,\kappa^2$. The operator L_2 has eigenfunctions $e^{-i\alpha\zeta}\,e^{i\beta\eta}$ with eigenvalues $-\,4\alpha\beta$. An elementary solution to the scalar wave equation (2.2.15) can be written as

$$\Psi_e(\vec{r}\,,\,t) \equiv \Psi_e(\rho,\zeta,\eta) = \left[C_n\,J_n(\kappa\rho) + D_n\,N_n(\kappa\rho)\right] e^{\pm in\phi}\,e^{-i\alpha\zeta}\,e^{i\beta\eta}\,, \tag{2.2.21a}$$

with the constraint

$$\alpha\beta = \frac{\kappa^2}{4} \,. \tag{2.2.21b}$$

This constraint limits the values of α and β either to be both negative or both positive. A general solution to the scalar wave equation can be written in the nonconventional form

$$\Psi(\rho,\zeta,\eta) = \frac{1}{(2\pi)^2} \sum_{l=1,-1} \sum_{n=0}^{\infty} \int_0^\infty d\kappa \int_0^\infty d(l\alpha) \int_0^\infty d(l\beta)\; C_n(l\alpha, l\beta, \kappa)\,\kappa\,J_n(\kappa\rho) \times e^{\pm in\phi}\,e^{-il\alpha\zeta}\,e^{il\beta\eta}\,\delta(\alpha\beta - \frac{\kappa^2}{4}) \,. \tag{2.2.22}$$

The two representations [cf. equations (2.2.18) and (2.2.22)] may appear to be very different. There exists, however, a one to one correspondence between these two superpositions through the change of variables

$$k_z = \alpha - \beta \quad , \quad \frac{\omega}{c} = \alpha + \beta \; . \tag{2.2.23}$$

Using these relationships, the new representation (2.2.22) can be transformed into the the Fourier synthesis given in equation (2.2.18), with the following connection between their spectra

$$A_n(\omega, k_z, \kappa) = \frac{2}{c} \, C_n\Big[\, \frac{1}{2} \left(\frac{\omega}{c} + k_z \right) , \frac{1}{2} \left(\frac{\omega}{c} - k_z \right) , \kappa \, \Big] , \tag{2.2.24}$$

It should be noted that this transformation requires a careful handling of the limits of integration. A complete discussion of this point will be given later when dealing with specific examples.

The representation (2.2.22) provides a fresh path through which exact solutions to the scalar wave equation can be obtained. Although such a representation is not a familiar one, solutions obtained using (2.2.22) can still be easily transformed into the more popular Fourier superposition, and one can link the bidirectional results to the more conventional Fourier interpretation. To emphasize these ideas, one can remove the constraint in (2.2.18) by integrating over ω, hence reducing (2.2.18) to a form similar to (2.2.2), with

$$\begin{aligned} \Psi(\vec{r}, t) = \frac{1}{(2\pi)^2} \sum_{n=0}^{\infty} \int_0^{\infty} d\kappa \int_{-\infty}^{+\infty} dk_z \Big[A_n[\, c\sqrt{\kappa^2 + k_z^2} \, , k_z, \kappa \,] \, e^{-i(k_z z - \sqrt{\kappa^2 + k_z^2}\, ct)} \\ + A_n[\, -c\sqrt{\kappa^2 + k_z^2} \, , k_z, \kappa \,] \, e^{-i(k_z z + \sqrt{\kappa^2 + k_z^2}\, ct)} \Big] \, \frac{\kappa \, J_n(\kappa\rho)}{2c\sqrt{\kappa^2 + k_z^2}} \, e^{\pm in\phi} \; . \end{aligned} \tag{2.2.25}$$

This is a special case of the superposition (2.2.2). A common problem that arises when dealing with such integrals is associated with the branch-cut type singularities. These can pose significant diffi-

culties even when the integrals are solved either asymptotically or computed numerically. On the other hand, when the constraint is integrated out of equation (2.2.22), one obtains

$$\Psi(\rho,\zeta,\eta)=\frac{1}{(2\pi)^2}\sum_{n=0}^{\infty}\int_0^{\infty}d\kappa\int_0^{\infty}d\beta\left[C_n\left(\frac{\kappa^2}{4\beta},\beta,\kappa\right)e^{-(i\kappa^2/4\beta)\zeta}\,e^{i\beta\eta}\right.$$
$$\left.-C_n\left(-\frac{\kappa^2}{4\beta},-\beta,\kappa\right)e^{i(\kappa^2/4\beta)\zeta}\,e^{-i\beta\eta}\right]\frac{\kappa}{\beta}\,J_n(\kappa\rho)\,e^{\pm in\phi}\,. \tag{2.2.26}$$

Similar to the Fourier synthesis where one can choose either the positive or negative ω-branch, we can choose to work with either the positive or the negative branch of α and β. In what follows, for convenience only, we choose the positive branch. Notice that, unlike equation (2.2.25), the terms in the above integral consist of products of two plane waves travelling in opposite directions. An important characteristic of the representation (2.2.26) is that the branch-cut singularities in equation (2.2.25) have been converted into algebraic singularities. This provides a novel approach to finding solutions to the scalar wave equation. New exact solutions can be obtained by choosing appropriate spectra C_n , for which the corresponding Fourier spectra A_n might be very complicated and could not have been guessed. Moreover, because of the nature of the branch-cut singularities in the Fourier synthesis, problems arise because of their multi-valuedness and because large oscillations accompany any attempt to evaluate them either numerically or asymptotically. We have found that one can circumvent such problems by dealing with the bidirectional synthesis and its tame algebraic singularities.

In summary, the procedure described in this section provides an alternate way of synthesizing solutions to different partial differential equations. Such representations are characterized by different types of singularities that may facilitate their asymptotic or numerical evaluation. This is a flexible procedure that changes with the types of equations considered. Moreover, solutions to the same equation may have different representations depending on how the operator L is partitioned.

2.3 MATHEMATICAL CONSIDERATIONS

A number of important mathematical issues dealing with the new bidirectional synthesis will be considered at this point. These will include the completeness of the expansions (2.2.22) and (2.2.26), the inversion properties for $C_n(\alpha, \beta, \kappa)$ and the sufficient and neccessary conditions that must be imposed on the spectrum in order to ensure square integrability. The feasibility of solving Cauchy-initial value problems on the basis of the new representation will be addressed in Chapter 3.

Completeness follows directly from the fact that the superimposed functions are either exponential or Bessel functions, which are both orthogonal functions and form their own complete sets. However, the inversion of $C_n(\alpha, \beta, \kappa)$ is not obvious. A generalization of Ziolkowski's formula (2.1.6), has to be used. Using the positive β branch in (2.2.26), $\Psi(\rho, \zeta, \eta)$ can be constructed as follows:

$$\Psi(\rho,\zeta,\eta)=\frac{1}{(2\pi)^2}\sum_{n=-\infty}^{+\infty}\int_0^{\infty}d\kappa\int_0^{\infty}d\beta\;\frac{1}{\beta}\;C_n(\frac{\kappa^2}{4\beta},\beta,\kappa)\,\kappa\,J_n(\kappa\rho)\,e^{in\phi}\,e^{-i(\kappa^2/4\beta)\zeta}\,e^{i\beta\eta}. \quad (2.3.1)$$

The inversion formula corresponding to this superposition is given by

$$C_m(\frac{\kappa^2}{4\beta},\beta,\kappa)=\frac{1}{4\sqrt{\pi}}\int_{-\pi}^{+\pi}d\phi\int_{-\infty}^{+\infty}d\zeta\,e^{-\zeta^2/16\beta^2}\int_{-\infty}^{+\infty}d\eta\int_0^{\infty}d\rho\;\rho\,J_m(\kappa\rho)\,\Psi(\rho,\zeta,\eta) \quad (2.3.2)$$
$$\times\,e^{-im\phi}\,e^{i(\kappa^2/4\beta)\zeta}\,e^{-i\beta\eta}\,.$$

Note the appearance of the Gaussian measure over ζ. A similar measure occured in Ziolkowski's inversion (2.1.5). However, in the more general inversion (2.3.2) the additional parameter a_1 has disappeared. The validity of the inversion will be demonstrated in Section 2.4 in connection to specific examples.

To investigate the possible restrictions on the spectrum C_0 which would ensure square integrability of the solution, one can consider the integral over β in equation (2.3.1), namely,

$$\psi(z,t) = \int_0^\infty d\beta \; \frac{1}{\beta} \; C_0\left(\frac{\kappa^2}{4\beta}, \beta, \kappa \right) \; e^{-i\kappa^2(z-ct)/4\beta} \; e^{i\beta(z+ct)} \; . \tag{2.3.3}$$

Rearranging the variables in the exponentials, one obtains

$$\psi(z,t) = \int_0^\infty d\beta \; \frac{1}{\beta} \; C_0\left(\frac{\kappa^2}{4\beta}, \beta, \kappa \right) \; \exp\left[-iz\left(\frac{\kappa^2}{4\beta} - \beta\right) \right] \; \exp\left[ict\left(\frac{\kappa^2}{4\beta} + \beta\right) \right] ,$$

or

$$\psi(z,t) = \int_0^\infty d\beta \; \frac{1}{\beta} \; C_0\left(\frac{\kappa^2}{4\beta}, \beta, \kappa \right) \; \exp\left[\frac{i\kappa z}{2}\left(\frac{2\beta}{\kappa} - \frac{\kappa}{2\beta}\right) \right] \; \exp\left[\frac{\kappa ct}{2}\left(\frac{i2\beta}{\kappa} - \frac{\kappa}{i2\beta}\right) \right] . \tag{2.3.4}$$

Using the Laurent expansion of the Bessel generating function, viz.,

$$\exp\left[\frac{x}{2}\left(t - \frac{1}{t}\right) \right] = \sum_{n=-\infty}^{+\infty} J_n(x) \, t^n \; , \tag{2.3.5}$$

the exponentials in (2.3.4) can be rewritten as

$$\exp\left[\frac{i\kappa z}{2}\left(\frac{2\beta}{\kappa} - \frac{\kappa}{2\beta}\right) \right] = \sum_{n=-\infty}^{+\infty} (i)^n \, I_n(\kappa z) \left[\frac{2\beta}{\kappa} \right]^n ,$$

$$\exp\left[\frac{\kappa ct}{2}\left(\frac{i2\beta}{\kappa}-\frac{\kappa}{i2\beta}\right)\right]=\sum_{m=-\infty}^{+\infty}(i)^m J_m(\kappa ct)\left[\frac{2\beta}{\kappa}\right]^m .$$

Using these expansions, equation (2.3.4) can be rewritten as

$$\psi(z,t)=\sum_{n=-\infty}^{+\infty}\sum_{m=-\infty}^{+\infty} C_{mn}\, I_n(\kappa z)\, J_m(\kappa ct)\,, \tag{2.3.6a}$$

where

$$C_{mn}=\int_0^{\infty} d\beta\left[\frac{2\beta}{\kappa}\right]^{m+n} i^{m+n}\, C_0\left(\frac{\kappa^2}{2\beta},\beta,\kappa\right). \tag{2.3.6b}$$

A necessary condition for the convergence of (2.3.6a) is that $C_{mn}<\infty$ for all values of m and n ranging from $-\infty$ to $+\infty$. Considering the integral (2.3.6b), it is then obvious that $C_0(\frac{\kappa^2}{\beta},\beta,\kappa)$ should obey the conditions

$$\lim_{\beta\to 0}\ \frac{1}{\beta^r}\ C_0\left(\frac{\kappa^2}{4\beta},\beta,\kappa\right)<\infty\,, \tag{2.3.7a}$$

$$\lim_{\beta\to\infty}\ \beta^r\ C_0\left(\frac{\kappa^2}{4\beta},\beta,\kappa\right)<\infty\,, \tag{2.3.7b}$$

for arbitrary β , and $r=m+n$, for any integer values of m and n . A good candidate is a spectrum of the form

$$C_0\left(\frac{\kappa^2}{4\beta},\beta,\kappa\right)=\beta^r\ \exp\left[-\{\beta a_1+(\kappa^2/4\beta)\,a_2\}\right]. \tag{2.3.8}$$

This is similar to the one used for the splash pulses and EDEPT solutions, as will be demonstrated in Section 2.4, where the bidirectional representation (2.2.22) will be used as a natural superposition for the synthesis of Brittingham-like solutions, e.g., focus wave modes, splash pulses, Bessel beams and EDEPT solutions. This will enable us to gain a better understanding of these unusual solutions, and by using the transformation (2.2.23), to obtain more information about their Fourier spectral content.

We would like to derive, next, the sufficient condition that should be imposed on the spectra chosen, in order to ensure the square integrability of the resulting wave function. The condition for square integrability can be expressed as follows:

$$\mathscr{I} = 2\pi \int_0^\infty dz \int_0^\infty d\rho\, \rho\, |\Psi(\rho, \zeta, \eta)|^2 \;<\; \infty\,, \tag{2.3.9}$$

where $\Psi(\rho, \zeta, \eta)$ is given in equation (2.3.1). With no loss of generality, we will treat only the case $n = 0$. Substituting equation (2.3.1) into the condition (2.3.9), we get

$$\begin{aligned}\mathscr{I} = \frac{1}{(2\pi)^3} \int_0^\infty d\kappa \int_0^\infty d\beta \int_0^\infty d\kappa' \int_0^\infty d\beta'\, \frac{\kappa\kappa'}{\beta\beta'}\, C_0(\kappa^2/4\beta, \beta, \kappa)\, C_0^*(\kappa'^2/4\beta', \beta', \kappa') \\ \times \int_0^\infty d\rho\, \rho\, J_0(\kappa\rho)\, J_0(\kappa'\rho)\, e^{i[(\beta + \kappa^2/4\beta) - (\beta' + \kappa'^2/4\beta')]ct} \\ \times \int_{-\infty}^{+\infty} dz\, e^{-i[(\beta' - \kappa'^2/4\beta') - (\beta - \kappa^2/4\beta)]z}\,.\end{aligned} \tag{2.3.10}$$

Using the orthogonality relation of the Bessel function, viz.,

$$\int_0^\infty dt\, t\, J_n(xt)\, J_n(yt) = \frac{1}{x}\, \delta(x - y)\,, \tag{2.3.11}$$

we can manipulate equation (2.3.10) and bring it into the form

$$\mathcal{I} = \frac{1}{(2\pi)^3} \int_0^\infty d\kappa \int_0^\infty d\beta \int_0^\infty d\beta' \, \frac{\kappa}{\beta\beta'} \, C_0(\kappa^2/4\beta, \beta, \kappa) \, C_0^*(\kappa^2/4\beta', \beta', \kappa) \times e^{i[(\beta + \kappa^2/4\beta) - (\beta' + \kappa^2/4\beta')]ct} \int_{-\infty}^{+\infty} dz \, e^{i(\beta - \beta')(1 + \kappa^2/4\beta\beta')z} \,. \tag{2.3.12}$$

Using the relationship

$$\frac{1}{2\pi} \int_{-\infty}^{+\infty} dz \, e^{i(\beta - \beta')(1 + \kappa^2/4\beta\beta')z} = \frac{\delta(\beta - \beta')}{(1 + \kappa^2/4\beta\beta')} \,, \tag{2.3.13}$$

we arrive at the sufficient condition

$$\mathcal{I} = \frac{1}{\pi^2} \int_0^\infty d\beta \int_0^\infty d\kappa \, \frac{\kappa}{(\kappa^2 + 4\beta^2)} \, |C_0(\kappa^2/4\beta, \beta, \kappa)|^2 < \infty \tag{2.3.14}$$

that ensures the square integrability of the solution $\Psi(\vec{r}, t)$ corresponding to the spectrum $C_0(\kappa^2/4\beta, \beta, \kappa)$.

2.4 THE BIDIRECTIONAL DECOMPOSITION OF KNOWN SOLUTIONS

It was demonstrated in the previous section that the main achievement of the embedding technique is to introduce a time-symmetric bidirectional representation. For the scalar wave equation, such a representation is given in equation (2.2.22). It turns out that such a superposition provides the most natural approach for synthesizing Brittingham-like solutions. This section is de-

voted, mainly, to substantiating this claim. Starting with the scalar analog of Brittingham's FWMs, it will be shown that by choosing very simple spectra $C_n(\alpha, \beta, \vec{\kappa})$, mostly of the type given in equation (2.3.8), all known Brittingham-like solutions can be synthesized. Because of the simple transformation (2.2.23), it will be easy to transform such solutions to their Fourier picture, from which a basic understanding of their spectral content can be achieved. These examples can also provide a vehicle through which the inversion formula can be checked. The following discussion will be restricted to the zeroth order mode $(n = 0)$.This is a matter of convenience and does not affect the generality of the procedure.

2.4.1 FOCUS WAVE MODES

The FWMs were originally stimulated by the work of Brittingham [1] who derived their vector form in connection with Maxwell's equations. Their scalar form was derived by Belanger [7], Sezginer [5] and Ziolkowski [9]. These modes, the zeroth order of which is given in equation (2.1.2), are characterized by an infinite total energy content. Motivated by the bidirectional character of the solution (2.1.2), it will be shown below that the representation (2.2.22) can be used to synthesize the FWMs associated with the scalar wave equation.

Consider the spectrum

$$C_0(\alpha, \beta, \kappa) = \frac{\sqrt{\pi}}{2}\ \sigma\, e^{-\sigma^2(\beta-\beta')^2}\ e^{-\alpha a_1}\ . \tag{2.4.1}$$

Substituting it into equation (2.2.22) results in the expression

$$\Psi(\rho, \zeta, \eta) = \frac{1}{(2\pi)^2} \int_0^\infty d\kappa \int_0^\infty d\beta \int_0^\infty d\alpha\ \frac{\sqrt{\pi}\,\sigma}{2}\ e^{-\sigma^2(\beta-\beta')^2}\, e^{-\alpha a_1}\, \kappa\, J_0(\kappa\rho) \times e^{-i\alpha\zeta}\, e^{i\beta\eta}\, \delta\left[\alpha\beta - \frac{\kappa^2}{4}\right]. \tag{2.4.2}$$

An integration over α reduces equation (2.4.2) to

$$\Psi(\rho,\zeta,\eta)=\frac{\sigma}{8\pi^{3/2}}\int_0^\infty d\kappa\int_0^\infty d\beta\ \frac{\kappa}{\beta}\ J_0(\kappa\rho)\,e^{-\sigma^2(\beta-\beta')^2}\,e^{-\kappa^2(a_1+i\zeta)/4\beta}\,e^{i\beta\eta}\ .$$

Using equation (6.631.4) in Gradshteyn and Ryzhik [47], viz.,

$$\int_0^\infty dx\,x^{\nu+1}\ e^{-ax^2}\,J_\nu(\alpha x)=\frac{\alpha^\nu}{(2a)^{\nu+1}}\ e^{-\alpha^2/4a}\ , \tag{2.4.3}$$

the integration over κ can be carried out explicitly, yielding

$$\Psi(\rho,\zeta,\eta)=\frac{\sigma}{4\pi^{3/2}}\int_o^\infty d\beta\ \frac{1}{(a_1+i\zeta)}\ e^{-\sigma^2(\beta-\beta')^2}\,e^{-\beta\rho^2/(a_1+i\zeta)}\,e^{i\beta\eta}\ .$$

To carry out the final integration over β, equation (3.4621.1) in Gradshteyn and Ryzhik [47] is used, viz.,

$$\int_0^\infty dx\,x^{\nu-1}\,e^{-\gamma x}\,e^{-\beta x^2}=\frac{\Gamma(\nu)}{(2\beta)^{\nu/2}}\ e^{\gamma^2/8\beta}\,D_{-\nu}\left(\frac{\gamma}{\sqrt{2\beta}}\right),$$

to give the solution

$$\Psi(\rho,\zeta,\eta)=\frac{1}{4\pi(a_1+i\zeta)}\ \frac{e^{-\sigma^2\beta'^2}}{\sqrt{2\pi}}\ e^{(\Lambda-i\eta-2\sigma^2\beta')^2/8\sigma^2}\,D_{-1}\left(\frac{\Lambda-i\eta-2\sigma^2\beta'}{\sqrt{2}\,\sigma}\right), \tag{2.4.4a}$$

where D_{-1} is the parabolic cylinder function of order -1 and

$$\Lambda=\frac{\rho^2}{(a_1+i\zeta)}\ .$$

The solution (2.4.4a) is a generalization of the scalar FWMs; the latter can be recovered by taking the limit $\sigma \to \infty$, for which the spectrum in (2.4.1) reduces to

$$C_0(\alpha, \beta, \kappa) = \frac{\pi}{2}\, \delta(\beta - \beta')\, e^{-\alpha a_1} .$$

In what follows, we shall use $\hat{\delta}$ to denote the part of the spectrum in (2.4.1) that reduces to the Dirac delta function as $\sigma \to \infty$. This will yield less cumbersome expressions and will make our discussion more transparent. As for the solution in (2.4.4a) it is more convenient to compute the limit $\sigma \to \infty$ after rewriting the parabolic cylinder function in an alternate form using the identity (9.254.1) in Gradshteyn and Ryzhik [47]; namely,

$$D_{-1}(z) = e^{z^2/4} \sqrt{\frac{\pi}{2}}\, \left[1 - \Phi(z/\sqrt{2})\right] ,$$

where $\Phi(z)$ is the probability integral defined as follows:

$$\Phi(z) = \frac{2}{\sqrt{\pi}} \int_o^z e^{-t^2} dt .$$

Rewriting the wave function (2.4.4a) in terms of the probability integral, viz,

$$\Psi(\rho, \zeta, \eta) = \frac{e^{-\beta'(\Lambda - i\eta)}}{8\pi(a_1 + i\zeta)}\, e^{(\Lambda - i\eta)^2/4\sigma^2} \left[1 - \Phi\left(\frac{\Lambda - i\eta}{2\sigma} - \sigma\beta'\right)\right] ,$$

facilitates taking the limit $\sigma \to \infty$ since $\Phi(-\infty) = -1$. Hence, as σ goes to ∞, the above expression reduces to the scalar FWM solution

$$\Psi(\rho, \zeta, \eta) = \frac{1}{4\pi\,(a_1 + i\zeta)}\; e^{-\beta'(\Lambda - i\eta)} . \qquad (2.4.4b)$$

Heyman and Felsen [36] have established the acausal nature of the FWMs, in the limit where $\beta' a_1 >> 1$, using their approximate STT theory. The causality issue can be handled in a more direct way by transforming (2.4.2) into the Fourier picture using the relationships

$$\beta = \frac{1}{2}\left(\frac{\omega}{c} - k_z\right) \qquad , \qquad \alpha = \frac{1}{2}\left(\frac{\omega}{c} + k_z\right) . \tag{2.4.5}$$

If $\Psi(\rho, \zeta, \eta)$ in equation (2.4.2) is rewritten as

$$\Psi(\rho, \zeta, \eta) = \frac{1}{(2\pi)^2} \int_0^\infty d\kappa\, \kappa\, J_0(\kappa\rho)\, \tilde{\psi}(\kappa, \zeta, \eta) , \tag{2.4.6a}$$

with

$$\tilde{\psi}(\kappa, \zeta, \eta) = \int_0^\infty d\beta \int_0^\infty d\alpha\, \frac{\pi}{2}\, \hat{\delta}(\beta - \beta')\, e^{-\alpha a_1}\, e^{-i\alpha\zeta}\, e^{i\beta\eta}\, \delta\left[\alpha\beta - \frac{\kappa^2}{4}\right], \tag{2.4.6b}$$

one can use equation (2.4.5) to express $\tilde{\psi}(\kappa, z, t)$ as follows:

$$\begin{aligned}\tilde{\psi}(\kappa, z, t) = \int_0^\infty dk_z \int_{ck_z}^\infty d\omega\, \frac{\pi}{4c}\, \hat{\delta}\left[\frac{((\omega/c) - k_z)}{2} - \beta'\right] e^{-\frac{a_1}{2}((\omega/c) + k_z)} \\ \times \delta\left[\frac{\omega^2}{4c^2} - \frac{k_z^2}{4} - \frac{\kappa^2}{4}\right] e^{-i(k_z z - \omega t)} \\ + \int_{-\infty}^0 dk_z \int_{-ck_z}^\infty d\omega\, \frac{\pi}{4c}\, \hat{\delta}\left[\frac{((\omega/c) - k_z)}{2} - \beta'\right] e^{-\frac{a_1}{2}((\omega/c) + k_z)} \\ \times \delta\left[\frac{\omega^2}{4c^2} - \frac{k_z^2}{4} - \frac{\kappa^2}{4}\right] e^{-i(k_z z - \omega t)} .\end{aligned} \tag{2.4.7}$$

An integration over ω simplifies (2.4.7) to

$$\tilde{\psi}(\kappa, z, t) = \int_0^\infty dk_z \frac{\pi}{\sqrt{k_z^2 + \kappa^2}} \hat{\delta}\left[\sqrt{k_z^2 + \kappa^2} - k_z - 2\beta'\right] e^{-\frac{a_1}{2}\left[\sqrt{k_z^2 + \kappa^2} + k_z\right]} e^{-i(k_z z - \bar{\omega} t)}$$
$$+ \int_0^\infty dk_z \frac{\pi}{\sqrt{k_z^2 + \kappa^2}} \hat{\delta}\left[\sqrt{k_z^2 + \kappa^2} + k_z - 2\beta'\right] e^{-\frac{a_1}{2}\left[\sqrt{k_z^2 + \kappa^2} - k_z\right]} e^{i(k_z z + \bar{\omega} t)}, \tag{2.4.8}$$

where $\bar{\omega} = c\sqrt{k_z^2 + \kappa^2}$. Referring to Figures 2.1 and 2.2, it is clear that the first integral in (2.4.8) vanishes for $\beta' < \kappa/2$ while the second one vanishes for $\beta' > \kappa/2$. As a result, $\Psi(\vec{r}, t)$ can be divided into two parts, one travelling in the positive z-direction and the other in the negative z-direction, viz.,

$$\Psi(\vec{r}, t) = \Psi^+(\vec{r}, t) + \Psi^-(\vec{r}, t),$$

where

$$\Psi^+(\vec{r}, t) = \frac{1}{(2\pi)^2} \int_{2\beta'}^\infty d\kappa\, \kappa\, J_0(\kappa\rho) \int_0^\infty dk_z\, F(k_z, \kappa)\, e^{-i(k_z z - \bar{\omega} t)}, \tag{2.4.9a}$$

$$\Psi^-(\vec{r}, t) = \frac{1}{(2\pi)^2} \int_0^{2\beta'} d\kappa\, \kappa\, J_0(\kappa\rho) \int_0^{\beta'} dk_z\, F(-k_z, \kappa)\, e^{i(k_z z + \bar{\omega} t)}, \tag{2.4.9b}$$

and

$$F(k_z, \kappa) = \frac{\pi}{\sqrt{k_z^2 + \kappa^2}} \hat{\delta}\left[\sqrt{k_z^2 + \kappa^2} - k_z - 2\beta'\right] e^{-\left[\sqrt{k_z^2 + \kappa^2} + k_z\right] a_1/2}. \tag{2.4.10}$$

If the parameter a_1 is large, the spectrum $F(k_z, \kappa)$ in (2.4.10) has a very narrow bandwidth, while $F(-k_z, \kappa)$ can maintain a balance between $\sqrt{k_z^2 + \kappa^2}$ and k_z in the exponential and, conse-

quently, can have a much larger bandwidth bounded by the upper limits of integration over κ and k_z in (2.4.9b). In this case, the predominant contribution to $\Psi(\vec{r}, t)$ comes from $\Psi^{-}(\vec{r}, t)$. This contribution is primarily a nonlocalized plane wave moving in the negative z-direction. If, on the other hand a_1 is very small, both $F(k_z, \kappa)$ and $F(-k_z, \kappa)$ have large bandwidths and because of the limited range of integration in the expression for $\Psi^{-}(\vec{r}, t)$ compared to the infinite range for $\Psi^{+}(\vec{r}, t)$, one expects that $\Psi^{+}(\vec{r}, t)$ becomes much larger than $\Psi^{-}(\vec{r}, t)$. In this case, the solution $\Psi(\vec{r}, t)$ behaves like a localized pulse moving in the positive z-direction.

In closing this subsection, we shall check the validity of the inversion given in equation (2.3.2). A substitution of (2.4.4b) into equation (2.3.2), leads to the expression

$$C_0\left(\frac{\kappa^2}{4\beta}, \beta, \kappa\right) = \frac{\sqrt{\pi}}{2} \int_{-\infty}^{+\infty} d\zeta\, e^{-\zeta^2/16\beta^2} \int_{-\infty}^{+\infty} d\eta \int_0^{+\infty} d\rho\, \rho\, J_0(\kappa\rho)\, \frac{e^{i\beta'\eta}}{4\pi\,(a_1 + i\zeta)} \times e^{-\beta'\rho^2/(a_1 + i\zeta)}\, e^{(i\kappa^2/4\beta)\zeta}\, e^{-i\beta\eta}\,. \tag{2.4.11}$$

Integrating over η and making use of equation (2.4.3) in order to carry out the integration over ρ, it follows that

$$C_0\left(\frac{\kappa^2}{4\beta}, \beta, \kappa\right) = \frac{\sqrt{\pi}}{8} \int_{-\infty}^{+\infty} d\zeta\, e^{-\zeta^2/16\beta^2}\, \delta(\beta - \beta')\, \frac{1}{\beta'}\, e^{-\kappa^2 a_1/4\beta'}\,.$$

The relation

$$\int_{-\infty}^{+\infty} d\zeta\, e^{-\zeta^2/16\beta^2} = \sqrt{16\pi}\ \beta$$

yields, finally, the result

$$C_0\left(\frac{\kappa^2}{4\beta}, \beta, \kappa\right) = \frac{\pi}{2}\, e^{-\kappa^2 a_1/4\beta}\, \delta(\beta - \beta') \tag{2.4.12}$$

which is identical to the spectrum given in equation (2.4.1) provided that $\alpha = \kappa^2 / 4\beta$. The latter follows from the constraint embodied in equation (2.2.21b)

2.4.2 SPLASH MODES

The original "Splash Mode" was introduced by Ziolkowski [9] as the first example of the class of finite energy solutions constructed from superpositions of the original FWMs. Hillion [12,13] has extended the FWM and the Splash Mode concepts to the realm of spinors. Ziolkowski's splash pulse can be derived within the framework of the bidirectional representation by choosing the spectrum $C_0(\alpha, \beta, \kappa)$ as follows:

$$C_0(\alpha, \beta, \kappa) = \frac{\pi}{2} \ \beta^{q-1} \ e^{-(\alpha a_1 + \beta a_2)} . \tag{2.4.13}$$

It should be noted that this choice is a specific example of the general class of spectra given in equation (2.3.8). Substituting (2.4.13) into equation (2.2.22) yields

$$\Psi(\rho, \zeta, \eta) = \frac{1}{(2\pi)^2} \int_0^\infty d\kappa \int_0^\infty d\beta \int_0^\infty d\alpha \ \frac{\pi}{2} \ \beta^{q-1} \ e^{-(\alpha a_1 + \beta a_2)} \ \kappa \ J_0(\kappa\rho) \times e^{-i\alpha\zeta} \ e^{i\beta\eta} \ \delta\left[\alpha\beta - \frac{\kappa^2}{4} \right] . \tag{2.4.14}$$

The integration over α can be carried out explicitly, viz.,

$$\Psi(\rho, \zeta, \eta) = \frac{1}{8\pi} \int_0^\infty d\kappa \int_0^\infty d\beta \ \kappa \ J_0(\kappa\rho) \ \beta^{q-2} \ e^{-\frac{\kappa^2}{4\beta}(a_1 + i\zeta)} \ e^{-\beta(a_2 - i\eta)} .$$

Equation (3.471.9) in Gradshteyn and Ryzhik [47], viz.,

$$\int_0^\infty d\beta\, \beta^{q-1}\, \exp\left[-\frac{a}{\beta} - b\beta \right] = 2\left[\frac{a}{b} \right]^{q/2} K_q\left[2\sqrt{ab} \right], \tag{2.4.15}$$

facilitates the integration over β; specifically,

$$\Psi(\rho, \zeta, \eta) = \frac{1}{8\pi} \int_0^\infty d\kappa\, \kappa^q\, J_0(\kappa\rho)\, 2\left(\frac{(a_1 + i\zeta)}{4(a_2 - i\eta)} \right)^{(q-1)/2} K_{q-1}\left[\kappa \sqrt{(a_1 + i\zeta)\,(a_2 - i\eta)} \right], \tag{2.4.16}$$

where K_q is the modified Bessel function of the second kind. To carry out the final integration over κ, formula (6.576.3) in Gradshteyn and Ryzhik [47] is used, viz.,

$$\begin{aligned} \int_0^\infty dx\, x^{-\lambda}\, K_\mu(ax)\, J_\nu(bx) = {} & \frac{b^\nu\, \Gamma(\,(\nu - \lambda + \mu + 1)/2\,)\; \Gamma(\,(\nu - \lambda - \mu + 1)/2\,)}{2^{\lambda+1}\; a^{\nu-\lambda+1}\; \Gamma(\nu + 1)} \\ & \times F\left(\frac{\nu - \lambda + \mu + 1}{2}, \frac{\nu - \lambda - \mu + 1}{2}, 1, -\frac{b^2}{a^2} \right). \end{aligned} \tag{2.4.17}$$

This leads to the result

$$\Psi(\rho, \zeta, \eta) = \frac{\Gamma(q)}{4\pi} \left(\frac{(a_1 + i\zeta)}{(a_2 - i\eta)} \right)^{(q-1)/2} \frac{F\left(q, 1, 1, -\dfrac{\rho^2}{(a_1 + i\zeta)\,(a_2 - i\eta)} \right)}{\left[\, (a_1 + i\zeta)\,(a_2 - i\eta)\, \right]^{(q+1)/2}}, \tag{2.4.18}$$

where $F(q, 1, 1, -p)$ is the hypergeometric function. The latter has the property that

$$F(q, 1, 1, -p) = \frac{1}{(1 + p)^q}.$$

Hence, (2.4.18) takes the form

$$\Psi(\rho,\zeta,\eta)=\frac{\Gamma(q)}{4\pi\,(a_1+i\zeta)}\left[\,(a_2-i\eta)+\frac{\rho^2}{(a_1+i\zeta)}\,\right]^{-q}, \tag{2.4.19}$$

which is identical to that for the splash pulse introduced by Ziolkowski [9].

It is interesting to note in connection with equation (2.4.16) that the transverse components are separated from ζ and η. The portion of $\Psi(\rho,\zeta,\eta)$ depending on ζ and η only, viz.,

$$\tilde{\psi}(\kappa,\zeta,\eta)\equiv\pi\left(\frac{(a_1+i\zeta)}{4(a_2-i\eta)}\right)^{(q-1)/2}\kappa^{q-1}\,K_{q-1}\left[\,\kappa\sqrt{(a_1+i\zeta)\,(a_2-i\eta)}\,\right] \tag{2.4.20}$$

is a solution to the 1-D Klein-Gordon equation.

The scalar wave equation analog to Hillion's "Splash Modes" [12] can easily be derived by choosing the spectrum

$$C_0(\alpha,\beta,\kappa)=\frac{\pi}{2}\,J_\nu(\beta b)e^{-\alpha a_1}\,. \tag{2.4.21}$$

In this case,

$$\Psi(\rho,\zeta,\eta)=\frac{1}{(2\pi)^2}\int_0^\infty d\kappa\int_0^\infty d\beta\int_0^\infty d\alpha\;\frac{\pi}{2}\;J_\nu(\beta b)\,e^{-\alpha a_1}\,\kappa\,J_0(\kappa\rho)\,e^{-i\alpha\zeta}\,e^{i\beta\eta}\,\delta\left[\,\alpha\beta-\frac{\kappa^2}{4}\,\right], \tag{2.4.22}$$

or

$$\Psi(\rho,\zeta,\eta)=\frac{1}{8\pi}\int_0^\infty d\kappa\int_0^\infty d\beta\;\frac{\kappa}{\beta}\;J_0(\kappa\rho)\,J_\nu(\beta b)\,e^{-\kappa^2(a_1+i\zeta)/4\beta}\,e^{i\beta\eta}$$

upon integrating over α. The integration over κ can be carried out using equation (2.4.3). One finds

$$\Psi(\rho,\zeta,\eta)=\frac{1}{4\pi}\int_0^\infty d\beta\ \frac{J_\nu(\beta b)}{(a_1+i\zeta)}\ e^{-\beta s}\ ,$$

where

$$s=\frac{\rho^2}{(a_1+i\zeta)}-i\eta\ . \tag{2.4.23}$$

Using relation (6.611.1) in Gradshteyn and Ryzhik [47], viz.,

$$\int_0^\infty dx\, e^{-\alpha x}\ J_\nu(\beta x)=\frac{\beta^{-\nu}\left[\sqrt{\alpha^2+\beta^2}-\alpha\right]^\nu}{\sqrt{\alpha^2+\beta^2}}\ , \tag{2.4.24}$$

$\Psi(\rho,\zeta,\eta)$ assumes, finally, the form

$$\Psi(\rho,\zeta,\eta)=\frac{1}{4\pi\,(a_1+i\zeta)}\ \ \frac{b^{-\nu}\left[\sqrt{s^2+b^2}-s\right]^\nu}{\sqrt{s^2+b^2}}\ , \tag{2.4.25}$$

which is a solution to the 3-D scalar wave equation analogous to Hillion's spinors. The Bessel function $J_\nu(\beta b)$ entering into (2.4.21) forms a complete orthogonal set. This means that any spectrum expressed as

$$C_0(\alpha,\beta,\kappa)=\frac{\pi}{2}\ \ F(\beta)\ \ e^{-\alpha a_1}\ ,$$

with

$$F(\beta)=\int_0^\infty db\ \ B(b)\ \ J_\nu(\beta b)\ ,$$

can result in the solution

$$\Psi(\rho,\zeta,\eta)=\frac{1}{4\pi\,(a_1+i\zeta)}\int_0^\infty db\,B(b)\,\frac{b^{-\nu}\left[\sqrt{s^2+b^2}-s\right]^\nu}{\sqrt{s^2+b^2}}\,, \tag{2.4.26}$$

which is a generalization of Hillion's result.

The Fourier spectral content of Ziolkowski's splash pulse will be discussed in the next section in conjunction with the "Modified Power Spectrum" (MPS) pulse. The Fourier picture corresponding to Hillion's solution can be obtained using the same procedure as in Section 2.4.1. Starting with the function

$$\tilde{\psi}(\kappa,\zeta,\eta)=\int_0^\infty d\beta\int_0^\infty d\alpha\;\frac{\pi}{2}\;J_\nu(\beta b)\,e^{-\alpha a_1}\,e^{-i\alpha\zeta}\,e^{i\beta\eta}\,\delta\left[\alpha\beta-\frac{\kappa^2}{4}\right], \tag{2.4.27}$$

the relationships given in equation (2.4.5) can be used to find the corresponding Fourier representation; specifically,

$$\begin{aligned}\tilde{\psi}(\kappa,z,t)=&\int_0^\infty dk_z\int_{ck_z}^\infty d\omega\;\frac{\pi}{4c}\;J_\nu\left[\frac{b}{2}\;((\omega/c)-k_z)\right]e^{-\frac{a_1}{2}\;((\omega/c)+k_z)}\\ &\times\delta\left[\frac{\omega^2}{4c^2}-\frac{k_z^2}{4}-\frac{\kappa^2}{4}\right]e^{-i(k_z z-\omega t)}\\ &+\int_{-\infty}^0 dk_z\int_{-ck_z}^\infty d\omega\;\frac{\pi}{4c}\;J_\nu\left[\frac{b}{2}\;((\omega/c)-k_z)\right]e^{-\frac{a_1}{2}\;((\omega/c)+k_z)}\\ &\times\delta\left[\frac{\omega^2}{4c^2}-\frac{k_z^2}{4}-\frac{\kappa^2}{4}\right]e^{-i(k_z z-\omega t)}\,.\end{aligned} \tag{2.4.28}$$

Integrating over ω, it follows that

$$\tilde{\psi}(\kappa, z, t) = \int_0^\infty dk_z \frac{\pi}{2\sqrt{k_z^2 + \kappa^2}} J_\nu\left[\frac{b}{2}\{\sqrt{k_z^2 + \kappa^2} - k_z\}\right] \times e^{-\frac{a_1}{2}\left[\sqrt{k_z^2 + \kappa^2} + k_z\right]} e^{-i(k_z z - \bar{\omega} t)} + \int_0^\infty dk_z \frac{\pi}{2\sqrt{k_z^2 + \kappa^2}} J_\nu\left[\frac{b}{2}\{\sqrt{k_z^2 + \kappa^2} + k_z\}\right] \times e^{-\frac{a_1}{2}\left[\sqrt{k_z^2 + \kappa^2} - k_z\right]} e^{i(k_z z - \bar{\omega} t)} . \tag{2.4.29}$$

It is seen, then, that $\Psi(\vec{r}, t)$ can be divided into two portions, $\Psi^+(\vec{r}, t)$ and $\Psi^-(\vec{r}, t)$, given by

$$\Psi^+(\vec{r}, t) = \frac{1}{(2\pi)^2} \int_0^\infty d\kappa\, \kappa J_0(\kappa\rho) \int_0^\infty dk_z F(k_z, \kappa) e^{-i(k_z z - \bar{\omega} t)} \tag{2.4.30a}$$

and

$$\Psi^-(\vec{r}, t) = \frac{1}{(2\pi)^2} \int_0^\infty d\kappa\, \kappa J_0(\kappa\rho) \int_0^\infty dk_z F(-k_z, \kappa) e^{i(k_z z + \bar{\omega} t)} , \tag{2.4.30b}$$

where

$$F(k_z, \kappa) = \frac{\pi}{2\sqrt{k_z^2 + \kappa^2}} J_\nu\left[\frac{b}{2}\{\sqrt{k_z^2 + \kappa^2} - k_z\}\right] e^{-\frac{a_1}{2}[\sqrt{k_z^2 + \kappa^2} + k_z]} . \tag{2.4.31}$$

Unlike the FWMs, the spectrum in this case is not singular. As in the case of the FWMs, however, the $\Psi^-(\vec{r}, t)$ part will predominate for large values of the parameter a_1. On the other hand, the contributions from both parts of the spectrum are almost equal for small values of a_1. This can be seen from the ratio

$$\frac{F(k_z, \kappa)}{F(-k_z, \kappa)} = \frac{J_\nu\left[\frac{b}{2}\{\sqrt{k_z^2+\kappa^2}-k_z\}\right]}{J_\nu\left[\frac{b}{2}\{\sqrt{k_z^2+\kappa^2}+k_z\}\right]}\ e^{-a_1 k_z}.$$

As indicated earlier,

$$F(k_z, \kappa) << F(-k_z, \kappa)$$

for large values of a_1. This is true for most of the frequency range contributing to the integrations (2.4.30a) and (2.4.30b). On the other hand, for a_1 very small,

$$F(k_z, \kappa) \simeq F(-k_z, \kappa)$$

for the most significant components of this spectrum.

2.4.3 EDEPTs

These solutions, which were first introduced by Ziolkowski [16,32], have finite energy, are extremely localized and they are highly directive. Another important feature of these solutions is that they contain certain parameters that can be "tweaked up" so that a pulse is predominantly propagating in one direction. An interesting example of the EDEPT solutions is the MPS pulse which can be synthesized in the context of the bidirectional representation using the shifted spectrum

$$\begin{aligned} C_0(\alpha, \beta, \kappa) &= \frac{\pi p}{2\Gamma(q)}\ (p\beta - b)^{q-1}\ e^{-[\alpha a_1 + (p\beta - b)a_2]}, \qquad \beta > \frac{b}{p}, \\ &= 0, \qquad\qquad \frac{b}{p} > \beta \geq 0. \end{aligned} \tag{2.4.32}$$

A substitution of this spectrum into (2.2.22) leads to the following solution:

$$\Psi(\rho,\zeta,\eta)=\frac{1}{(2\pi)^2}\int_0^\infty d\kappa\int_{b/p}^\infty d\beta\int_0^\infty d\alpha\;\frac{\pi p}{2\Gamma(q)}\;(p\,\beta-b)^{q-1}\;e^{-[\alpha a_1+(p\beta-b)\,a_2]} \times \kappa\,J_0(\kappa\rho)\,e^{-i\alpha\zeta}\,e^{i\beta\eta}\,\delta\left[\alpha\beta-\frac{\kappa^2}{4}\right]. \tag{2.4.33}$$

Integrating over α, it follows that

$$\Psi(\rho,\zeta,\eta)=\frac{1}{8\pi}\int_0^\infty d\kappa\int_{b/p}^\infty d\beta\;\kappa\,J_0(\kappa\rho)\;\frac{p\,(p\beta-b)^{q-1}}{\beta\,\Gamma(q)}\;e^{-\kappa^2(a_1+i\zeta)/4\beta}\,e^{-(p\beta-b)a_2}\,e^{i\beta\eta}\,.$$

The integration over κ can be performed by resorting to the change of variables $\beta'=\beta-b/p$, and making use of equation (2.4.3):

$$\Psi(\rho,\zeta,\eta)=\frac{1}{4\pi}\int_0^\infty d\beta'\;\frac{p^q\,\beta'^{q-1}}{\Gamma(q)}\;e^{-\beta'(s+pa_2)}\;\frac{e^{-bs/p}}{(a_1+i\zeta)}\;.$$

The integration over β' can be carried out explicitly, resulting in the wave function

$$\Psi(\rho,\zeta,\eta)=\frac{1}{4\pi\,(a_1+i\zeta)}\;\frac{e^{-bs/p}}{\left[\,a_2+\frac{s}{p}\,\right]^q}\;, \tag{2.4.34}$$

which is identical to the MPS pulse introduced by Ziolkowski [16,32].

A detailed analysis of the behavior of the MPS has been presented elsewhere [16,32]. Our main interest, at this point, is to transfer (2.4.33) into the corresponding Fourier representation in order to study the contributions from the positive- and negative-going components of the solution. A procedure identical to that introduced earlier yields, in this case,

$$\tilde{\psi}(\kappa, z, t) = \int_0^{\infty} d\omega \int_{-\infty}^{+\infty} dk_z \, \frac{\pi p}{4c\,\Gamma(q)} \left[\frac{p}{2} \{ (\frac{\omega}{c}) - k_z \} - b \right]^{q-1} e^{-\frac{a_1}{2}(\frac{\omega}{c} + k_z)} \times e^{-a_2 [\frac{p}{2}(\frac{\omega}{c} - k_z) - b]} \delta \left[\frac{\omega^2}{4c^2} - \frac{k_z^2}{4} - \frac{\kappa^2}{4} \right] e^{-i(k_z z - \omega t)} \tag{2.4.35a}$$

for $\frac{1}{2}(\frac{\omega}{c} - k_z) > \frac{b}{p}$, and

$$\tilde{\psi}(\kappa, z, t) = 0 \tag{2.4.35b}$$

for $\frac{1}{2}(\frac{\omega}{c} + k_z) < \frac{b}{p}$. The indicated ranges in the ω, k_z plane can be seen clearly by referring to Figures 2.3 and 2.4. Carrying out the integration over ω changes (2.4.35) to

$$\tilde{\psi}(\kappa, z, t) = \int_{-\infty}^{+\infty} dk_z \, \frac{\pi p}{2\Gamma(q)} \left[\frac{p}{2} \{ \sqrt{k_z^2 + \kappa^2} - k_z \} - b \right]^{q-1} e^{ba_2} \times e^{-a_1 \{ \sqrt{k_z^2 + \kappa^2} + k_z \}/2} e^{-a_2 p \{ \sqrt{k_z^2 + \kappa^2} - k_z \}/2} e^{-i(k_z z - \bar{\omega} t)}$$

for $\sqrt{k_z^2 + \kappa^2} - k_z > \frac{2b}{p}$, and

$$\tilde{\psi}(\kappa, z, t) = 0$$

for $\sqrt{k_z^2 + \kappa^2} - k_z < \frac{2b}{p}$. Solving for k_z and splitting $\tilde{\psi}(\kappa, z, t)$ into positive- and negative-going parts, results, finally, in the components

$$\Psi^+(\vec{r}, t) = \frac{1}{(2\pi)^2} \int_{\frac{2b}{p}}^{\infty} d\kappa \, \kappa \, J_0(\kappa\rho) \int_0^{\frac{\kappa^2 p}{4b} - \frac{b}{p}} dk_z \, F(k_z, \kappa) \, e^{-i(k_z z - \bar{\omega} t)} , \tag{2.4.36a}$$

$$\Psi^{-}(\vec{r}, t) = \frac{1}{(2\pi)^2} \int_0^{\frac{2b}{p}} d\kappa\, \kappa J_0(\kappa\rho) \int_{\frac{b}{p} - \frac{\kappa^2 p}{4b}}^{\infty} dk_z F(-k_z, \kappa)\, e^{i(k_z z + \bar{\omega} t)}$$
$$+ \frac{1}{(2\pi)^2} \int_{\frac{2b}{p}}^{\infty} d\kappa\, \kappa J_0(\kappa\rho) \int_0^{\infty} dk_z F(-k_z, \kappa)\, e^{i(k_z z + \bar{\omega} t)}, \tag{2.4.36b}$$

where

$$F(k_z, \kappa) = \frac{\pi p}{2\Gamma(q)} \left[\frac{p}{2} \{\sqrt{k_z^2 + \kappa^2} - k_z\} - b \right]^{q-1} e^{ba_2}$$
$$\times e^{-\sqrt{k_z^2 + \kappa^2}\,(a_1 + a_2 p)/2}\, e^{-k_z (a_1 - a_2 p)/2}. \tag{2.4.37}$$

The strength of the MPS pulse arises from the introduced asymmetry in the positive- and negative-going components. This can be easily demonstrated by examining the ratio

$$\frac{F(k_z, \kappa)}{F(-k_z, \kappa)} = e^{(pa_2 - a_1)k_z}$$

for $q = 1$. By an appropriate choice of the parameters p, a_1 and a_2, the positive-going frequency components can be made much larger than the negative-going ones. This can be achieved by using large values of the product pa_2. It is also straightforward to demonstrate that in the limit $b \to 0$ and $p \to 1$ the MPS given in equation (2.4.34) is reduced to the splash pulse [cf. equation (2.4.19)]. Therefore, the Fourier spectral content of the splash pulse can be obtained directly from equation (2.4.36) by setting $b = 0$ and $p = 1$; specifically,

$$\Psi^{+}(\vec{r}, t) = \frac{1}{(2\pi)^2} \int_0^{\infty} d\kappa\, \kappa J_0(\kappa\rho) \int_0^{\infty} dk_z F(k_z, \kappa) e^{-i(k_z z - \bar{\omega} t)}, \tag{2.4.38a}$$

$$\Psi^{-}(\vec{r}, t) = \frac{1}{(2\pi)^2} \int_0^\infty d\kappa\, \kappa\, J_0(\kappa\rho) \int_0^\infty dk_z\, F(-k_z, \kappa) e^{i(k_z z + \bar{\omega} t)}\,, \qquad (2.4.38b)$$

with

$$F(k_z, \kappa) = \frac{\pi}{2} \left[\frac{1}{2}\sqrt{k_z^2 + \kappa^2} - \frac{k_z}{2} \right]^{q-1} e^{-\sqrt{k_z^2 + \kappa^2}\,(a_1 + a_2)/2}\, e^{-k_z (a_1 - a_2)/2}\,. \qquad (2.4.39)$$

To compare $\Psi^{+}(\vec{r}, t)$ to $\Psi^{-}(\vec{r}, t)$, consider the following ratio for $q = 1$:

$$\frac{F(k_z, \kappa)}{F(-k_z, \kappa)} = e^{(a_2 - a_1)k_z}\,.$$

It is clear from this expression that one can have a predominantly positive component if a_2 is chosen to be large and a_1 very small. However, unlike the MPS pulse, the splash pulse is not localized in the transverse directions. This is due to the absence of the parameters b and p that provide some control over the transverse localization through the factor exp $(-bs/p)$ in equation (2.4.34).

2.4.4 BESSEL BEAMS

The "Bessel Beams" were introduced by Durnin [24] and, like Brittingham's FWMs, they are characterized by an infinite energy content. It is of interest that such beams have been realized experimentally [26], primarily because of the manner in which the behavior of an infinite energy beam can be realized approximately. It is possible to show that these beams can be represented by the time-symmetric bidirectional superposition (2.2.22). One can choose, in this case,

$$C_0(\alpha, \beta, \kappa) = 4\pi\, \sigma\, \tau\, e^{-\sigma^2(\alpha + \beta - \frac{\omega_0}{c})^2}\, e^{-\tau^2(\alpha - \beta - \lambda)^2}\,, \qquad (2.4.40)$$

for which equation (2.2.22) specializes to

$$\Psi(\rho,\zeta,\eta)=\frac{1}{(2\pi)^2}\int_0^\infty d\kappa\int_0^\infty d\beta\int_0^\infty d\alpha\, 4\pi\,\sigma\,\tau e^{-\sigma^2(\alpha+\beta-\frac{\omega_0}{c})^2}\,e^{-\tau^2(\alpha-\beta-\lambda)^2} \times \kappa\, J_0(\kappa\rho)\,e^{-i\alpha\zeta}\,e^{i\beta\eta}\,\delta\left[\alpha\beta-\frac{\kappa^2}{4}\right]. \tag{2.4.41}$$

Integrating first over κ, one has

$$\Psi(\rho,\zeta,\eta)=\frac{2\sigma\tau}{\pi}\int_0^\infty d\beta\int_0^\infty d\alpha\, e^{-\sigma^2(\alpha+\beta-\frac{\omega_0}{c})^2}\,e^{-\tau^2(\alpha-\beta-\lambda)^2}\,J_0(2\sqrt{\alpha\beta}\,\rho)\,e^{-i\alpha\zeta}\,e^{i\beta\eta}\,. \tag{2.4.42}$$

This integration is very hard to evaluate exactly; nevertheless, an asymptotic solution can be obtained for large values of $\sigma\,\tau$. Without any loss of generality we can take $\sigma=\tau$ and equation (2.4.42) can be rewritten as follows:

$$\Psi(\rho,\zeta,\eta)=\frac{2\sigma^2}{\pi}\int_0^\infty d\beta\int_0^\infty d\alpha\, e^{-\sigma^2[(\frac{\omega_0}{c})^2+\lambda^2-2(\lambda+\frac{\omega_0}{c})\alpha-2(\frac{\omega_0}{c}-\lambda)\beta+2\alpha^2+2\beta^2]} \times J_0(2\sqrt{\alpha\beta}\,\rho)\,e^{-i\alpha\zeta}\,e^{i\beta\eta}\,. \tag{2.4.43}$$

This is a double integral of the Laplace type and can be evaluated asymptotically for large σ^2. Following Bleistein and Handelsman [48], the function

$$\phi(\alpha,\beta)=-\left[(\frac{\omega_0}{c})^2+\lambda^2-2(\lambda+\frac{\omega_0}{c})\alpha-2(\frac{\omega_0}{c}-\lambda)\beta+2\alpha^2+2\beta^2\right] \tag{2.4.44}$$

has critical points at $\phi_\alpha=\phi_\beta=0$, or at

$$\alpha_0=\frac{((\omega_0/c)+\lambda)}{2}\qquad \beta_0=\frac{((\omega_0/c)-\lambda)}{2}\,. \tag{2.4.45}$$

Since $\phi_{\alpha\alpha} = \phi_{\beta\beta} = -4$ and $\phi_{\alpha\beta} = 0$, it follows that

$$\phi_{\alpha\alpha}(\alpha_0, \beta_0) < 0 , \quad \phi_{\beta\beta}(\alpha_0, \beta_0) < 0 ,$$

$$\phi_{\alpha\alpha}(\alpha_0, \beta_0)\, \phi_{\beta\beta}(\alpha_0, \beta_0) - \phi^2_{\alpha\beta}(\alpha_0, \beta_0) = 16 > 0$$

and the critical point given by (2.4.45) is a maximum. Hence, the integration (2.4.43) can be approximated by

$$\Psi(\rho, \zeta, \eta) = \frac{2\pi\sigma^{-2}\, e^{\sigma^2 \phi(\alpha_0, \beta_0)}}{\sqrt{\phi_{\alpha\alpha}(\alpha_0, \beta_0)\, \phi_{\beta\beta}(\alpha_0, \beta_0) - \phi^2_{\alpha\beta}(\alpha_0, \beta_0)}} \; \frac{2\sigma^2}{\pi} \; J_0(2\sqrt{\alpha_0\beta_0}\,\rho)\, e^{-i\alpha_0\zeta}\, e^{i\beta_0\eta} + O(\sigma^{-2}) .$$

Rearranging the terms and using equation (2.4.45), one gets

$$\Psi(\rho, \zeta, \eta) = J_0\left[\sqrt{(\frac{\omega_0}{c})^2 - \lambda^2}\;\rho\right] e^{-i\lambda(\eta+\zeta)/2}\, e^{i\omega_0(\eta-\zeta)/2c} + O(\sigma^{-2}) , \tag{2.4.46}$$

which in the limit $\sigma \to \infty$ reduces to

$$\Psi(\rho, \zeta, \eta) = J_0\left[\sqrt{(\frac{\omega_0}{c})^2 - \lambda^2}\;\rho\right] e^{-i\lambda(\eta+\zeta)/2}\, e^{i\omega_0(\eta-\zeta)/2c} . \tag{2.4.47a}$$

Although the wave function given in (2.4.47a) was obtained from the asymptotic evaluation of the double integration (2.4.43), it turns out to be an exact solution to the scalar wave equation. In fact, it is same as Durnin's Bessel beam, which can be obtained by substituting

$$\zeta = z - ct \qquad , \qquad \eta = z + ct$$

into equation (2.4.47a) and rewriting it as follows:

$$\Psi(\rho, \zeta, \eta) = J_0\left[\sqrt{(\frac{\omega_0}{c})^2 - \lambda^2}\;\rho\right] e^{-i(\lambda z - \omega_0 t)} . \tag{2.4.47b}$$

As in the case of Brittingham's FWMs, the spectrum associated with a Bessel beam is singular; specifically, the spectrum given in (2.4.40) reduces to a product of two Dirac delta functions as σ goes to ∞. On the other hand, the conversion to a Fourier picture is trivial in this case since (2.4.47b) is totally travelling in the positive z-direction.

2.5 THE BIDIRECTIONAL SYNTHESIS OF NEW SOLUTIONS

Up to this point we have mainly dealt with two types of unusual solutions to the 3-D scalar wave equation. First, solutions that do not disperse at all as they propagate in free space, e.g., Brittingham's FWMs [1] and Durnin's Bessel Beams [24]. As mentioned earlier, these solutions are characterized by finite energy densities but they have infinite total energies. We have also examined solutions that hold together without spreading out for a particular distance, beyond which they start decaying very quickly, e.g., Ziolkowski's MPS pulse [16]. Such solutions can have finite total energies. In this section, we would like to utilize the full potential of the bidirectional superposition to derive new solutions analogous to the ones given in Section 2.4.

Recall that for the FWM the spectrum

$$C_0(\alpha, \beta, \kappa) = \frac{\pi}{2}\, \delta(\beta - \beta')\, e^{-\alpha a_1}$$

does not depend on κ. This property is shared by all other solutions given in the preceding section. To generalize such a spectrum, one can introduce a κ dependence into it. A possible choice is the spectrum

$$C_0(\alpha, \beta, \kappa) = \frac{\pi}{2}\, \delta(\beta - \beta')\, e^{-\alpha a_1}\, I_0(a_2 \kappa)\,, \tag{2.5.1}$$

where I_0 is the zeroth order modified Bessel function of the first kind. Substituting the spectrum (2.5.1) into equation (2.2.22) gives

$$\Psi(\rho,\zeta,\eta)=\frac{1}{(2\pi)^2}\int_0^\infty d\kappa\int_0^\infty d\beta\int_0^\infty d\alpha\ \frac{\pi}{2}\ \delta(\beta-\beta')\,e^{-\alpha a_1}\,I_0(a_2\kappa)\,\kappa\,J_0(\kappa\rho) \times e^{-i\alpha\zeta}\,e^{i\beta\eta}\,\delta\left[\alpha\beta-\frac{\kappa^2}{4}\right]. \tag{2.5.2}$$

The integration over β and α reduces equation (2.5.2) to

$$\Psi(\rho,\zeta,\eta)=\frac{1}{(8\pi)}\int_0^\infty d\kappa\ \frac{\kappa}{\beta'}\ I_0(a_2\kappa)\,J_0(\kappa\rho)\,e^{-\kappa^2(a_1+i\zeta)/4\beta'}\,e^{i\beta'\eta}\,. \tag{2.5.3}$$

Using equation (6.633.4) in Gradshteyn and Ryzhik [47], viz.,

$$\int_0^\infty dx\,x\,e^{-\alpha x^2}\,I_\nu(\beta x)\,J_\nu(\gamma x)=\frac{1}{2\alpha}\ e^{(\beta^2-\gamma^2)/4\alpha}\,J_\nu(\beta\gamma/2\alpha)\,, \tag{2.5.4}$$

the integration over κ can be carried out to give

$$\Psi(\rho,\zeta,\eta)=\frac{1}{4\pi(a_1+i\zeta)}\ e^{\beta'(a_2^2-\rho^2)/(a_1+i\zeta)}\,J_0\left(\frac{2a_2\beta'\rho}{(a_1+i\zeta)}\right)e^{i\beta'\eta}\,. \tag{2.5.5}$$

It should be noted that in the limit $a_2\to 0$ the above solution reduces to the scalar FWM. Thus, for small arguments of J_0, i.e., for $|2a_2\beta'\rho/(a_1+i\zeta)|<<1$ the solution given in equation (2.5.5) behaves, basically, as the scalar FWM. The only deviation occurs for large values of ρ, such that $|2a_2\beta'\rho/(a_1+i\zeta)|>>1$. In this case,

$$J_0\left(\frac{2a_2\beta'\rho}{(a_1+i\zeta)}\right) \sim \sqrt{\frac{(a_1+i\zeta)}{\pi a_2\beta'\rho}}\ \cos\left(\frac{2a_2\beta'\rho}{(a_1+i\zeta)}-\frac{\pi}{4}\right),$$

and for large values of ρ the wave function $\Psi(\rho,\zeta,\eta)$ falls off as $1/(a_1+i\zeta)^{1/2}$ instead of $1/(a_1+i\zeta)$ as in the case of the FWM.

Another possible spectrum, namely,

$$C_0(\alpha,\beta,\kappa)=\frac{\pi}{2}\ \delta(\beta-\beta')\,e^{-\alpha a_1}\,J_0(a_2\kappa) \tag{2.5.6}$$

can be used in the synthesis (2.2.22) to give the wave function

$$\Psi(\rho,\zeta,\eta)=\frac{1}{(8\pi)}\int_0^\infty d\kappa\ \frac{\kappa}{\beta'}\ J_0(a_2\kappa)\,J_0(\kappa\rho)\,e^{-\kappa^2(a_1+i\zeta)/4\beta'}\ e^{i\beta'\eta}\,, \tag{2.5.7}$$

where the integrations over α and β has been carried out. Equation (6.633.2) in Gradshteyn and Ryzhik [47], viz.,

$$\int_0^\infty dx\,x\,e^{-\rho^2x^2}\,J_p(\alpha x)\,J_p(\beta x)=\frac{1}{2\rho^2}\ e^{-(\alpha^2+\beta^2)/4\rho^2}\,I_p(\alpha\beta/2\rho^2)\,, \tag{2.5.8}$$

can be used to carry out the integration in (2.5.7), the final result is

$$\Psi(\rho,\zeta,\eta)=\frac{1}{4\pi(a_1+i\zeta)}\ e^{-\beta'(a_2^2+\rho^2)/(a_1+i\zeta)}\,I_0\left(\frac{2a_2\beta'\rho}{(a_1+i\zeta)}\right)e^{i\beta'\eta}\,. \tag{2.5.9}$$

Similarly to the solution (2.5.5), this wave function reduces to the FWM pulse in the limit $a_2\to 0$. However, for large values of a_2, such that $|2a_2\beta'\rho/(a_1+i\zeta)|>>1$, the solution (2.5.9) will have its

maxima away from $\rho = 0$. To verify this claim, consider the large argument approximation of $I_0(z)$; namely,

$$I_0(z) \sim \frac{e^z}{\sqrt{2\pi z}} .$$

This approximation reduces the wave function $\Psi(\rho, \zeta, \eta)$ given in equation (2.5.9) to

$$\Psi(\rho, \zeta, \eta) = \frac{1}{8\pi^{3/2}[\beta' a_2 (a_1 + i\zeta)\, \rho]^{1/2}} \; e^{-\beta'(\rho - a_2)^2/(a_1 + i\zeta)} \, e^{i\beta'\eta} . \tag{2.5.10}$$

The argument of the exponential function has a minimum at $\rho = a_2$. This means that the peak value of the amplitude of $\Psi(\rho, \zeta, \eta)$ is situated at the circle $\rho = a_2$ centered around $\rho = 0$. As a_2 decreases, the peak value of the amplitude shifts towards the origin.

Another possibility is to choose the spectrum

$$C_0(\alpha, \beta, \kappa) = \frac{\pi}{2} \; \delta(\beta - \beta') \, e^{-\alpha a_1} \, J_0(a_2 \kappa^2/4) , \tag{2.5.11}$$

which leads to the following integration:

$$\Psi(\rho, \zeta, \eta) = \frac{1}{(8\pi)} \int_0^\infty d\kappa \; \frac{\kappa}{\beta'} \; J_0(a_2 \kappa^2/4) \, J_0(\kappa\rho) \, e^{-\kappa^2(a_1 + i\zeta)/4\beta'} \, e^{i\beta'\eta} . \tag{2.5.12}$$

Using equation (6.651.6) in Gradshteyn and Ryzhik [47], viz.,

$$\int_0^\infty dx \, x \, e^{-\alpha x^2/4} \, J_{\nu/2}(\beta x^2/4) \, J_\nu(\gamma x) = \frac{2}{\sqrt{\alpha^2 + \beta^2}} \; e^{-\alpha\gamma^2/(\alpha^2 + \beta^2)} \, J_{\nu/2}\left(\frac{\beta\gamma^2}{(\alpha^2 + \beta^2)} \right) , \tag{2.5.13}$$

the wave function $\Psi(\rho, \zeta, \eta)$ assumes the form

$$\Psi(\rho,\zeta,\eta)=\frac{1}{4\pi[(a_1+i\zeta)^2+a_2^2\beta'^2]^{1/2}}\,e^{-\beta'(a_1+i\zeta)\rho^2/[(a_1+i\zeta)^2+a_2^2\beta'^2]}$$
$$\times J_0\left(\frac{a_2\beta'^2\rho^2}{(a_1+i\zeta)^2+a_2^2\beta'^2}\right)e^{i\beta'\eta}\,. \tag{2.5.14}$$

Similarly to the FWMs, the three solutions given in equations (2.5.5), (2.5.9) and (2.5.14) have infinite energies. It is of interest to point out the possibility of integrating these solutions over the parameter β in analogy to Ziolkowski's EDEPT superposition. Consider, for example, the wave function given in equation (2.5.9). A superposition of the form

$$\Psi(\rho,\zeta,\eta)=\frac{1}{4\pi(a_1+i\zeta)}\int_0^\infty d\beta\,e^{-\beta a_3}I_0\left(\frac{2a_2\beta'\rho}{(a_1+i\zeta)}\right)e^{-\beta\bar{s}}\,, \tag{2.5.15}$$

with

$$\bar{s}=\frac{a_2^2+\rho^2}{(a_1+i\zeta)}-i\eta\,, \tag{2.5.16}$$

is an exact solution to the scalar wave equation. The relationship

$$\int_0^\infty dt\,\frac{\sqrt{\pi}}{\Gamma(k)}\,(\frac{t}{2a})^{k-1/2}\,I_{(k-1/2)}(at)\,e^{-st}=\frac{1}{(s^2-a^2)^k}\,, \tag{2.5.17}$$

facilitates the integration over β and results in the wave function

$$\Psi(\rho,\zeta,\eta)=\frac{1}{4\pi(a_1+i\zeta)}\left[\left\{\frac{a_2^2+\rho^2}{(a_1+i\zeta)}+(a_3-i\eta)\right\}^2-\frac{4\rho^2a_2^2}{(a_1+i\zeta)^2}\right]^{-1/2}. \tag{2.5.18}$$

It should be noted that as $a_2 \to 0$, this solution reduces to the splash pulse given in equation (2.4.19). It should be pointed out also that the wave function given in equation (2.5.18) can be derived directly from the bidirectional superposition by making use of the spectrum

$$C_0(\alpha, \beta, \kappa) = \frac{\pi}{2}\, e^{-\alpha a_1}\, e^{-\beta a_3}\, J_0(a_2 \kappa)\,. \tag{2.5.19}$$

Other solutions can be obtained using similar spectra. These solutions are generalizations of Brittingham's FWMs and Ziolkowski's EDEPTs. Another important feature is that these novel solutions cannot be derived from Ziolkowski's superposition (2.1.3).

In closing this section, we would like to point out that the spectrum

$$C_0(\alpha, \beta, \kappa) = \frac{\pi}{2}\, \alpha\, e^{-\alpha a_1}\, e^{-\beta a_2}\, e^{-a_3/\alpha} \tag{2.5.20}$$

will give a solution which behaves like the MPS pulse. Substituting $C_0(\alpha, \beta, \kappa)$ into equation (2.2.22) and integrating over β, we get

$$\Psi(\rho, \zeta, \eta) = \frac{1}{8\pi} \int_0^\infty d\kappa \int_0^\infty d\alpha\, \kappa\, J_0(\kappa\rho)\, e^{-(a_1 + i\zeta)\alpha}\, e^{-\kappa^2(a_2 - i\eta)/4\alpha}\, e^{-a_3/\alpha}\,. \tag{2.5.21}$$

The use of equation (2.4.3) allows the integration over κ to be carried out; we obtain as a result

$$\Psi(\rho, \zeta, \eta) = \frac{1}{4\pi(a_2 - i\eta)} \int_0^\infty d\alpha\, \alpha\, e^{-a_3/\alpha}\, e^{-\alpha[(a_1 + i\zeta) + \rho^2/(a_2 - i\eta)]}\,. \tag{2.5.22}$$

Performing, finally, the integration over α [cf. equation (2.4.15)], we obtain

$$\Psi(\rho, \zeta, \eta) = \frac{a_3}{2\pi[\rho^2 + (a_1 + i\zeta)(a_2 - i\eta)]}\, K_2\Big[2\sqrt{a_3[(a_1 + i\zeta) + \rho^2/(a_2 - i\eta)]}\,\Big]\,, \tag{2.5.23}$$

where K_2 is the second order modified Bessel function of the second kind.

Like the MPS pulse, the behavior of the wave function (2.5.23) is determined by the choice of the parameters a_1, a_2 and a_3. One possibility is to choose $a_1 << 1$ and $a_3 > a_2 >> 1$, with $a_3 a_1 \sim 5$. It should be noted that a_3 acts as an amplification factor in the argument of the modified Bessel function K_2, while the condition $a_3 a_1 \sim 5$ ensures that the large argument approximation

$$K_2(z) \sim \sqrt{\frac{\pi}{2z}}\, e^{-z} \tag{2.5.24}$$

can be used for all the values of ρ, ζ and η. The parameter a_2 determines the range within which the pulse (2.5.23) does not undergo any spreading, while a_1 determines the amplitude of the pulse at the center, where $\rho = 0$ and $z = ct$. If the center of the pulse is initially situated at $z = ct = 0$, then the behavior of the wave function (2.5.23) is quite distinct in two regions; specifically, for $z < a_2/2$

$$\begin{aligned} \Psi(\rho, \zeta = 0) &= \frac{a_3}{2\pi(\rho^2 + a_1 a_2)}\, K_2\Big[2\sqrt{a_3 a_1 + \rho^2 a_3/a_2}\,\Big] \\ &\sim \frac{a_3^{3/4} a_2^{1/4}}{4\pi^{1/2}(\rho^2 + a_1 a_2)^{5/4}}\, e^{-2\sqrt{a_3 a_1 + \rho^2 a_3/a_2}}, \end{aligned} \tag{2.5.25a}$$

while for $z > a_2/2$,

$$\begin{aligned} \Psi(\rho, \zeta = 0) &= \frac{a_3}{2\pi(\rho^2 - i2a_1 z)}\, K_2\Big[2\sqrt{a_3 a_1 + i\rho^2 a_3/2z}\,\Big] \\ &\sim \frac{a_3^{3/4}(-i2z)^{1/4}}{4\pi^{1/2}(\rho^2 - i2a_1 z)^{5/4}}\, e^{-2\sqrt{a_3 a_1 + i\rho^2 a_3/2z}}. \end{aligned} \tag{2.5.25b}$$

The amplitude of the center of the pulse stays constant as long as $z < a_2/2$. When the pulse travels beyond this point it disperses as $1/z$ a feature indicated clearly in equation (2.5.25b). In the transverse direction, the pulse is exponentially localized with a radius equal to $[\sqrt{a_1 a_3} + \sqrt{a_2/a_3}\,]$ for $z < a_2/2$; this radius increases to $[\sqrt{a_1 a_3} + \sqrt{2z/a_3}\,]$ for $z > a_2/2$. The shape of the pulse along the direction of propagation can be determined by considering the amplitude at $z - ct = \varepsilon$; specifically,

$$\Psi(\rho = 0, \zeta = \varepsilon) = \frac{a_3}{2\pi\, a_2(a_1 + i\varepsilon)}\, K_2\left[2\sqrt{a_3(a_1 + i\varepsilon)}\,\right]$$
$$\sim \frac{a_3^{3/4}}{4\pi^{1/2}\, a_2(a_1 + i\varepsilon)^{5/4}}\, e^{-2\sqrt{a_3(a_1 + i\varepsilon)}}\,, \tag{2.5.26}$$

for $z < a_2/2$. This shows that the center of the pulse has a constant amplitude in the region around the center for which $\varepsilon < a_1$. Farther away from the center, the pulse falls off exponentially as $\exp[-2(a_3\varepsilon)^{1/2}]$. It is, thus, established that the wave function $\Psi(\rho, \zeta, \eta)$ given in equation (2.5.23) is a pulse confined exponentially in the direction of propagation as well as in the transverse direction. Such a pulse holds together and does not undergo any dispersion for a distance equal to $a_2/2$. Beyond this point, the pulse will start spreading out and will eventually decay to zero at infinity.

2.6 *EXTENSIONS OF THE BIDIRECTIONAL SYNTHESIS*

In this section, we shall extend the ideas discussed in Sections 2.2 and 2.3 to other classes of problems. The most natural extension is an application involving the 3-D Klein-Gordon equation which describes the propagation of waves in a dispersive medium. Another one deals with the use of the bidirectional representation in connection with dissipative problems modelled, for example, by the 3-D dissipative scalar wave equation and the telegraph equation; in these cases the operator $\hat{\Omega}(-i\nabla)$ is nonpositive. Using these two classes of problems, we shall show that solutions obtained via the bidirectional representation will be as easy to evaluate analytically, asymptotically or numerically as those for the 3-D wave equation. By the virtue of this observation, new exact solutions can be obtained trivially using spectra similar to those in Sections 2.4 and 2.5.

The spectral analysis in the preceding sections was carried out over the β-dependent part of the integral in equation (2.3.1). We were led to this procedure because the 3-D wave equation has the same structure as the 1-D Klein-Gordon equation. In particular, a Fourier transformation with respect to the transverse coordinates x and y reduces the 3-D wave equation into a 1-D Klein-Gordon equation of the following form:

$$\left[c^{-2} \partial_t^2 - \partial_z^2 + \kappa^2 \right] \tilde{u}(\vec{\kappa}, z, t) = 0 . \tag{2.6.1}$$

It should be observed that the functions $[I_n(\kappa z)\, J_m(\kappa t)]$ in the expression (2.3.6a) are not solutions to the 1-D Klein-Gordon equation. Only their sums over integer values of m and n constitute a solution to (2.6.1) and a delicate balance between the coefficients of $[I_n(\kappa z)\, J_m(\kappa t)]$ must be maintained in order to give finite solutions.

A natural extension is the 3-D Klein-Gordon equation describing the evolution of a signal propagating in dispersive media. For this case, the operator $\hat{\Omega}(-i\nabla)$ equals $-\nabla^2 + \mu^2$ and equation (2.2.1a) takes the form

$$\left[c^{-2} \partial_t^2 - \nabla^2 + \mu^2 \right] u(\vec{r}, t) = 0 . \tag{2.6.2}$$

A general solution to this equation is analogous to that given by (2.2.18), namely,

$$u(\vec{r}, t) = 2\, Re \{ \Psi(\vec{r}, t) \} ,$$

where $\Psi(\vec{r}, t)$ can be represented by the following bidirectional superposition:

$$\Psi(\rho, \zeta, \eta) = \frac{1}{(2\pi)^2} \sum_{l=1,-1} \sum_{n=0}^{\infty} \int_0^{\infty} d\kappa \int_0^{\infty} d(l\alpha) \int_0^{\infty} d(l\beta)\; C_n(l\alpha, l\beta, \kappa)\, \kappa\, J_n(\kappa\rho) \times e^{\pm in\phi}\, e^{-il\alpha\zeta}\, e^{il\beta\eta}\, \delta\left[\alpha\beta - \frac{1}{4} (\kappa^2 + \mu^2) \right] . \tag{2.6.3}$$

In this case, a partitioning of $\hat{\Omega}(-\vec{\kappa}, -i\partial_z)$ was induced through the operators $\hat{A}(-i\partial_z) = -\partial_z^2$, $\hat{B}(\vec{\kappa}, -i\partial_z) = \kappa^2 + \mu^2$, and the new constraint relation is given by

$$\alpha\beta = \frac{1}{4}(\kappa^2 + \mu^2) . \tag{2.6.4}$$

Using the relationship (2.2.23), the representation (2.6.3) can be transformed into the conventional Fourier picture; specifically,

$$\Psi(\vec{r}, t) = \frac{1}{(2\pi)^2} \sum_{n=0}^{\infty} \int_0^{\infty} d\kappa \int_{-\infty}^{+\infty} d\omega \int_{-\infty}^{+\infty} dk_z A_n(\omega, k_z, \kappa)\, \kappa\, J_n(\kappa\rho) e^{\pm in\phi} \times e^{-ik_z z} e^{i\omega t} \delta\left[\frac{\omega^2}{c^2} - \kappa^2 - k_z^2 - \mu^2\right] . \tag{2.6.5}$$

The only difference between (2.6.5) and (2.2.18) is the more complicated constraint relationship. For the problem under consideration, the constraint requires that

$$\frac{\omega^2}{c^2} - \kappa^2 - k_z^2 = \mu^2 . \tag{2.6.6}$$

When the Klein-Gordon equation is used to model massive particles, with $\mu = mc/\hbar$, the constraint given in equation (2.6.6) recovers the well known energy relation $E^2 = p^2c^2 + m^2c^4$. Recall that very few exact solutions to the 3-D Klein-Gordon equation are available. In this sense, the representation (2.6.3) is very valuable because it is characterized by the same algebraic singularities as (2.2.22). As a consequence, (2.6.3) allows the analytical computation of a rich class of novel exact and approximate solutions with as much facility as shown in Sections 2.4 and 2.5 for the 3-D scalar wave equation. For example, all the spectra used in preceding sections can be used trivially to reproduce new solutions to the 3-D Klein-Gordon equation.

For physical situations requiring a nonpositive operator $\hat{\Omega}(-i\nabla)$, e.g., those modelled by the dissipative scalar wave equation and the telegraph equation, one can still obtain novel, exact sol-

utions using the bidirectional synthesis procedure. Along these lines, consider the 3-D dissipative scalar wave equation

$$\left[c^{-2} \partial_t^2 - \nabla^2 + (c_1 + c_2) c^{-1} \partial_t + c_1 c_2 \right] \Psi(\vec{r}, t) = 0 , \tag{2.6.7}$$

which describes a wave travelling in a dissipative medium. Although equation (2.6.7) has a different structure than equation (2.2.1), an exponential transformation of the form

$$\Psi(\vec{r}, t) = \exp \left[-\frac{1}{2} (c_1 + c_2) ct \right] \hat{\Psi}(\vec{r}, t) \tag{2.6.8}$$

reduces it to

$$\left[c^{-2} \partial_t^2 - \nabla^2 - \frac{1}{2} (c_1 - c_2)^2 \right] \hat{\Psi}(\vec{r}, t) = 0 , \tag{2.6.9}$$

which is a special case of equation (2.1) with $\hat{\Omega}(- i \nabla) = - \nabla^2 - (c_1 - c_2)^2 / 2$. Notice that the above equation is similar to the Klein-Gordon equation (2.6.2) with an imaginary μ (i.e., $\mu^2 = - (c_1 - c_2)^2 / 2$). The bidirectional representation can be written directly as

$$\begin{aligned} \hat{\Psi}(\rho, \zeta, \eta) = \frac{1}{(2\pi)} \sum_{l=1,-1} \sum_{n=0}^{\infty} \int_0^{\infty} d\kappa \int_0^{\infty} d(l\alpha) \int_{-\infty}^{0} d(l\beta) \; C_n(l\alpha, l\beta, \kappa) \, \kappa \, J_n(\kappa\rho) \\ \times \; e^{\pm in\phi} \, e^{-il\alpha\zeta} \, e^{il\beta\eta} \, \delta\left[\alpha\beta + \frac{1}{8} (c_1 - c_2)^2 - \frac{\kappa^2}{4} \right] , \end{aligned} \tag{2.6.10}$$

with the constraint

$$\alpha \beta = - \frac{1}{8} (c_1 - c_2)^2 + \frac{\kappa^2}{4} . \tag{2.6.11}$$

The same discussion concerning the nature of the singularities of this solution follows automatically, except for the fact that the hyperbolic constraint (2.6.11) can lie in the second or the fourth

quadrants of the $\alpha\beta$ plane for $(c_1 - c_2)^2/2 > \kappa^2$, and in the first or third quadrants for $(c_1 - c_2)^2/2 < \kappa^2$. This also explains the difference in the α and β limits of the integration in equation (2.6.10).

The dissipative wave equation can be reduced to the telegraph equation by removing the dependence of equation (2.6.7) on the transverse coordinates x and y. The telegraph equation, which can be written as

$$\left[c^{-2}\,\partial_t^2 - \partial_z^2 + (c_1 + c_2)\,c^{-1}\,\partial_t + c_1\,c_2 \right] \psi(z, t) = 0 , \tag{2.6.12}$$

models the transmission of electromagnetic signals through wire cables. Using an exponential transformation of the form

$$\psi(z,t) = \exp\left[-\frac{1}{2}\,(c_1 + c_2)\,ct \right] \hat{\psi}(z, t) , \tag{2.6.13}$$

reduces the telegraph equation to

$$\left[c^{-2}\,\partial_t^2 - \partial_z^2 - \frac{1}{2}\,(c_1 - c_2)^2 \right] \hat{\psi}(z, t) = 0 . \tag{2.6.14}$$

A celebrated solution due to Lord Kelvin involves the choice $c_1 = c_2$. This restriction reduces equation (2.6.14) to a 1-D scalar wave equation which has the distortion-free solutions $\hat{\psi}(z - t)$ and $\hat{\psi}(z + t)$. In an attempt to find solutions to equation (2.6.14) in the general case where $c_1 \neq c_2$, one runs into the same complications as those discussed earlier in connection to the Fourier representation of the 1-D Klein-Gordon equation, or the 3-D scalar wave equation. An alternative is to use the bidirectional representation

$$\hat{\psi}(\zeta, \eta) = \frac{1}{(2\pi)} \sum_{l=1,-1} \int_0^\infty d(l\alpha) \int_{-\infty}^0 d(l\beta)\; c_0(\alpha, \beta)\; e^{-il\alpha\zeta}\, e^{il\beta\eta}\, \delta\left[\alpha\,\beta + \frac{1}{8}\,(c_1 - c_2)^2 \right] \tag{2.6.15}$$

with the constraint

$$\alpha\,\beta = -\frac{1}{8}\,(c_1 - c_2)^2\,. \tag{2.6.16}$$

(Only the second or the fourth quadrants of the $\alpha\beta$ plane need be used in this case since α and β must have different signs.) The Fourier synthesis corresponding to (2.6.15) can be obtained by using the transformation (2.2.23). This leads to

$$\hat{\psi}(z,t) = \frac{1}{2\pi}\int_{-\infty}^{+\infty} d\omega \int_{-\infty}^{+\infty} dk_z\; A_n(\omega, k_z)\; e^{-ik_z z}\; e^{i\omega t}\; \delta[\frac{\omega^2}{c^2} - k_z^2 + \frac{1}{2}(c_1 - c_2)^2]\,, \tag{2.6.17}$$

with the constraint

$$\frac{\omega^2}{c^2} - k_z^2 = -\frac{1}{2}\,(c_1 - c_2)^2\,. \tag{2.6.18}$$

Again, exact solutions to the telegraph can be easily derived by using spectra analogous to those used in Sections 2.4 and 2.5.

As a demonstration, we consider the following choice of spectra to provide new solutions to the Klein-Gordon equation. Corresponding solutions to the 3-D dissipative wave equation or the telegraph equation can be easily derived, nevertheless, these will no be given explicitly.

Analogous to the FWM one can choose the spectrum

$$C_0(\alpha, \beta, \kappa) = \frac{\pi}{2}\,\delta(\beta - \beta')\,e^{-\alpha a_1} \tag{2.6.19}$$

which yields the solution

$$\Psi(\rho, \zeta, \eta) = \frac{1}{4\pi(a_1 + i\zeta)}\; e^{-\beta'(a_2^2 + \rho^2)/(a_1 + i\zeta)}\; e^{i\beta'\eta}\; e^{-\mu^2(a_1 + i\zeta)/4\beta'}\,. \tag{2.6.20}$$

This solution was first derived by Ziolkowski [9], it is nondipersive for all times and it behaves exactly like Brittingham's FWM.

The spectrum

$$C_0(\alpha, \beta, \kappa) = \frac{\pi}{4\beta^2}\, e^{-(\alpha a_1 + \beta a_2)} \tag{2.6.21}$$

produces the solution

$$\Psi(\rho, \zeta, \eta) = \frac{1}{4\pi(a_1 + i\zeta)}\, K_0\left[\mu\sqrt{(a_1 + i\zeta)(a_2 - i\eta) + \rho^2}\,\right]. \tag{2.6.22}$$

For $a_1 > \mu >> 1$, $a_2 << 1$ and $a_1 a_2 \sim \mu^2$, the solution given in equation (2.6.22) behaves like a localized pulse. Such a pulse does not decay as it propagates along the negative z-direction as long as $2|z| < a_1$. With the indicated choice of parameters the pulse has a compact support that falls off to exponentially small values determined by the large argument behavior of the modified Bessel function K_0. It should be noted, however, that all these solutions have centers that move at the speed of light c. This is not a very appealing property, because one expects a pulse travelling in a medium to move with a group velocity $v_g < c$. This requirement will be addressed in Chapters 5 and 6.

2.7 *SUMMARY AND CONCLUSION*

A novel bidirectional decomposition of solutions to partial differential equations into backward and forward travelling plane waves was introduced in this chapter. The bidirectional decomposition, which was developed within the framework of a more general embedding procedure, allows the construction of general solutions by means of a superposition of elementary bidirectional

blocks. Such a novel superposition differs significantly from the more conventional ones, e.g., the Fourier synthesis. In particular, it is characterized by algebraic singularities that can be much easier to handle than the branch-cut singularities arising usually in the Fourier synthesis. In spite of these differences, there is a one-to-one correspondence between the new synthesis and the Fourier method and these two methods complement each other.

Several mathematical aspects of the new synthesis were addressed. It was shown that the elementary blocks entering into this superposition are composed of exponential and Bessel functions which form complete sets of orthogonal functions. This led to an inversion formula, from which different spectra can be calculated from the knowledge of exact solutions. Necessary and sufficient conditions for the choice of the spectra leading to convergent solutions were discussed.

The bidirectional decomposition was applied to the 3-D scalar wave equation, the 3-D Klein-Gordon equation, the 3-D dissipative wave equation and the telegraph equation. For all these equations, it was demonstrated that new, exact solutions can be easily obtained. It was noted that the new synthesis provides the most natural basis for the construction of the unusual Brittingham-like solutions and that it can be used as a vehicle to find the Fourier spectral content of these solutions in order to gain a better understanding of their properties.

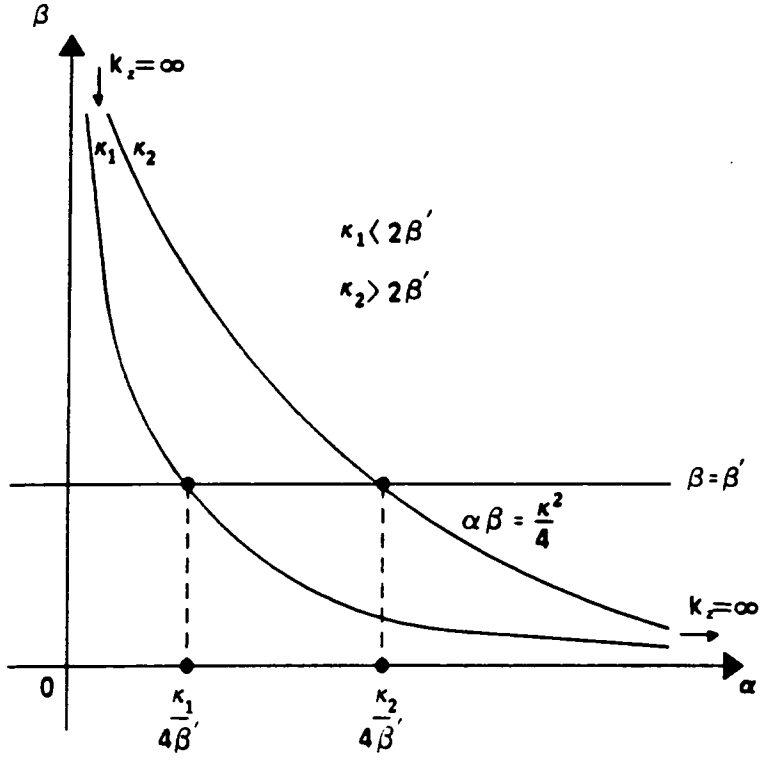

Figure 2.1 The constraints in the $\alpha\beta$ plane.

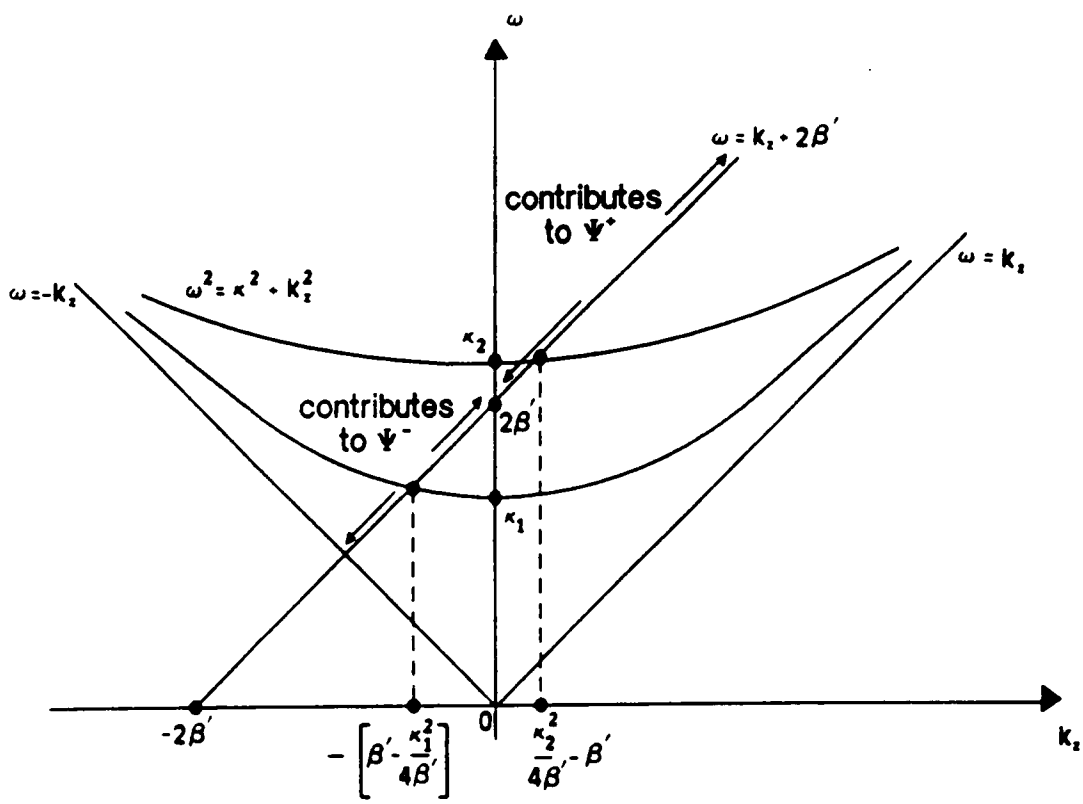

Figure 2.2 The constraints in the $k_z\omega$ plane.

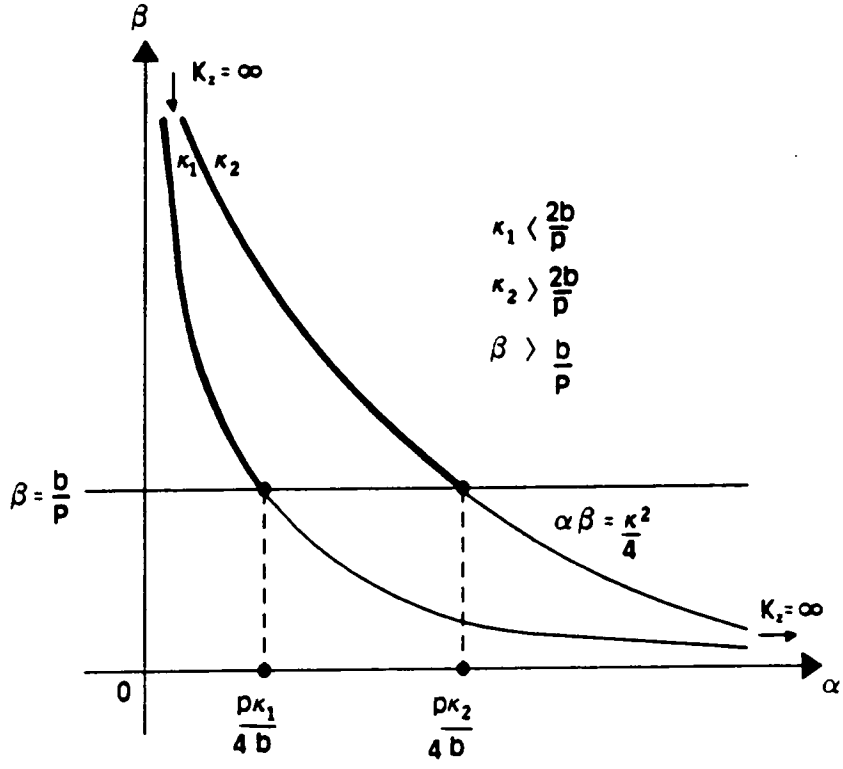

Figure 2.3 The constraints of the MPS pulse in the $\alpha\beta$ plane.

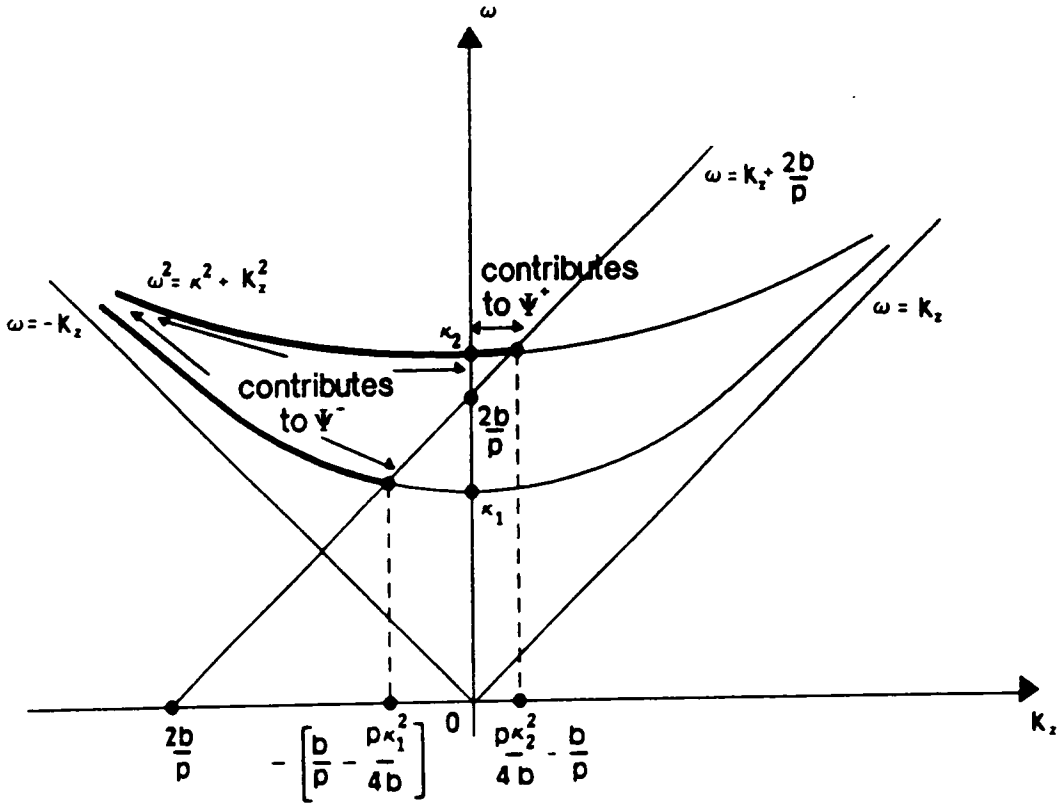

Figure 2.4 The constraints of the MPS pulse in the $k_z\omega$ plane.

3.0 PROPAGATION OF LOCALIZED PULSE TRAINS IN WAVEGUIDES

In this section we shall demonstrate the efficacy of the bidirectional method in geometries involving boundaries. After a general discussion of an initial boundary value problem in Section 3.1, we shall examine the propagation of a localized pulse train in an infinite circular waveguide. This will be followed with a detailed study of a semi-infinite waveguide excited by a localized initial pulse whose shape is related directly to parameters similar to those arising in Ziolkowski's EDEPT solutions. The far fields outside the semi-infinite waveguide will be computed using Kirchhoff's integral formula with a time-retarded Green's function. The resulting approximate solutions are causal, have finite energy and exhibit a slow energy decay behavior.

3.1 AN INITIAL BOUNDARY VALUE PROBLEM

One should not get the wrong impression that the bidirectional method introduced in the previous chapter is meant to replace the Fourier synthesis; on the contrary, the bidirectional syn-

thesis complements it. As it was shown in equation (2.2.17), a Fourier decomposition is simply a special case of a general partitioning of the operator L. In many instances dealing with single frequency phenomena, the Fourier synthesis is the most intuitive one; however, this does not rule out all other representations, particularly when they can lead to new exact solutions. Consider, for instance, initial value problems. Even though the bidirectional representation is characterized by an implicit dependence on time through the variables ζ and η, an initial value problem can still be handled successfully. As an example, consider the specific problem of pulse propagation through an infinitely long cylindrical waveguide. This problem is modelled by the 3-D scalar wave equation

$$\left[c^{-2}\,\partial_t^2 - \nabla^2\right]\, u(\vec{r}\,, t) = 0\,, \tag{3.1.1}$$

with the initial conditions

$$u(\vec{r}\,, 0) = F(\rho, z)\,, \tag{3.1.2a}$$

$$u_t(\vec{r}\,, 0) = G(\rho, z)\,, \tag{3.1.2b}$$

and the boundary condition

$$u(R, z, t) = 0\,, \tag{3.1.2c}$$

where R is the radius of the cross section of the waveguide. The functions $F(\rho, z)$ and $G(\rho, z)$ are assumed to be real. For this problem, it is advantageous to begin with the expression (2.3.1). A typical solution can then be written as

$$u(\vec{r}\,, t) \equiv u(\rho, \zeta, \eta) = c_0(\kappa, \beta)\, J_0(\kappa\rho)\, e^{-i(\kappa^2/4\beta)\zeta}\, e^{i\beta\eta}\,. \tag{3.1.3}$$

Applying the boundary condition (3.1.2c), one obtains $J_0(\kappa R) = 0$. It immediately follows that $\kappa R = \kappa_{0m}$, where κ_{0m} are the zeros of the zeroth order Bessel function. Summing over all modes and integrating over β, the general waveguide solution can be given as

$$u(\rho, \zeta, \eta) = Re \sum_{m=1}^{\infty} \int_0^{\infty} d\beta \, c_0(\kappa_{0m}, \beta) \, J_0\left(\frac{\kappa_{0m}\rho}{R}\right) e^{-i(\kappa_{0m}^2/4\beta R^2)\zeta} \, e^{i\beta\eta} \, . \tag{3.1.4}$$

The initial condition (3.1.2a) is satisfied if

$$F(\rho, z) = Re \sum_{m=1}^{\infty} \int_0^{\infty} d\beta \, c_0(\kappa_{0m}, \beta) \, J_0\left(\frac{\kappa_{0m}\rho}{R}\right) e^{-i(\kappa_{0m}^2/4\beta R^2 - \beta)z} \, . \tag{3.1.5}$$

The spectrum $c_0(\kappa_{0m}, \beta)$, which is, in general, a complex function of κ_{0m} and β, can be determined by taking first the Fourier transform with respect to z and then the Hankel transform with respect to ρ in equation (3.1.5). This gives

$$\begin{aligned} f(\kappa_{0m}, k_z) = \int_0^{\infty} d\beta \, \frac{R^2}{2} \, [J_1(\kappa_{0m})]^2 \int_{-\infty}^{+\infty} \frac{dz}{2} \Big[& c_0(\kappa_{0m}, \beta) \, e^{-i(\kappa_{0m}^2/4\beta R^2 - \beta - k_z)z} \\ & + c_0^*(\kappa_{0m}, \beta) \, e^{i(\kappa_{0m}^2/4\beta R^2 - \beta + k_z)z} \Big] , \end{aligned} \tag{3.1.6}$$

where $c_0^*(\kappa_{0m}, \beta)$ is the Hermitian conjugate of $c_0(\kappa_{0m}, \beta)$ and $f(\kappa_{0m}, k_z)$ is defined as

$$f(\kappa_{0m}, k_z) = \int_{-\infty}^{+\infty} dz \int_0^R d\rho \, \rho \, J_0\left(\frac{\kappa_{0m}\rho}{R}\right) F(\rho, z) \, e^{ik_z z} \, . \tag{3.1.7}$$

Integrating the right-hand side of equation (3.1.6) over z, it follows that

$$\begin{aligned} f(\kappa_{0m}, k_z) = \frac{\pi}{2} R^2 \, [J_1(\kappa_{0m})]^2 \int_0^{\infty} d\beta \Bigg[& c_0(\kappa_{0m}, \beta) \, \delta\left(\frac{\kappa_{0m}^2}{4\beta R^2} - \beta - k_z\right) \\ & + c_0^*(\kappa_{0m}, \beta) \, \delta\left(\frac{\kappa_{0m}^2}{4\beta R^2} - \beta + k_z\right) \Bigg] . \end{aligned} \tag{3.1.8}$$

Performing, finally, the integration over β, the following relation is obtained:

$$\frac{c_0(\kappa_{0m}, \beta_1)}{\sqrt{k_z^2 + (\frac{\kappa_{0m}}{R})^2}} \beta_1 + \frac{c_0^*(\kappa_{0m}, \beta_2)}{\sqrt{k_z^2 + (\frac{\kappa_{0m}}{R})^2}} \beta_2 = \frac{2f(\kappa_{0m}, k_z)}{\pi R^2 [J_1(\kappa_{0m})]^2} \quad . \tag{3.1.9}$$

Here,

$$\beta_1 = \frac{1}{2}\left[-k_z + \sqrt{(k_z^2 + (\frac{\kappa_{0m}}{R})^2)} \right] \quad , \qquad \beta_2 = \frac{1}{2}\left[k_z + \sqrt{(k_z^2 + (\frac{\kappa_{0m}}{R})^2)} \right] .$$

Similarly, it turns out that the initial condition (3.1.2b) is satisfied if

$$c_0(\kappa_{0m}, \beta_1)\, \beta_1 - c_0^*(\kappa_{0m}, \beta_2)\, \beta_2 = \frac{2g(\kappa_{0m}, k_z)}{\pi R^2 [J_1(\kappa_{0m})]^2} \quad , \tag{3.1.10}$$

where

$$g(\kappa_{0m}, k_z) = \int_{-\infty}^{+\infty} dz \int_0^R d\rho\, \rho\, J_0(\frac{\kappa_{0m}\rho}{R})\, G(\rho, z)\, e^{ik_z z} \quad . \tag{3.1.11}$$

A combination of equations (3.1.9) and (3.1.10) results in the spectrum

$$c_0(\kappa_{0m}, \beta_1) = \frac{1}{\beta_1\, \pi\, R^2\, [J_1(\kappa_{0m})]^2} \left(f(\kappa_{0m}, k_z) \sqrt{k_z^2 + (\frac{\kappa_{0m}}{R})^2} + g(\kappa_{0m}, k_z) \right) . \tag{3.1.12}$$

The relation $\beta_1 \equiv \beta(k_z)$ must be inverted in order to obtain $k_z \equiv k_z(\beta)$. Equation (3.1.12) can be written, then, as

$$c_0(\kappa_{0m}, \beta) = \frac{1}{\beta\, \pi\, R^2\, [J_1(\kappa_{0m})]^2} \left(f(\kappa_{0m}, k_z(\beta)) \sqrt{k_z^2(\beta) + (\frac{\kappa_{0m}}{R})^2} + g(\kappa_{0m}, k_z(\beta)) \right) ,$$

and the solution to the original problem can be expressed as

$$u(\rho,\zeta,\eta) = Re \sum_{m=1}^{\infty} \frac{1}{\pi R^2 [J_1(\kappa_{0m})]^2} \int_0^{\infty} d\beta \; e^{-i(\kappa_{0m}^2/4\beta R^2)\zeta} \, e^{i\beta\eta} \, J_0(\frac{\kappa_{0m}\rho}{R}) \\ \times \frac{1}{\beta} \left(f(\kappa_{0m}, k_z(\beta)) \sqrt{k_z^2(\beta) + (\frac{\kappa_{0m}}{R})^2} + g(\kappa_{0m}, k_z(\beta)) \right) , \tag{3.1.13}$$

in terms of a superposition of the elementary blocks $e^{-i\alpha\zeta}e^{i\beta\eta}$. Obviously, the shape of the field $u(\rho,\zeta,\eta)$ depends on the choice of $F(\rho,z)$ and $G(\rho,z)$. If, for example, $F(\rho,z)$ is chosen in the following separable form

$$F(\rho,z) = F_1(\rho)\, F_2(z) ,$$

and

$$G(\rho,z) = 0 ,$$

equation (3.1.13) can be rewritten as

$$u(\rho,\zeta,\eta) = Re \sum_{m=1}^{\infty} \frac{1}{\pi R^2 [J_1(\kappa_{0m})]^2} \int_0^{\infty} d\beta \; \frac{\hat{F}_2(k_z(\beta))}{\beta} \sqrt{k_z^2(\beta) + (\frac{\kappa_{0m}}{R})^2} \; e^{-i(\kappa_{0m}^2/4\beta R^2)\zeta} \\ \times e^{i\beta\eta} \, J_0(\frac{\kappa_{0m}\rho}{R}) \int_0^R d\rho' \, \rho' \, F_1(\rho') \, J_0(\frac{\kappa_{0m}}{R}\rho') , \tag{3.1.14}$$

where $\hat{F}_2(k_z)$ is the Fourier transform of $F_2(z)$.

3.2 THE INFINITE WAVEGUIDE

In this section we will consider the case of a pulsed initial condition. To be more specific, let

$$F_1(\rho) = \frac{1}{4\pi} J_0\left(\frac{\kappa_{0m}\rho}{R}\right), \tag{3.2.1a}$$

$$F_2(z) = K_0\left[\frac{\kappa_{0m}}{R}\sqrt{a^2+z^2}\right], \tag{3.2.1b}$$

where K_0 is the zero order modified Bessel function of the second kind. The initial conditions in this case have the form

$$u(\vec{r}, 0) = \frac{1}{4\pi} J_0\left(\frac{\kappa_{0m}\rho}{R}\right) K_0\left[\frac{\kappa_{0m}}{R}\sqrt{a^2+z^2}\right], \tag{3.2.2a}$$

$$u_t(\vec{r}, 0) = 0 . \tag{3.2.2b}$$

The Fourier transform of the function $F_2(z)$, required in equation (3.1.14), is given in this case by

$$\hat{F}_2(k_z) = \frac{\pi}{\sqrt{k_z^2 + \left(\frac{\kappa_{0m}}{R}\right)^2}} e^{-a\sqrt{k_z^2+\left(\frac{\kappa_{0m}}{R}\right)^2}} . \tag{3.2.3}$$

The expression for the root β_1, viz.,

$$(2\beta + k_z)^2 = k_z^2 + \frac{\kappa_{0m}^2}{R^2} ,$$

can be used to invert $k_z = k_z(\beta)$. This leads to the relations

$$k_z = \frac{\kappa_{0m}^2}{4\beta R^2} - \beta \ , \tag{3.2.4}$$

$$k_z^2 + \frac{\kappa_{0m}^2}{R^2} = \left(\frac{\kappa_{0m}^2}{4\beta R^2} + \beta\right)^2 . \tag{3.2.5}$$

Equations (3.2.3) and (3.2.5) can be used in conjunction with (3.1.14) to obtain

$$\begin{aligned} u(\rho, \zeta, \eta) = Re \sum_{n=1}^{\infty} \frac{J_0\left(\frac{\kappa_{0n}\rho}{R}\right)}{\pi R^2 [J_1(\kappa_{0n})]^2} \int_0^{\infty} d\beta \ \frac{\pi}{\beta} \ e^{-\left(\frac{\kappa_{0n}^2}{4\beta R^2} + \beta\right)a} \ e^{-i\frac{\kappa_{0n}^2}{4\beta R^2}\zeta} \ e^{i\beta\eta} \\ \times \frac{(\beta + \kappa_{0n}^2/4\beta R^2)}{(\beta + \kappa_{0m}^2/4\beta R^2)} \int_0^R d\rho' \ \frac{\rho'}{4\pi} \ J_0\left(\frac{\kappa_{0n}}{R}\rho'\right) J_0\left(\frac{\kappa_{0m}}{R}\rho'\right) . \end{aligned} \tag{3.2.6}$$

Integrating over ρ', equation (3.2.6) simplifies to

$$u(\rho, \zeta, \eta) = Re\left\{ \int_0^{\infty} \frac{d\beta}{8\pi\beta} \ e^{-\frac{\kappa_{0m}^2}{4\beta R^2}(a+i\zeta)} \ e^{-\beta(a-i\eta)} \ J_0\left(\frac{\kappa_{0m}\rho}{R}\right) \right\} . \tag{3.2.7}$$

The remaining integration over β can be carried out using equation (3.478.4) in Gradshteyn and Ryzhik [47]. The solution to the initial boundary value problem under consideration then assumes the form

$$u(\vec{r}, t) = Re\left\{ \frac{1}{4\pi} \ K_0\left[\frac{\kappa_{0m}}{R}\sqrt{(a+i\zeta)(a-i\eta)} \ \right] J_0\left(\frac{\kappa_{0m}\rho}{R}\right) \right\} . \tag{3.2.8}$$

This solution is of some interest because it is fairly localized at $t = 0$, where

$$u(\vec{r}, 0) = \frac{1}{4\pi} \ J_0\left(\frac{\kappa_{0m}\rho}{R}\right) K_0\left[\frac{\kappa_{0m}}{R}\sqrt{a^2 + z^2} \ \right] , \tag{3.2.9a}$$

$$u_t(\vec{r}, 0) = 0 \,. \tag{3.2.9b}$$

From the asymptotic expansion of K_0 for large arguments [49], viz.,

$$K_0(z) \simeq \sqrt{\frac{\pi}{2z}}\, e^{-z} \left\{ 1 - \frac{1}{8z} + \frac{9}{2(8z)^2} + \cdots \right\}, \tag{3.2.10}$$

it is seen that the initial pulse $u(\vec{r}, 0)$ given by (3.12a) dies off exponentially along the z-direction as $\exp[- \kappa_{0m}\sqrt{a^2 + z^2}\,/R\,]$. As a consequence, the initial pulse is fairly localized for large κ_{0m}/R. For small arguments, on the other hand, the modified Bessel function K_0 has the following behavior [49]:

$$K_0(z) \simeq - \ln(z) \,. \tag{3.2.11}$$

Therefore, at $z = ct = 0$, the initial pulse $u(\vec{r}, 0)$ becomes

$$u(\rho, 0, 0) = \frac{1}{4\pi}\, K_0\!\left[\frac{\kappa_{0m}}{R}\, a \right] J_0\!\left(\frac{\kappa_{0m}\rho}{R}\right), \tag{3.2.12}$$

and for a very small, such that $\kappa_{0m}a/R << 1$, it reduces to

$$u(\rho, 0, 0) \simeq - \frac{1}{4\pi}\, \ln\!\left[\frac{\kappa_{0m}}{R}\, a \right] J_0\!\left(\frac{\kappa_{0m}\rho}{R}\right).$$

This shows that the smaller the value of a is chosen, the larger the amplitude of the initial pulse becomes, and that parameters analogous to those arising in Ziolkowski's EDEPT solutions can now be related to some physical quantities.

It will be of interest, next, to look at the solution (3.2.8) at times $t > 0$. In this case κ_{0m}/R is large enough to keep the initial pulse localized, and a is very small so that $\kappa_{0m}a/R << 1$. Looking at the center of the pulse $z - ct = 0$, it follows that

$$u(\rho, z, z) = Re\left\{ \frac{1}{4\pi} J_0\left(\frac{\kappa_{0m}\rho}{R}\right) K_0\left[\frac{\kappa_{0m}}{R} \sqrt{a(a - i2z)} \right] \right\} .$$

If $z >> a$, and for small values of $|\kappa_{0m}\sqrt{-i2az}\,/R|$, the center of the pulse exhibits the behavior

$$u(\rho, z, z) \simeq Re\left\{ -\frac{1}{4\pi} J_0\left(\frac{\kappa_{0m}\rho}{R}\right) \ln\left[\frac{\kappa_{0m}}{R} \sqrt{-i2az} \right] \right\} ,$$

or

$$u(\rho, z, z) \simeq -\frac{1}{4\pi} J_0\left(\frac{\kappa_{0m}\rho}{R}\right) \ln\left[\frac{\kappa_{0m}}{R} \sqrt{2az} \right] . \tag{3.2.13}$$

In this case the center of the pulse decays logarithmically as it propagates down the waveguide. The same analysis applies to the pulse travelling in the negative z-direction; its center will decay according to equation (3.2.13).

As the pulses travel further in the waveguide, and z is such that $\left| \frac{\kappa_{0m}}{R} \sqrt{-i2az} \right|$ becomes large, the asymptotic expansion (3.2.10) can be used to show that the centers of the pulses will decay exponentially as

$$u(\rho, z, \pm z) \simeq Re\left\{ \frac{1}{4\pi} J_0\left(\frac{\kappa_{0m}\rho}{R}\right) \sqrt{\frac{\pi R}{2\kappa_{0m}\sqrt{2az}}}\, e^{\pm i\frac{\pi}{8}} e^{-\frac{\kappa_{0m}}{R}\sqrt{az}\,(1-i)} \right\} ,$$

or

$$u(\rho, z, \pm z) \simeq \frac{1}{4\pi} J_0\left(\frac{\kappa_{0m}\rho}{R}\right) \sqrt{\frac{\pi R}{2\kappa_{0m}\sqrt{2az}}}\, e^{-\frac{\kappa_{0m}}{R}\sqrt{az}} \cos\left(\frac{\kappa_{0m}}{R}\sqrt{az} + \frac{\pi}{8}\right). \tag{3.2.14}$$

The initial pulse (3.2.9) splits into two halves, with the centers of the individual pulses decaying logarithmically as long as $\kappa_{0m}\sqrt{2az}\,/R << 1$. For large z, the centers of the pulses start

decaying exponentially as $\exp[-\kappa_{0m}\sqrt{az}/R]$. It is easy to see how the initial pulse divides into two pulses because at the points $ct = z \pm \varepsilon$ with $\varepsilon >> a$, approximate results can be written as

$$u(\rho, z, z \pm \varepsilon) \simeq Re\left\{ \frac{1}{4\pi} J_0\left(\frac{\kappa_{0m}\rho}{R}\right) \sqrt{\frac{\pi R}{2\kappa_{0m}\sqrt{2\varepsilon z}}}\, e^{\pm i\frac{\pi}{4}} e^{-\frac{\kappa_{0m}}{R}\sqrt{\pm 2\varepsilon z}} \right\},$$

or

$$u(\rho, z, z + \varepsilon) \simeq \frac{1}{4\pi} J_0\left(\frac{\kappa_{0m}\rho}{R}\right) \sqrt{\frac{\pi R}{4\kappa_{0m}\sqrt{2\varepsilon z}}}\, e^{-\frac{\kappa_{0m}}{R}\sqrt{2\varepsilon z}} \qquad (3.2.15a)$$

and

$$u(\rho, z, z - \varepsilon) \simeq \frac{1}{4\pi} J_0\left(\frac{\kappa_{0m}\rho}{R}\right) \sqrt{\frac{\pi R}{2\kappa_{0m}\sqrt{2\varepsilon z}}}\, \cos\left(\frac{\kappa_{0m}}{R}\sqrt{2\varepsilon z} + \frac{\pi}{4}\right). \qquad (3.2.15b)$$

Similar expressions can be obtained for the pulse travelling in the negative z-direction. From these results it can be seen that the front part of the pulse dies off exponentially away from the center, while the right-going and left-going halves separate at a very slow rate. This follows from the expression (3.2.15b), where the pulse falls off as $(z\varepsilon)^{-1/4}$ behind its center.

At this point it should be mentioned that, in analogy to the free space solution (2.2.22), one can write directly the corresponding superposition for the bounded problem under consideration by replacing the integration over κ in (2.2.22) by a summation over the discrete values κ_{0m}; specifically,

$$u(\rho, \zeta, \eta) = \frac{1}{(2\pi)^2} \sum_{m=1}^{\infty} \int_0^{\infty} d\alpha \int_0^{\infty} d\beta\, C_0(\alpha, \beta, \kappa_{0m})\, J_0\left(\frac{\kappa_{0m}\rho}{R}\right) \times e^{-i\alpha\zeta}\, e^{i\beta\eta}\, \delta\left[\alpha\beta - \frac{\kappa_{0m}^2}{4R^2}\right]. \qquad (3.2.16)$$

A choice of spectrum analogous to that related to Ziolkowski's "splash pulse", namely,

$$C_0(\alpha, \beta, \kappa_{0m}) = \frac{\pi}{2}\ e^{-(\alpha+\beta)a} \tag{3.2.17}$$

leads to the solution

$$u(\vec{r}, t) = Re \sum_{m=1}^{\infty} \left\{ \frac{1}{4\pi} J_0\left(\frac{\kappa_{0m}\rho}{R}\right) K_0\left[\frac{\kappa_{0m}}{R} \sqrt{(a + i\zeta)(a - i\eta)} \right] \right\}, \tag{3.2.18}$$

which is identical to the wavefunction (3.2.8), except for the summation over all modes as indicated in equation (3.2.18).

As demonstrated earlier, the initial pulse corresponding to the solution (3.2.18) splits into two halves travelling in opposite directions and they separate at a very slow rate. Such a solution is not optimal for the transfer of energy in a waveguide. A small modification can produce a more efficient system for the transmission of localized pulses in waveguides. This can be achieved by using two parameters a_1 and a_2 instead of the one parameter a . In this case the spectrum

$$C_0(\alpha, \beta, \kappa_{0m}) = \frac{\pi}{2}\ e^{-(\alpha a_1 + \beta a_2)} \tag{3.2.19}$$

gives the solution

$$u(\vec{r}, t) = Re \sum_{m=1}^{\infty} \left\{ \frac{1}{4\pi} J_0\left(\frac{\kappa_{0m}\rho}{R}\right) K_0\left[\frac{\kappa_{0m}}{R} \sqrt{(a_1 + i\zeta)(a_2 - i\eta)} \right] \right\}. \tag{3.2.20}$$

Even though the wave function $u(\rho, \zeta, \eta)$ is expressed as a summation over all modes, our subsequent discussion will be restricted to a single one.

The solution (3.2.20), for a characteristic modal number m, is of some interest because it can model a fairly localized pulse propagating in a waveguide, where at $t = 0$,

$$u(\vec{r}, 0) = \frac{1}{4\pi} J_0\left(\frac{\kappa_{0m}\rho}{R}\right) Re\left\{ K_0\left[\frac{\kappa_{0m}}{R}\sqrt{(a_1 + iz)(a_2 - iz)} \right] \right\} \qquad (3.2.21a)$$

and

$$u_t(\vec{r}, 0) = \frac{\kappa_{0m}\, c}{8\pi R} J_0\left(\frac{\kappa_{0m}\rho}{R}\right) Re\left\{ i K_1\left[\frac{\kappa_{0m}}{R}\sqrt{(a_1 + iz)(a_2 - iz)} \right] \frac{a_1 + a_2}{\sqrt{(a_1 + iz)(a_2 - iz)}} \right\} . \qquad (3.2.21b)$$

The initial pulse can be extremely localized for large a_2. This can be demonstrated by using the asymptotic expansion of K_0 for large arguments [cf. equation (3.2.10)] in order to rewrite the initial condition (3.2.21a) approximately as follows:

$$u(\rho, z, 0) \simeq \frac{1}{4\pi} J_0\left(\frac{\kappa_{0m}\rho}{R}\right) \sqrt{\frac{\pi R}{2\kappa_{0m}\sqrt{a_2 z}}}\, e^{-\kappa_{0m}\sqrt{a_2 z/2}\ /R} \cos\left(\frac{\kappa_{0m}}{R}\sqrt{\frac{a_2 z}{2}} + \frac{\pi}{8}\right) . \qquad (3.2.22)$$

The initial pulse $u(\vec{r}, 0)$ falls off exponentially along the z direction as $\exp[-\kappa_{0m}\sqrt{a_2 z/2}\ /R]$. This approximate form is valid away from the pulse's center. To determine the shape of the initial pulse around $z = 0$, one can use the small argument approximation of the modified Bessel function K_0, given in equation (3.2.11). At $z = 0$, the amplitude of the initial pulse $u(\vec{r}, 0)$ has the value

$$u(\rho, 0, 0) = \frac{1}{4\pi} K_0\left[\frac{\kappa_{0m}}{R}\sqrt{a_1 a_2} \right] J_0\left(\frac{\kappa_{0m}\rho}{R}\right) . \qquad (3.2.23)$$

If the product $a_1 a_2$ is very small so that $\kappa_{0m}\sqrt{a_1 a_2}\ /R << 1$, equation (3.2.11) yields

$$u(\rho, 0, 0) \simeq -\frac{1}{4\pi} \ln\left[\frac{\kappa_{0m}}{R}\sqrt{a_1 a_2} \right] J_0\left(\frac{\kappa_{0m}\rho}{R}\right) . \qquad (3.2.24)$$

This expression shows that small values of $\sqrt{a_1 a_2}$ correspond to large amplitudes of the initial pulse. Noting, also, that the oscillatory term $\cos[\frac{\pi}{8} + \frac{\kappa_{0m}}{R}\sqrt{a_2 z/2}\,]$ in equation (3.2.22) depends on a_2,

it is clear that the parameters a_1 and a_2 can now be related to physically meaningful quantities, such as the width of the initial pulse and its amplitude. A similar discussion applies to the second initial condition (3.2.21b) but will not be carried out here.

The behavior of the pulse solution (3.2.20) is very sensitive to the values of the parameters a_1 and a_2. If these parameters are equal, the solution (3.2.20) models a pulse that splits into two halves travelling in opposite directions. This situation is not optimal for the transmission of energy in the waveguide. On the other hand, because of the asymmetric dependence on the values of a_1 and a_2, the pulse given in equation (3.2.20) can be made to travel mainly in one direction. Such a claim can be verified by referring to equations (2.4.38) and (2.4.39) which give the positive-going and the negative-going components of the splash pulse. The only difference entails the replacement of the integration over κ by a summation over κ_{0m} . The backward and forward spectra have the following ratio:

$$\frac{F(k_z, \kappa_{0m})}{F(-k_z, \kappa_{0m})} = e^{(a_2 - a_1)k_z} .$$

It is seen that for $a_2 = a_1$, the positive and the negative components have the same strength. On the other hand, for $a_2 > 1$ and $a_1 << 1$, $F(k_z, \kappa_{0m}) >> F(-k_z, \kappa_{0m})$ and the pulse moves predominantly in the positive z-direction. Moreover, in contradistinction to the splash pulse (2.4.19), the solution (3.2.20) is localised by the walls of the waveguide and one does not have to worry about its localization in the transverse direction. Thus, launching a pulse that travels primarily in the positive z-direction requires that $a_2 > 1$ and $a_1 << 1$, with the condition $\kappa_{0m}\sqrt{a_1 a_2} \; / \; R << 1$. To see this, one can look at the pulse centers at $z = ct$ and $z = -ct$, where

$$u(\rho, z, z) = Re\left\{ \frac{1}{4\pi} J_0\left(\frac{\kappa_{0m}\rho}{R}\right) K_0\left[\frac{\kappa_{0m}}{R} \sqrt{a_1(a_2 - i2z)} \right] \right\} \qquad (3.2.25)$$

and

$$u(\rho, z, -z) = Re\left\{ \frac{1}{4\pi} J_0\left(\frac{\kappa_{0m}\rho}{R}\right) K_0\left[\frac{\kappa_{0m}}{R}\sqrt{a_2(a_1 + i2z)} \right] \right\}. \qquad (3.2.26)$$

As long as $2z << a_2$, $u(\rho, z, z)$ in equation (3.2.25) remains constant with

$$u(\rho, z, z) \simeq \frac{1}{4\pi} J_0\left(\frac{\kappa_{0m}\rho}{R}\right) K_0\left[\frac{\kappa_{0m}}{R}\sqrt{a_1 a_2} \right]. \qquad (3.2.27)$$

This expression is identical to the amplitude of the initial pulse. We conclude that the parameter a_2 determines the range through which the pulse can travel before it starts decaying. Beyond this range the pulse starts decaying logarithmically, viz.,

$$u(\rho, z, z) \simeq \frac{-1}{4\pi} J_0\left(\frac{\kappa_{0m}\rho}{R}\right) \ln\left[\frac{\kappa_{0m}}{R}\sqrt{2a_1 z} \right], \qquad (3.2.28)$$

as long as $\kappa_{0m}\sqrt{2a_1 z}\ /R << 1$. Thus, the pulse travelling in the positive z-direction stays almost unchanged as long as $2z << a_2$, decays logarithmically for $\kappa_{0m}\sqrt{2a_1 z}\ /R << 1$, beyond which it dies off exponentially as exp $[-\kappa_{0m}\sqrt{2a_1 z}\ / R]$. As for the pulse travelling in the negative z-direction, it can be easily seen that for $a_1 << 1$ the expression (3.2.26) can be simplified as follows:

$$u(\rho, z, -z) = Re\left\{ \frac{1}{4\pi} J_0\left(\frac{\kappa_{0m}\rho}{R}\right) K_0\left[\frac{\kappa_{0m}}{R}\sqrt{i2a_2 z} \right] \right\}. \qquad (3.2.29)$$

But for $a_2 > 10$ the center of the pulse in (3.2.26) will decay exponentially as exp$[-\kappa_{0m}\sqrt{2a_2 z}\ /R]$ and the pulse will die off within a very short distance from the origin.

With an appropriate choice of the parameters a_1 and a_2, one is capable of launching a pulse in one direction down an infinite cylinder. Another interesting aspect of this solution is its ability to resist the dispersive effects of the waveguide. It has been demonstrated that the pulse can travel with almost no decay in its center for a distance $\simeq a_2/2$, beyond which the decay in the center of the pulse is only logarithmic for $a_2/2 < z << [\, R^2/2\kappa_{0m}^2 a_1\,]$. For example, if one chooses $a_1 = 10^{-13}$ m,

$a_2 = 10^3$ m and $\kappa_{0m}/R = 1000$ m^{-1}, then the pulse can travel down the waveguide a distance of approximately 500 m without any decay in the pulse center, and will spread very little for the following 5×10^4 m . To see how little does it decay, consider the amplitude of the center of the initial pulse, which is proportional to $K_0[\kappa_{0m}\sqrt{a_1 a_2}\ /R]$ or, asymptotically, to $-\ \ln(10^{-2}) \simeq 2\ \ln(10)$. The pulse center after travelling a distance of 50 km will have an amplitude proportional to ln(10). Thus, over a distance of 50 km , the pulse's center decays only to half its original value.

One would hope that such pulses could still hold themselves together when launched in free space from an open end of the waveguide, and that they could still exhibit a slow decay behavior. In this case the pulses would be analogous to Ziolkowski's EDEPTs and the open waveguide could act as their source. This scheme will be pursued in the next section where it will be shown that a semi-infinite waveguide can be used as a source for slowly decaying pulses.

3.3 THE SEMI-INFINITE WAVEGUIDE

A natural extension of the previous section is to consider the case of a semi-infinite waveguide. The initial pulse is the same as that given by equation (3.2.21) and the waveguide is open at the position $z = L$, where L is large enough so that the amplitude of the tail of the initial pulse is extremely small, and for all practical purposes can be taken equal to zero, while the waveguide appears to be practically infinite. It is assumed, furthermore, that the radius of the cylinder is large compared to the wavelengths of the excited modes. In this case, upon reaching the guide's opening, the pulse is basically launched in the forward direction and the reflected field from the edges of the cylinder can be neglected. This setup is shown in Figure 3.2.

Under the assumptions made above one can use Kirchhoff's diffraction formula to find an expression for the far field in terms of the field illuminating the aperture or the cylinder's opening. Kirchhoff's formula has the form [50]

$$\hat{\Psi}(x', y', z', \omega) = \frac{1}{4\pi} \int_s da \left\{ \frac{\partial}{\partial z} \hat{\Psi}(x, y, z, \omega) \frac{e^{-i\omega r}}{r} - \frac{\partial}{\partial z} \left(\frac{e^{-i\omega r}}{r} \right) \hat{\Psi}(x, y, z, \omega) \right\}, \tag{3.3.1}$$

where (x', y', z') is the point of observation, the integration is carried over the area of the aperture, and the normal to the aperture is in the z-direction. $\hat{\Psi}(x, y, z, \omega)$ is the Fourier transform of $\Psi(x,y,z, t)$ with respect to time, and is defined as follows:

$$\hat{\Psi}(x, y, z, \omega) = \int_{-\infty}^{+\infty} dt \ \Psi(x, y, z, t) \ e^{-i\omega t} . \tag{3.3.2}$$

The variable r appearing in (3.3.1) is the distance between the aperture and the observation point; it is given explicitly as follows:

$$r = \sqrt{\rho^2 + \rho'^2 + 2\rho \rho' \cos(\theta - \theta') + (z' - L)^2} . \tag{3.3.3}$$

Only the amplitude of the pulse along the line of sight ($\rho' = 0$) will be considered in the sequel. In this case, Kirchhoff's formula can be rewritten as

$$\hat{\Psi}(0, 0, z', \omega) = \frac{1}{4\pi} \int_0^{2\pi} d\phi \int_0^R d\rho \ \rho \left[\frac{\partial}{\partial z} \hat{\Psi}(x, y, z, \omega) \frac{e^{-i\omega r}}{r} - \frac{\partial}{\partial z} \left(\frac{e^{-i\omega r}}{r} \right) \hat{\Psi}(x, y, z, \omega) \right]_{z=L}, \tag{3.3.4}$$

with

$$r = \sqrt{\rho^2 + (z' - z)^2} \Big|_{z=L} . \tag{3.3.5}$$

From Kirchhoff's integrals (3.3.1) and (3.3.4), together with the definition of the Fourier transform (3.3.2), it can be seen that the time-retarded Green's function has been used. As a consequence, the resulting pulse is causal and it propagates away from the aperture into free space.

As mentioned earlier, the initial pulse given in (3.2.21) will be used, with L large enough so that the waveguide appears to be infinitely long. For all practical purposes, the basic solution derived in Section 3.2 can be used to illuminate the open end of the waveguide. This solution is rewritten here for convenience, viz.,

$$\Psi(\vec{r}, t) = \frac{1}{4\pi} J_0\left(\frac{\kappa_{0m}\rho}{R}\right) K_0\left[\frac{\kappa_{0m}}{R}\sqrt{(a_1 + i\zeta)(a_2 - i\eta)}\right]. \tag{3.3.6}$$

This pulse is located initially at the origin, and with an appropriate choice of a_1 and a_2 it can be made to travel in the positive z-direction. All the discussion pertaining to the initial conditions and the conditions required for localization are the same as in Section 3.2.

Substituting (3.3.6) into equations (3.3.1) and (3.3.4), Kirchhoff's integral formula (3.3.4) assumes the following form after an integration over ϕ:

$$\begin{aligned}\hat{\Psi}(0, 0, z', \omega) = {} & \frac{f_2(\omega)}{8\pi}\int_0^R d\rho\,\rho\,\frac{e^{-i\omega r}}{r} J_0\left(\frac{\kappa_{0m}\rho}{R}\right) \\ & - \frac{f_1(\omega)}{8\pi}\int_0^R d\rho\,\rho\left[\frac{(z' - L)}{r^3} + \frac{i\omega(z' - L)}{r^2}\right] e^{-i\omega r}.\end{aligned} \tag{3.3.7}$$

Here, $f_1(\omega)$ and $f_2(\omega)$ are defined as follows:

$$f_1(\omega) = \int_{-\infty}^{+\infty} dt\, e^{-i\omega t} K_0\left[\frac{\kappa_{0m}}{R}\sqrt{(a_1 + i(z - ct))(a_2 - i(z + ct))}\right]\Bigg|_{z=L}, \tag{3.3.8}$$

$$f_2(\omega) = \int_{-\infty}^{+\infty} dt\, e^{-i\omega t}\frac{\partial}{\partial z} K_0\left[\frac{\kappa_{0m}}{R}\sqrt{(a_1 + i(z - ct))(a_2 - i(z + ct))}\right]\Bigg|_{z=L}. \tag{3.3.9}$$

For $(z' - L) >> \rho$, the quantity r can be approximated by

$$r \simeq (z' - L) + \frac{\rho^2}{2(z' - L)} , \tag{3.3.10}$$

and equation (3.3.7) can be rewritten as

$$\hat{\Psi}(0, 0, z', \omega) = e^{-i\omega\hat{z}} \left[\frac{f_2(\omega)}{8\pi\,\hat{z}} - \frac{f_1(\omega)}{8\pi} \left\{ \frac{1}{\hat{z}^2} + \frac{i\omega}{\hat{z}} \right\} \right] \int_0^R d\rho\, \rho\, J_0\left(\frac{\kappa_{0m}\rho}{R}\right) e^{-i\omega\rho^2/2\hat{z}} , \tag{3.3.11}$$

where $\hat{z} = z' - L$. An evaluation of the integral

$$I = \int_0^R d\rho\, \rho\, J_0\left(\frac{\kappa_{0m}\rho}{R}\right) e^{-i\omega\rho^2/2\hat{z}} \tag{3.3.12}$$

is needed. This integral can be related to Lommel's function of two variables. Making use of the relations (3) and (4), p. 543 of Watson [51], it is easy to show that

$$\begin{aligned} I = \frac{\hat{z}}{\omega}\; e^{-i\omega R^2/2\hat{z}} & \left\{ - U_1\left(\frac{\hat{z}\kappa_{0m}^2}{\omega R^2}, \kappa_{0m} \right) + i\, U_0\left(\frac{\hat{z}\kappa_{0m}^2}{\omega R^2}, \kappa_{0m} \right) \right\} \\ & + \frac{\hat{z}}{\omega} \left\{ U_1\left(\frac{\hat{z}\kappa_{0m}^2}{\omega R^2}, 0 \right) - i\, U_0\left(\frac{\hat{z}\kappa_{0m}^2}{\omega R^2}, 0 \right) \right\} . \end{aligned} \tag{3.3.13}$$

At this stage, one can go back to equation (3.3.11), find $\Psi(0, 0, z', \omega)$, carry out the inverse transform and find $\Psi(0, 0, z', t)$. The integrations become quite involved, however, and it will be a very tedious task to find a closed form solution. To simplify the integrals involved in the Fourier inversion, one can use the asymptotic expansion of $U_\nu(\mu, \lambda)$ for large μ, while ν and λ are kept constant. The quantity $\hat{z}\kappa_{0m}^2/\omega R^2$ entering into equation (3.3.13) must be large. A reasonable limit can be chosen as

$$\frac{\hat{z}\kappa_{0m}^2}{\omega R^2} > 1000 . \tag{3.3.14}$$

One can use the asymptotic expansions given in equations (3) and (4) p. 550 of Watson [51] to write

$$U_\nu(\mu, 0) \simeq \cos(\frac{\mu}{2} - \frac{\nu\pi}{2}) + \sum_{m=0}^{\infty} \frac{(-1)^m}{\Gamma(\nu - 1 - 2m)\ [\frac{\mu}{2}]^{2m-\nu+2}} \tag{3.3.15}$$

and

$$U_\nu(\mu, \lambda) \simeq \cos\left[\ \frac{\mu}{2} + \frac{\lambda^2}{2\mu} - \frac{\nu\pi}{2}\ \right] + \sum_{m=0}^{\infty} (-1)^m \left[\ \frac{\lambda}{\mu}\ \right]^{2m-\nu+2} J_{\nu-2-2m}(\lambda) . \tag{3.3.16}$$

Using these expansions in equation (3.3.13), it follows that

$$I = \frac{\hat{z}}{\omega}\ e^{-i\omega R^2/2\hat{z}} \sum_{m=0}^{\infty} (-1)^m \left[\ -\left(\frac{\omega R^2}{\hat{z}\kappa_{0m}}\right)^{2m+1} J_{-1-2m}(\kappa_{0m}) + i\left(\frac{\omega R^2}{\hat{z}\kappa_{0m}}\right)^{2m+2} J_{-2-2m}(\kappa_{0m})\ \right] .$$

For small values of of $\omega R^2/\hat{z}\kappa_{0m}$ (e.g., < 0.1), the first term in the above expression can be retained, while the rest of the terms are neglected. Thus, I can be approximated by

$$I = J_1(\kappa_{0m})\ \frac{R^2}{\kappa_{0m}}\ e^{-i\omega R^2/2\hat{z}} + O(\frac{1}{\hat{z}}) . \tag{3.3.17}$$

This approximate result is valid for large $\hat{z}$ or, more generally, for large $\hat{z}\kappa_{0m}/\omega R^2$. This requirement follows from the condition (3.3.14) as long as $\kappa_{0m} < 30$, i.e., for the lowest ten modes. As a result, the approximate expression (3.3.17) is valid for the following values of $\hat{z}$:

$$\hat{z} > 1000 \frac{\omega R^2}{\kappa_{0m}^2} .$$

Since $\omega > \kappa_{0m}/R$ for the waveguide, the above inequality can be rewritten as

$$\hat{z} > 1000 \frac{R}{\kappa_{0m}} . \tag{3.3.18}$$

Substituting (3.3.17) into (3.3.11), the wave function $\hat{\Psi}(0, 0, \hat{z}, \omega)$ along the line of sight can be found to be equal to

$$\hat{\Psi}(0, 0, \hat{z}, \omega) = \frac{J_1(\kappa_{0m}) R^2}{8\pi \kappa_{0m} \hat{z}} \exp\left\{ - i\omega \left(\hat{z} + \frac{R^2}{2\hat{z}} \right) \right\} \left[f_2(\omega) - i\omega f_1(\omega) \right] , \tag{3.3.19}$$

where all terms proportional to $\hat{z}^{-2}$ have been neglected. This approximate result is quite accurate for the range determined by (3.3.18). It is not hard, now, to find the inverse Fourier transform of the expression (3.3.19); it can be expressed as

$$\Psi(0, 0, \hat{z}, t) = \frac{J_1(\kappa_{0m}) R^2}{8\pi \kappa_{0m} \hat{z}} \left[F_2(t') - \partial_t F_1(t') \right]_{z=L} , \tag{3.3.20}$$

where

$$F_2(t') = \partial_z K_0 \left[\frac{\kappa_{0m}}{R} \sqrt{(a_1 + i(z - ct'))(a_2 - i(z + ct'))} \right] ,$$

$$F_1(t') = K_0 \left[\frac{\kappa_{0m}}{R} \sqrt{(a_1 + i(z - ct'))(a_2 - i(z + ct'))} \right]$$

and

$$ct' = ct - \hat{z} - \frac{R^2}{2\hat{z}} \ .$$

Using the identity $K_0'(z) = -K_1(z)$, the result (3.3.20) can be reduced to the following form:

$$\Psi(0,0,\hat{z},t) = -\frac{iJ_1(\kappa_{0m})\,R}{8\pi\,\hat{z}}\ K_1\Big[\ \frac{\kappa_{0m}}{R}\sqrt{(a_1 + i(L-ct'))(a_2 - i(L+ct'))}\ \Big] \times \frac{a_2 - i(L+t')}{\sqrt{(a_1 + i(L-ct'))(a_2 - i(L+ct'))}} \ . \tag{3.3.21}$$

At the center of the pulse (i.e., $\hat{z} - ct + L = 0$), the wave amplitude becomes

$$\Psi(0,0,\hat{z},t) = -\frac{iJ_1(\kappa_{0m})\,R}{8\pi\,\hat{z}}\ K_1\Big[\ \frac{\kappa_{0m}}{R}\sqrt{(a_1 + i\frac{R^2}{2\hat{z}})(a_2 - i(2L - \frac{R^2}{2\hat{z}}))}\ \Big] \times \frac{a_2 - i(2L - \frac{R^2}{2\hat{z}})}{\sqrt{(a_1 + i\frac{R^2}{2\hat{z}})(a_2 - i(2L - \frac{R^2}{2\hat{z}}))}} \ . \tag{3.3.22}$$

As discussed in Section 3.2, one can choose the condition $\kappa_{0m}\sqrt{(a_1 + iR^2/2\hat{z})a_2}\ /R << 1$. If, furthermore, $a_2 >> L$, an asymptotic expansion for small arguments yields $K_1(z) \simeq z^{-1}$ [49]. Under these restrictions, (3.3.22) becomes

$$\Psi(0,0,\hat{z},t) \simeq \frac{-\,iJ_1(\kappa_{0m})\,R^2}{4\pi\,\kappa_{0m}}\ \frac{1}{(2a_1\,\hat{z} + i\,R^2)} \ , \tag{3.3.23}$$

or, after rearranging the terms,

$$\Psi(0,0,\hat{z},t) \simeq \frac{J_1(\kappa_{0m})}{4\pi\,\kappa_{0m}}\ \frac{R^2\ e^{-i\phi}}{\sqrt{(2a_1\,\hat{z})^2 + R^4}} \ , \tag{3.3.24}$$

with $\phi = \tan^{-1} \frac{R^2}{2a_1 z} + \frac{\pi}{2}$. This result is interesting because, for $a_1 << 1$, the real part of the solution given by (3.3.24) does not decay for $2a_1\hat{z} << R^2$, and is given approximately by

$$Re\{\Psi(0,0,\hat{z},t)\} \simeq \frac{J_1(\kappa_{0m})}{4\pi\kappa_{0m}} \cos\phi \tag{3.3.25}$$

for

$$\hat{z} < \frac{R^2}{2a_1} . \tag{3.3.26}$$

Combining equations (3.3.26) and (3.3.18), the range of validity of the approximate solution (3.3.24) can be stated as follows:

$$1000 \frac{R}{\kappa_{0m}} < \hat{z} < \frac{R^2}{2a_1} . \tag{3.3.27}$$

Note that the lower bound in equation (3.3.27) may not be strong enough to ensure the validity of the condition $\kappa_{0m}\sqrt{(a_1 + iR^2/2\hat{z})\, a_2} \;/\; R << 1$. This can occur when $\hat{z}$ is fairly small; in that case we can set the limit

$$\frac{\kappa_{0m}}{R} \sqrt{(a_1 + \frac{iR^2}{2\hat{z}})\, a_2} < 0.1 ,$$

and for $a_1 << 1$ the range given by equation (3.3.27) has to be modified to

$$\frac{\kappa_{0m}^2 a_2}{.02} < \hat{z} < \frac{R^2}{2a_1} . \tag{3.3.28}$$

The values of the different parameters will determine the correct range. Choose, for example, $\kappa_{0m}/R \simeq O(1)$, $a_2 = 5\text{m}$ and $a_1 << 1$. This choice of parameters is typical for a waveguide a few meters long, with an openning of radius equal to one meter and with mainly the first mode excited.

In this case, $1000R/\kappa_{0m} = \kappa_{0m}^2 a_2/0.02 \simeq 1000$ and both ranges are identical. On the other hand, if higher modes are excited, the range (3.3.28) is valid, while the range (3.3.27) is correct if a waveguide of a larger radius is used.

The solution given in (3.3.24) has the unusual feature of hiding the $\hat{z}$ parameter within the $(2a_1\hat{z})^2 + R^4$ term since, for a small a_1, the effect of $\hat{z}$ does not appear until $2a_1\hat{z}$ takes over the R^4 term. This feature is shared by the EDEPT solutions of Ziolkowski [9,16]. As mentioned earlier, such solutions contain certain parameters that can be adjusted in order to slow down their decay. (For the semi-infinite waveguide, the parameters a_1 and a_2 are related directly to physical quantities, e.g., the amplitude of the initial pulse and its bandwidth.) Such behavior is not possible for the more conventional solutions. A good example along this direction is the following solution to the infinite waveguide problem [52]

$$\Psi(\vec{r}, t) = J_0\left(\frac{\kappa_{0m}\rho}{R}\right) J_0\left[\frac{\kappa_{0m}}{R}\sqrt{c^2t^2 - z^2}\right] u(ct - z) . \tag{3.3.29}$$

It consists of a pulse travelling in the positive z-direction with amplitude $J_0\left(\frac{\kappa_{0m}\rho}{R}\right)$ at $z = ct$. An analysis analogous to that followed earlier in this section results in equation (3.3.20) with

$$F_2(t') = \partial_z\left(J_0\left[\frac{\kappa_{0m}}{R}\sqrt{c^2t'^2 - z^2}\right] u(ct' - z)\right)$$

and

$$F_1(t') = J_0\left[\frac{\kappa_{0m}}{R}\sqrt{c^2t'^2 - z^2}\right] u(ct' - z) .$$

Using the identity $J_0'(z) = -J_1(z)$ and carrying out the differentiations, one obtains

$$\hat{\Psi}(0,0,z,t)=\frac{J_1(\kappa_{0m})\,R^2}{2\kappa_{0m}\,\hat{z}}\left[J_1\left[\frac{\kappa_{0m}}{R}\sqrt{c^2t'^2-L^2}\right]u(ct'-L)\,\frac{\kappa_{0m}}{R}\,\frac{(ct'+L)}{\sqrt{(ct'-L)(ct'+L)}}\right.$$
$$\left.+\,2J_0\left[\frac{\kappa_{0m}}{R}\sqrt{c^2t'^2-L^2}\right]\delta(ct'-L)\right]. \tag{3.3.30}$$

If the peak of the pulse is taken at $ct'=L$, and one recalls that $J_1(z)$ behaves as $z/2$ for small arguments, the above expression can be approximated around its peak as follows:

$$\hat{\Psi}(0,0,z,t)=\frac{J_1(\kappa_{0m})\,R^2}{2\kappa_{0m}\,\hat{z}}\left[\frac{\kappa_{0m}^2}{R^2}\cdot 2L+2\;\delta(0)\right]. \tag{3.3.31}$$

It is seen that the wave amplitude dies off as $\hat{z}^{-1}$, even for higher modes. The unusual behavior observed earlier in connection with our original problem does not show up in this case. It should be pointed out that the $\delta(0)$ term appears in (3.3.31) because of the discontinuity in the pulse amplitude at $z=ct$.

3.4 *SUMMARY AND CONCLUSION*

It was demonstrated in this chapter that Brittingham-like pulsed solutions can be realized physically. Such pulses can be fairly localized in a waveguide and the parameters arising within the context of their solution can be related to physically meaningful quantities. Travelling down the waveguide, which is highly dispersive, these pulses have unusual decay patterns. Basically, the waveguide can be divided into three regions, with the center of the pulses undergoing no decay in the first, a logarithmic decay in the second, and an exponential decay in the last portion. When launched in free space, these pulses were shown to have finite energy, to be causal and to exhibit

an unusual decay pattern. (A similar behavior was not exhibited by other, more conventional solutions even if higher modes where used.)

Although the decay properties of the pulses studied here are similar to Wu's electromagnetic missiles [33], the approach adopted in our work is quite different, mainly because it is of the Brittingham-Ziolkowski type. There are additional differences: (1) the missile solutions are restricted to TE_{01} modes only, whereas the solutions presented in this thesis can incorporate a larger number of modes; (2) Wu analyzed the Poynting vector integrated over time and over the surface of a receiver located at variable distances, while in our analysis we dealt with peak field intensities along the line of sight of the aperture; (3) our pulses are initiated in a Cauchy initial-value fashion, with $\Psi(\vec{r}, 0)$ and $\Psi_t(\vec{r}, 0)$ specified, while in Wu's work the pulses are initiated with a rising edge proportional to $t^{\varepsilon/2}$, with $\varepsilon < 1$. The parameter ε is related directly to the slowness of the energy decay of the missiles. As a consequence, a pulse with a sharper rising edge will give a missile that decays at a slower rate as the distance to the receiver increases; in contrast, our solutions pertain to bounded distances depending primarily on the parameter a_1. In spite of these differences, it seems that the two approaches are pointing out to the same underlying physical reality that needs to be investigated further.

The usual R^{-1} decay of a signal in the far field of an antenna calls upon defining some limit that separates the far from the near field. A very popular candidate is the Fresnel limit which is defined as $2D^2/\lambda$, where D is a characteristic dimension of the aperture and λ is a characteristic wave length of the signal. Such a definition has been developed primarily for monochromatic or modulated signals with a very narrow bandwidth. In the case of time-limited pulses, a characteristic wavelength λ has no meaning since, by definition, such pulses have virtually an infinite bandwidth. As a consequence, the notion of a Fresnel limit is very ambiguous, and a clear distinction between a far and a near field is not possible. Because of such ambiguities one can only compare different types of pulses with each other. Our work has shown that certain types of pulses can spread much more slowly than others as they propagate in free space. These results point out to the fact that techniques and ideas used to handle the transmission of CW signals might not be adequate in cases where time-limited pulses are involved, and call for the undertaking of a serious theoretical and

experimental study of the propagation of pulses in free space. The hope is to establish that one can physically generate certain time-limited pulses which spread out at a much slower rate than CW signals.

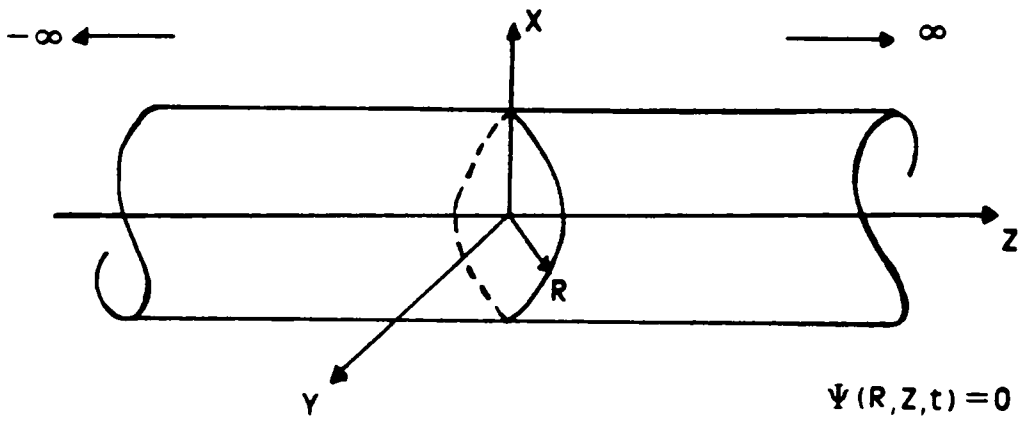

Figure 3.1 The infinite waveguide.

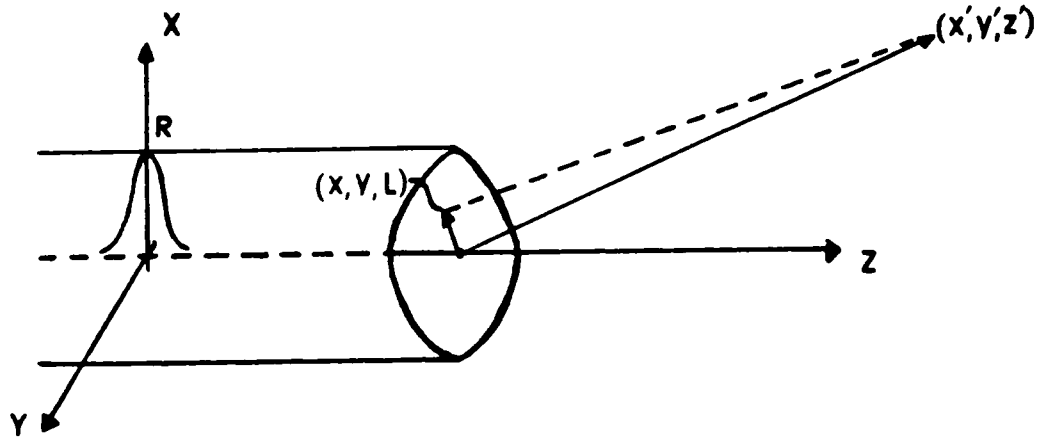

Figure 3.2 The semi-infinite waveguide.

4.0 THE FWM PULSE AND THE WAVE-PARTICLE DUALITY OF LIGHT

In this chapter we would like to investigate the possibility of using Brittingham-like solutions to represent light particles. It is a well established fact that a finite energy pulse solution to a linear partial differential equation has to spread out [6]. If such a solution is used to model a particle, the aforementioned limitation stresses the importance of the notion of the total energy content of a particle over its localization. On the other hand, one can regard the nondispersive character of particles (including light particles) as a more fundamental property. In this respect the total energy content can be foresaken and a continuous, nonsingular, nondispersive bump solution can be used. This field, which may not have a finite total energy content, consists of a central bump of a very large amplitude in comparison to its tails. The tails can provide the total field with a nonlocal character that should be contrasted with the localization of the central bump. For such a field the localized bump can be used to represent a particle, while the rest of the field will behave as a wave. Since the field exists everywhere, it depends on the configuration of an experimental setup. This endows individual microphysical processes with a nonlocal character, even if the size of the measuring devices and the separation between them are much larger than the extension of the central bump, i.e., much larger than the particle under consideration. This kind of nonlocality is reflected

in several quantum processes. Recent experiments [53-55] have confirmed this nonlocal character of the microphysical world. The simplest and most famous experiment that demonstrates such a nonlocal behavior is Young's two slit interference experiment. This experiment has been considered to be the most fundamental realization of quantum phenomena. According to Feynman [56] it is "... a phenomenon which is impossible, *absolutely* impossible, to explain in any classical way, and which has in it the heart of quantum mechanics. In reality it contains the *only* mystery."

In Young's two slit experiment single light particles or photons passing through a screen will end up on a photographic plate behind the screen as dots on the fringes of an interference pattern. At very low intensities, the photons go through the screen one at a time; as a result, there is no interaction between them. Therefore, a single photon of dimensions much smaller than the width of the slits must interfere with itself (i.e., must interact with both slits of the screen) to reproduce the interference pattern. In this chapter it will be shown that the FWM solution can be used to represent photons. It will be demonstrated that a single FWM pulse can interfere with itself. This is not the case for other localized pulses, e.g., a transverse Gaussian pulse. As discussed earlier, the central field can be chosen to represent the light particle which is incorporated in an extended wave structure of a very low intensity; the wave and particle aspects are, thus, combined in a single framework.

4.1 BACKGROUND MATERIAL

In 1905, Einstein [57] proposed that energy in a light beam is carried out by localized wave packets or photons. that hypothesis was introduced to explain the photoelectric effect. The idea that light can have a corpuscular nature and that photons can carry momentum and can be scattered off other massive particles like billiard balls, is in sharp contrast with Maxwell's electromagnetic wave theory. Maxwell's theory was very successful in accounting for all wave properties of light, e.g. refraction, diffraction and interference phenomena. One of the first experiments to confirm the

wave nature of light was Young's two slit experiment. In such an experiment, light is shone on a screen containing two narrow slits and it is observed on a photographic plate placed behind the screen. Because of the path difference between light waves passing through either slit, waves arriving at the photographic plate can either interfere constructively or destructively to form the interference fringes. Maxwell's theory, however, is incapable of explaining the photoelectric effect, whereby a beam of light incident on some materials knocks off electrons with an energy that does not depend on the intensity of the beam, but rather on its frequency. Higher intensities will only knock off a larger number of electrons. This unusual behavior led Einstein to introduce the concept of a light corpuscle or "photon" that carries an energy equal to $h\nu$, where h is Planck's constant and ν is the frequency of the light. This gave birth to the notion of a wave-particle duality. This concept was further encouraged by another dramatic development which took place in the early twenties. At that time de Broglie [30] hypothesized that a massive particle has a wave character associated with it. He proposed that such a particle wave has a wave length $\lambda = h/p$, where p is the momentum of the particle. This idea was confirmed experimently by showing that a two slit interference pattern can be obtained for a beam of electrons. This development broke completely the psychological barrier separating particles and waves, thus, firmly establishing their duality.

One attempt to explain how particles can form an interference pattern was based on the idea that a large number of particles interact with each other in such a way that most of them end up on the light fringes. This idea was proven incorrect in interference experiments with beams of extremely low intensities, in which only one particle went through the screen at any time. In that case the particle interactions were absent; nevertheless, the particles always ended up on one of the light fringes. After a long period of time an interference pattern was formed. Consequently, the interference was not caused by the interaction between the particles, but rather by the interference of a single particle (e.g., a photon) with itself through the presence of the two slit screen. The notion of a photon interfering with itself seems quite preplexing because a particle is always associated, in our minds, with a localized structure that has dimensions much smaller than the width of the slits, or the separation between them. If this was the case, a particle passing through one slit would in no way feel the presence of the other opening.

It is well known, on the other hand, that an interference pattern is formed only if the field is symmetrically distributed over the two slits. If a particle is then represented by a structure that stays localized for all points in space-time, it will never be symmetric with respect to the two slits. Consequently, an interference pattern will not be formed by the scattering of a localized packet from the two slit screen. This need for the field to be symmetrically distributed over both openings led to the idea that the photon might split into two parts, each part going through a different slit. These parts would interfere with each other, thus reproducing the interference pattern. However, photon detectors placed behind the two slits indicated that the photon passes through only one of the slits.

These dichotomies led to a construction which is at the foundation of quantum mechanics. The now accepted explanation of the two slit experiment is a probabilistic one where the photon is represented by the superposition of two abstract wave functions, these are the two eigenstates associated with the passage of the particle through either one of the two slits. The total probabilistic field is, thus symmetric over the two openings; and beyond the screen, the probability of detecting the photons forms a probabilistic interference pattern. Then, according to the Copenhagen interpretation [3] of the quantum theory: (1) a measurement carried out by the photographic plate will collapse the wave function onto a dot on one of the light fringes where the probability of having a photon is not zero, and (2) detectors placed behind the screen will collapse the wave function onto one of its eigenstates, destroying the interference pattern and forcing the photon to appear as though it had passed through one of the two slits.

Although Copenhagen interpretation is capable of explaining the results of Young's experiment, it has led to several paradoxes, especially in connection with causality and in relation to the mechanism of the collapse of the wave function. The orthodox interpretation of quantum mechanics asserts that this probabilistic explanation provides the most complete and the only possible description of reality. This means that the statistical laws of quantum mechanics are incompatible with the possibility of deeper laws governing individual processes, implying, hence, that there is no way to produce a nonstatistical model which can explain the phenomenon described above.

It is our aim in this chapter to point out that Brittingham's FWM solution [1] to Maxwell's equations can interfere with itself and, at the same time, can accommodate the wave and particle

properties of light. The results of this chapter are derived from the scalar form of the FWM given in equation (2.1.2), viz.,

$$\Psi(\vec{r}, t) = \frac{A(\beta)}{4\pi\,(a_1 + i(z - ct))}\; e^{-\beta\rho^2/(a_1 + i(z-ct))}\, e^{i\beta(z+ct)} . \qquad (4.1.1)$$

Even though this model does not incorporate polarization effects directly, the following analysis can be readily extended to the full electromagnetic situation. In equation (4.1.1), the parameter β is considered to be a characteristic wave number and a_1 is a constant. As demonstrated in Chapter 2, this solution consists of a Gaussian envelope of a waist $w = (a_1/\beta)^{1/2}$ moving in the positive z-direction, modulated by a plane wave moving in the opposite direction. The envelope travels in free space with the speed of light in a straight line, it does not disperse for all time, it is continuous and it has a finite energy density everywhere. The behavior of the FWM solution depends largely on the quantity βa_1 . It was shown in Section 2.4.1 that for $\beta a_1 >> 1$, $\Psi(\vec{r}, t)$ degenerates into a nonlocalized sinusoidal function travelling in the negative z-direction. On the other hand, for a_1 very small, such that $\beta a_1 << 1$, the FWM solution behaves like a localized pulse moving in the positive z-direction with speed c. In terms of the waist $w = (a_1/\beta)^{1/2}$, the above condition reduces to $w << 1/\beta$. For a photon of a wavelength $\lambda = 2\pi/\beta$, this condition becomes $w << \lambda$. Thus, for $\Psi(\vec{r}, t)$ to represent a localized light pulse (a photon) its waist must be much smaller than the characteristic wavelength of the wave structure associated with it. In what follows, it should be understood that the condition $\beta a_1 << 1$ is imposed whenever we refer to the FWM solution as the FWM "pulse".

There is a sharp contrast between this wave packet picture and other reperesentations of photons as wave packets formed by a superposition of wavelets of various wavelengths. Usually the constructed wave packets have dimensions much larger than the wavelengths of the constituent wavelets [58,59]. In such cases, one ends up with photons of extensions up to several meters along the direction of propagation. This causes severe problems for the explanation of interactions of such photons with other elementary particles of dimensions of order 10^{-15} m. Furthermore, the afore-mentioned superpositions are usually carried over wave numbers; as a result, the constructed wave

packets do not have any characterisitic wave numbers associated with them. In contrast, the FWM solution *has* the characteristic wave number β.

The FWM pulse is only localized near its center ($z - ct < a_1$ and $\rho < (a_1/\beta)^{1/2}$) where the field has a very large amplitude proportional to $1/a_1$ that falls off exponentially in the transverse direction and as $1/(z - ct)$ in the direction of propagation. Far away from the center of the pulse, for $z - ct >> a_1$, the amplitude of the field diminishes significantly. At the same time, the Gaussian envelope stretches out in the transverse direction to a waist equal to $(z - ct)/(\beta a_1)^{1/2}$. This fanning out of the amplitude to cover larger distances in the transverse direction as we move away from the center allows the FWM to feel both slits in Young's experiment. As such a pulse approaches the two slits, the small amplitude precursor field will be symmetrically distributed over the two slits. When the pulse passes through the screen, it will be guided by its diffracted precursor field to end up on one of the light fringes. This picture of a photon is nonlocal and consists of a bump field with a very large amplitude around its center. Its amplitude diminishes to very low values away from the center in such a way that the energy densities are too small to be detected, i.e., the fields in the tails are so small that their interactions with other particles (e.g., electrons) is unobservable. The central field, thus, can represent a compact light particle or a photon which is incorporated in an extended nonlocal wave structure. This conception of the photon is compatible with the wave particle duality advocated by de Broglie [30] who hypothesized that particles have wave structures associated with them and that the particle and wave aspects of matter should exist simultaneously. It also reflects Einstein's position that particles are manifestations of a highly dense concentration of some field, a "bunch" field, as he called it. This "bunch" field stays localized and does not spread out in free motion. These ideas are in sharp contrast with Bohr's "complementarity principle" which perceives the wave and particle natures of microevents as two complementary characters that manifest themselves in different situations. According to his interpretation, the wave and corpuscular aspects cannot exist simultaneously.

As mentioned earlier, the FWM pulse is an exact solution to the wave and Maxwell's equations. Thus, its field is a classical entity and it is not just an abstract wave function that gives only information about the probability of the outcome of a measurement procedure. Consequently,

we can trace a trajectory for the pulse, at least for its center, and we can restore the causality and the continuity of the measurement process that was abandoned in the Copenhagen interpretation of the quantum theory.

In the next sections we shall rederive the interference pattern for a plane wave using a spectral procedure which is capable of accomodating pulses of complex spectral content (e.g., the FWM pulse). The same analysis will be repeated for a transverse Gaussian pulse of an extension much smaller than the width of the slits. Since the field of such a pulse is not symmetrically distributed over both slits, it will not produce an interference pattern. In contradistinction, it will be established that a FWM pulse can interfere with itself through the mediation of the two slit screen. The energy and momentum content of the particle-like central portion of the FWM pulse will be calculated and the Lorentz invariance of the energy and momentum expressions will be demonstrated. Finally, possibilities of experimental verification will be discussed and a concise comparison between the consequences of our results and different interpretations of quantum mechanics will be given.

4.2 THE PLANE WAVE

In this section we will consider the case of a plane wave incident on a screen containing two narrow slits. The screen is placed at $z = 0$ along the transverse y-axis and the two openings are modelled by a pair of Gaussian slits of width $2b$ situated at $y = \pm d$, viz.,

$$S(y) = \frac{1}{2\sqrt{\pi}\, b}\left[e^{-(y-d)^2/2b^2} + e^{-(y+d)^2/2b^2}\right]. \tag{4.2.1}$$

The photographic plate is placed at $z = L$. This 2-D setup is shown in Figure 4.1. The plane wave incident on the screen can be represented by the 2-D function

$$\Psi_{inc}(y, z, t) = \Psi_0 \, e^{-i(k_1 z + k_2 y - \omega t)} \, . \tag{4.2.2}$$

For a wave propagating mainly in the z-direction, we have $k_1 >> k_2$. An interference pattern can be derived directly by making use of $\Psi_{inc}(y, z, t)$ given in equation (4.2.2). A more involved spectral procedure is needed in order to accomodate the complex spectral content of the FWM, as will be shown in Section 4.4. For such a purpose, $\Psi_{inc}(y, z, t)$ can be expressed in terms of the following synthesis:

$$\Psi_{inc}(y, z, t) = \frac{1}{(2\pi)^2} \int_{-\infty}^{+\infty} dk_y \int_{-\infty}^{+\infty} dk_z \int_0^{\infty} d\omega \, \Phi_{inc}(k_y, k_z, \omega) \, e^{-i(k_y y + k_z z)} \, e^{i\omega t} \times \delta[\omega - c(k_y^2 + k_z^2)^{1/2}] \, . \tag{4.2.3}$$

The plane wave given in equation (4.2.2) results from the spectrum

$$\Phi_{inc}(k_y, k_z, \omega) = (2\pi)^2 \, \Psi_0 \, \delta(k_z - k_1) \, \delta(k_y - k_2) \, . \tag{4.2.4}$$

The spectral components of the field beyond the screen can be obtained by convolving the spectrum given in equation (4.2.4) with the spatial spectral content of the screen transfer function $\hat{S}(k_y)$ obtained by the Fourier transformation of $S(y)$, viz.,

$$\hat{S}(k_y) = \frac{1}{\sqrt{2}} \, [e^{ik_y d} + e^{-ik_y d}] e^{-b^2 k_y^2/2} \, . \tag{4.2.5}$$

Carrying out the indicated operation, it follows that

$$\Phi_{out}(k_y, k_z, \omega) = \frac{1}{2\pi} \int_{-\infty}^{+\infty} dk'_y \, (2\pi)^2 \, \Psi_0 \, \delta(k_z - k_1) \, \delta(k_y - k'_y - k_2) \, \frac{1}{\sqrt{2}} \, [e^{ik'_y d} + e^{-ik'_y d}] e^{-b^2 k'^2_y/2} \, .$$

The integration over k'_y gives the spectrum

$$\Phi_{out}(k_y, k_z, \omega) = \frac{2\pi}{\sqrt{2}} \Psi_0 \, \delta(k_z - k_1) \left[e^{i(k_y - k_2)d} + e^{-i(k_y - k_2)d} \right] e^{-b^2(k_y - k_2)^2/2} \quad , \qquad (4.2.6)$$

which upon substitution into a synthesis similar to (4.2.3), results in the following wave function:

$$\Psi_{out}(y, z, t) = \frac{1}{(2\pi)^2} \int_{-\infty}^{+\infty} dk_y \int_{-\infty}^{+\infty} dk_z \int_0^{\infty} d\omega \, \frac{2\pi}{\sqrt{2}} \Psi_0 \, \delta(k_z - k_1) \left[e^{i(k_y - k_2)d} + e^{-i(k_y - k_2)d} \right]$$
$$\times e^{-b^2(k_y - k_2)^2/2} \, e^{-i(k_y y + k_z z)} \, e^{i\omega t} \, \delta[\omega - c(k_y^2 + k_z^2)^{1/2}] \, .$$

In the above superposition we have made use of the fact that the screen is placed at $z = 0$ and we have assumed that the plane wave reaches the screen at time $t = 0$. The integration over k_z and ω yields

$$\Psi_{out}(y, z, t) = \frac{\Psi_0 e^{-ik_1 z}}{2\sqrt{2}\,\pi} \int_{-\infty}^{+\infty} dk_y \, e^{-ik_y y} \, e^{i(k_1^2 + k_y^2)^{1/2} ct} \left[e^{i(k_y - k_2)d} + e^{-i(k_y - k_2)d} \right] e^{-b^2(k_y - k_2)^2/2} \quad (4.2.7)$$

It should be noted that the integrand is a Gaussian centered around $k_y = k_2$ with a bandwidth of order b^{-1}, multiplied by oscillatory terms. For $k_1 >> (k_2 + b^{-1})$, the argument $i(k_1^2 + k_y^2)^{1/2} ct$ can be approximated by $i(k_1 + (k_y^2/2k_1))ct$. For a wave predominantly moving in the z-direction we have $k_2 << k_1$, and the earlier condition becomes $k_1 >> b^{-1}$. In a typical two slit light interference experiment the width of the slits $2b$ and the separation between them $2d$ can have the values 10^{-5} m and 10^{-4} m, respectively. For the wavelength $\lambda \simeq 2\pi/k_1$, the above approximation is valid when $\lambda << 6 \times 10^{-5}$ m, which is quite satisfactory if we recall that for visible light $\lambda = 4 - 8 \times 10^{-7}$ m . In what follows, we will choose k_1 to be equal to 10^7 m^{-1}. Incorporating the indicated approximation, the integral in equation (4.2.7) reduces to

$$\Psi_{out}(y, z, t) = \frac{\Psi_0 e^{-ik_1 z}}{2\sqrt{2}\,\pi} \int_{-\infty}^{+\infty} dk_y \, e^{-ik_y y} \, e^{i(k_1 + (k_y^2/2k_1))ct} \left[e^{i(k_y - k_2)d} + e^{-i(k_y - k_2)d} \right] e^{-b^2(k_y - k_2)^2/2} \, .$$

The integration over k_y yields

$$\Psi_{out}(y, z, t) = \frac{\Psi_0}{2}\, e^{-ik_1(z-ct)}\, \frac{e^{-k_2^2 b^2/2}}{\sqrt{\pi\Delta}} \left[e^{-ik_2 d}\, e^{-(y-d+ib^2k_2)^2/2\Delta} + e^{ik_2 d}\, e^{-(y+d+ib^2k_2)^2/2\Delta} \right], \quad (4.2.8)$$

where $\Delta = b^2 - ict/k_1$. Since we have assumed that the plane wave goes through the screen at time $t = 0$, it will reach the photographic plate at $z = ct_L = L$. For k_2 extremely small (i.e. $k_2 \simeq 0$), the field $\Psi_{out}(y, L, t_L)$ at the photographic plate becomes

$$\Psi_{out}(y, L, t_L) = \frac{\Psi_0}{2[\pi(b^2 - iL/k_1)]^{1/2}} \left[e^{-(y-d)^2/2(b^2 - iL/k_1)} + e^{-(y+d)^2/2(b^2 - iL/k_1)} \right].$$

If $L^2/k_1^2 >> b^4$, which is the case for $b \simeq 10^{-5}$ m , $k_1 \simeq 10^7$ m^{-1} and $L = 0.2$ m, the square of the amplitude of the field at the photographic plate can be approximated by

$$|\Psi_{out}(y, L, t_L)|^2 = \frac{\Psi_0^2 k_1}{\pi L}\, e^{-k_1^2 b^2 (y^2 + d^2)/L^2} \cos^2(k_1 dy/L) . \quad (4.2.9)$$

The energy density of this field is proportional to $|\Psi_{out}|^2$ and will vary as $\exp(-k_1^2 b^2 y^2/L^2)$ $\cos^2(k_1 dy/L)$. This gives the all familiar interference pattern of width

$$\Delta y \simeq \frac{L}{bk_1} , \quad (4.2.10)$$

with the distance separating the fringes equal to

$$\delta y = \frac{\pi L}{dk_1} . \quad (4.2.11)$$

We are, therefore, capable of reproducing the usual interference pattern using a k-space formulation that makes use of the spectral content of the incident signal, together with that of the screen containing the two slits. Although this procedure is trivial in the case of the plane wave, it is extremely valuable when we have to deal with pulses of more complex spectral content like the transverse Gaussian pulse and the FWM pulse. The latter two will be dealt with in the next two sections.

4.3 THE TRANSVERSE GAUSSIAN PULSE

The procedure developed in the previous section will be applied to a transverse Gaussian pulse that can be obtained from a slight modification of the plane wave spectrum given in equation (4.2.4), viz.,

$$\Phi_{\text{inc}}(k_y, k_z, \omega) = (2\pi)^{3/2}\, \varepsilon\, \Psi_0\, \delta(k_z - k_1)\, e^{-\varepsilon^2(k_y - k_2)^2/2}\, e^{i(k_y - k_2)y_0}\,. \tag{4.3.1}$$

In the limit $\varepsilon \to \infty$ this spectrum reduces to that of a plane wave. The parameter y_0 determines the center of the pulse, while ε determines its width. This can be shown by substituting the spectrum given in (4.3.1) into equation (4.2.3) to get

$$\Psi_{\text{inc}}(y, z, t) = \frac{1}{(2\pi)^2} \int_{-\infty}^{+\infty} dk_y \int_{-\infty}^{+\infty} dk_z \int_0^{\infty} d\omega\, (2\pi)^{3/2}\, \varepsilon\, \Psi_0\, \delta(k_z - k_1)\, e^{-\varepsilon^2(k_y - k_2)^2/2}\, e^{i(k_y - k_2)y_0} \times e^{-i(k_y y + k_z z)}\, e^{i\omega t}\, \delta[\omega - c(k_y^2 + k_z^2)^{1/2}]\,.$$

The integrations over ω and k_z yield

$$\Psi_{\text{inc}}(y, z, t) = \frac{\varepsilon \Psi_0}{\sqrt{2\pi}}\, e^{-ik_1 z} \int_{-\infty}^{+\infty} dk_y\, e^{-\varepsilon^2(k_y - k_2)^2/2}\, e^{i(k_y - k_2)y_0} e^{-ik_y y}\, e^{i(k_y^2 + k_1^2)^{1/2} ct}\,. \tag{4.3.2}$$

If we assume that the pulse reaches the screen at $t = 0$, the integration in equation (4.3.2) can be carried out explicitly to give the field

$$\Psi_{\text{inc}}(y, 0, 0) = \Psi_0 \, e^{-ik_2 y} \, e^{-(y-y_0)^2/2\varepsilon^2}, \tag{4.3.3}$$

which is a Gaussian pulse of width $\sim 2\varepsilon$ when it is going through the screen. It should be pointed out that the width of such a pulse is not constant but it spreads out with time. By specifying that the pulse reaches the screen at $t = 0$, we have chosen its width to equal $2\varepsilon << 2b$ as it passes through the screen. To find $\Phi_{\text{out}}(k_y, k_z, \omega)$ beyond the screen we have to convolve the spectrum (4.3.1) with $\hat{S}(k_y)$ given in equation (4.2.5); specifically,

$$\Phi_{\text{out}}(k_y, k_z, \omega) = \frac{1}{2\pi} \int_{-\infty}^{+\infty} dk'_y \, (2\pi)^{3/2} \, \varepsilon \, \Psi_0 \, \delta(k_z - k_1) \, e^{-\varepsilon^2(k_y - k'_y - k_2)^2/2} \, e^{i(k_y - k'_y - k_2)y_0} \times \frac{1}{\sqrt{2}} \left[e^{ik'_y d} + e^{-ik'_y d} \right] e^{-b^2 k'^2_y/2}.$$

Upon integration we get

$$\Phi_{\text{out}}(k_y, k_z, \omega) = \frac{\sqrt{2}\,\pi\varepsilon\,\Psi_0}{(b^2 + \varepsilon^2)^{1/2}} \, \delta(k_z - k_1) \, e^{i(k_y - k_2)y_0} \left[e^{i\varepsilon^2(d - y_0)(k_y - k_2)/(b^2 + \varepsilon^2)} \, e^{-(d - y_0)^2/2(b^2 + \varepsilon^2)} + e^{-i\varepsilon^2(d + y_0)(k_y - k_2)/(b^2 + \varepsilon^2)} \, e^{-(d + y_0)^2/2(b^2 + \varepsilon^2)} \right] e^{-\varepsilon^2 b^2 (k_y - k_2)^2/2(b^2 + \varepsilon^2)}. \tag{4.3.4}$$

The wave function beyond the screen can be obtained by substituting equation (4.3.4) into a superposition similar to that given in equation (4.2.3). After carrying out the integrations over k_z and ω, it follows that

$$\Psi_{\text{out}}(y, z, t) = \frac{\varepsilon \, \Psi_0 \, e^{-ik_1 z}}{2^{3/2}\pi(b^2 + \varepsilon^2)^{1/2}} \int_{-\infty}^{+\infty} dk_y \, e^{i(k_y - k_2)y_0} \, e^{-\varepsilon^2 b^2 (k_y - k_2)^2/2(b^2 + \varepsilon^2)} \, e^{-ik_y y} \, e^{i(k_y^2 + k_1^2)^{1/2} ct} \times \left[e^{i\varepsilon^2(d - y_0)(k_y - k_2)/(b^2 + \varepsilon^2)} \, e^{-(d - y_0)^2/2(b^2 + \varepsilon^2)} + e^{-i\varepsilon^2(d + y_0)(k_y - k_2)/(b^2 + \varepsilon^2)} \, e^{-(d + y_0)^2/2(b^2 + \varepsilon^2)} \right]. \tag{4.3.5}$$

As mentioned earlier, we are interested in pulses with extensions much smaller than the width of the slits (i.e., $\varepsilon << b$); thus, ε^2 can be neglected compared to b^2 and equation (4.3.5) can be re-written in the form

$$\Psi_{\text{out}}(y, z, t) = \frac{1}{2\sqrt{\pi}\,(b^2 + \varepsilon^2)^{1/2}} \left[I_1\, e^{-(d - y_0)^2/b^2} + I_2\, e^{-(d + y_0)^2/b^2} \right], \qquad (4.3.6a)$$

where

$$I_1 = \frac{\varepsilon \Psi_0}{\sqrt{2\pi}}\, e^{-ik_1 z} \int_{-\infty}^{+\infty} dk_y\, e^{-\varepsilon^2 (k_y - k_2)^2/2}\, e^{i(k_y - k_2)(y_0 + (\varepsilon^2/b^2)d)}\, e^{-ik_y y}\, e^{i(k_y^2 + k_1^2)^{1/2} ct}, \qquad (4.3.6b)$$

$$I_2 = \frac{\varepsilon \Psi_0}{\sqrt{2\pi}}\, e^{-ik_1 z} \int_{-\infty}^{+\infty} dk_y\, e^{-\varepsilon^2 (k_y - k_2)^2/2}\, e^{i(k_y - k_2)(y_0 - (\varepsilon^2/b^2)d)}\, e^{-ik_y y}\, e^{i(k_y^2 + k_1^2)^{1/2} ct}. \qquad (4.3.6c)$$

There is no need to evaluate these integrals, because of their resemblence to those given in equation (4.3.2) representing the incident pulse. A comparison of these integrals shows that I_1 and I_2 represent Gaussian pulses of waists equal to 2ε at $t = 0$. At the later time $ct_L = L$, when the pulse reaches the photographic plate, I_1 and I_2 still represent Gaussian pulses, but with waists slightly larger than 2ε, and their centers slightly shifted to $y_0 \pm (\varepsilon^2/b^2)d$. These pulses are multiplied by the two factors $\exp[-(d - y_0)^2/2b^2]$ and $\exp[-(d + y_0)^2/2b^2]$ which determine the slit through which the incident pulse will pass. This depends on the center of the pulse y_0. If $d - b < y_0 < d + b$, the pulse will go through the upper slit, and when $-d - b < y_0 < -d + b$, the pulse will go through the lower one. Outside these ranges the amplitude of the pulse is multiplied by exponentially small factors that can be taken equal to zero. At the photograhic plate, the pulse will interact with the emulsion producing a dot lying in front of either opening A or B and no diffraction pattern will be produced. This is the case because the field of the transverse Gaussian pulse is spatially limited for all space-time

points. Despite the fact that such a pulse has tails that extend to infinity in the transverse direction, its field is never symmetric with respect to the two slits unless it spreads out so much that its localized character disappears. As long as its waist is much smaller than $2b$, a transverse Gaussian pulse going through one of the slits will never feel the existence of the other one. Consequently, a beam of such pulses will never produce a diffraction pattern.

4.4 THE FWM PULSE

The procedure used in the previous section was a two dimensional one. Therefore, the 3-D FWM pulse given in equation (4.1.1) can not be used. The Fourier spectrum of the 3-D FWM solution was derived in Section 2.4.1. A slight modification of that procedure gives the spectrum of the 2-D FWM pulse; specifically,

$$\Phi_{\text{inc}}(k_y, k_z, \omega) = \frac{\pi A(\beta)}{(k_y^2 + k_z^2)^{1/2}}\, \delta[(k_y^2 + k_z^2)^{1/2} - k_z - 2\beta]\, e^{ik_y y_0}\, e^{-[(k_y^2 + k_z^2)^{1/2} + k_z]a_1/2}\,. \quad (4.4.1)$$

Substituting this spectrum into equation (4.2.3) gives the 2-D FWM

$$\Psi_{\text{inc}}(y, z, t) = \frac{A(\beta)}{4[\pi\beta\,(a_1 + i(z - ct))]^{1/2}}\, e^{-\beta(y - y_0)^2/(a_1 + i(z-ct))}\, e^{i\beta(z+ct)}\,, \quad (4.4.2)$$

where y_0 is the center of the incident pulse. Following the same procedure as before, the spectrum of the pulse beyond the screen is obtained by convolving the spectrum of the incident pulse with the transverse spectral distribution of the two slits $\hat{S}(k_y)$. This is carried out explicitly to give

$$\Phi_{out}(k_y, k_z, \omega) = \frac{1}{2\pi} \int_{-\infty}^{+\infty} dk'_y \, \frac{1}{\sqrt{2}} \, e^{-b^2(k_y - k'_y)^2/2} \left[e^{id(k_y - k'_y)} + e^{-id(k_y - k'_y)} \right]$$
$$\times \frac{\pi A(\beta)}{(k'^2_y + k_z^2)^{1/2}} \, \delta[(k'^2_y + k_z^2)^{1/2} - k_z - 2\beta] \, e^{ik'_y y_0} \, e^{-[(k'^2_y + k_z^2)^{1/2} + k_z] a_1/2} \, . \tag{4.4.3}$$

The field $\Psi_{out}(y, z, t)$ can be obtained by substituting the spectrum (4.4.3) into a synthesis similar to that given in equation (4.2.3), for which the center of the pulse reaches the screen at $t = 0$. After carrying out the integration over k_z and ω, it follows that

$$\Psi_{out}(y, z, t) = \frac{A(\beta)}{16\pi^2\sqrt{2}\,\beta} \int_{-\infty}^{+\infty} dk_y \int_{-\infty}^{+\infty} dk'_y \, e^{-b^2(k_y - k'_y)^2/2} \left[e^{id(k_y - k'_y)} + e^{-id(k_y - k'_y)} \right] \tag{4.4.4}$$
$$\times \, e^{-ik_y y} \, e^{ik'_y y_0} \, e^{-(k'^2_y/4\beta) a_1} \, e^{-i((k'^2_y/4\beta) - \beta) z} \, e^{i[((k'^2_y/4\beta) - \beta)^2 + k_y^2]^{1/2} ct} \, .$$

The waist of the pulse is taken to be much smaller than the width of the slits; i.e., $w = (a_1/\beta)^{1/2} << 2b$. Using the same parameters as in the case of the plane wave, we have $2b = 10^{-5}$ m, $2d = 10^{-4}$ m and $\beta = 10^7$ m^{-1} . The parameter a_1 can be chosen to be equal to 10^{-15} m^{-1} . In this case, the pulse width w equals 10^{-11} m , which is much smaller than $2b$. Introducing the new variables

$$k_y = \tau \ , \ k'_y - \frac{2b^2}{2b^2 + w^2} k_y = \sigma \ , \tag{4.4.5}$$

reduces equation (4.4.4) into a double integral: one has a large bandwidth determined by the exponential $\exp(-\tau^2 w^2/4)$ and the other has a much smaller bandwidth of order b^{-1}, viz.,

$$\Psi_{out}(y, z, t) = \frac{A(\beta)}{16\pi^2\sqrt{2}\,\beta} \int_{-\infty}^{+\infty} d\sigma \int_{-\infty}^{+\infty} d\tau \, e^{-\tau^2 w^2/4} \, e^{-\sigma^2 b^2/2} \left[e^{i(dw^2/2b^2)\tau} \, e^{-id\sigma} + e^{-i(dw^2/2b^2)\tau} \, e^{id\sigma} \right] \tag{4.4.6}$$
$$\times \, e^{-i\tau(y - y_0)} \, e^{i\sigma y_0} \, e^{i\beta z} \, e^{-i(\sigma^2 + 2\sigma\tau + \tau^2) z/4\beta} \, e^{i[(4\beta^2 - \sigma^2 - 2\sigma\tau - \tau^2)^2 + 16\beta^2\tau^2]^{1/2} ct/4\beta} \, .$$

In this expression we have neglected w^2 in comparison to b^2. For the chosen value of $2b = 10^{-5}$ m, the integration over σ has an effective range of 4×10^5 m^{-1}, so that $\sigma << \beta = 10^7$ for all values of σ contributing to the integral. Using this property together with a binomial expansion of the square root, we can approximate the argument of the last exponential in equation (4.4.6) by

$$[(4\beta^2 - \sigma^2 - 2\sigma\tau - \tau^2)^2 + 16\beta^2\tau^2]^{1/2} \frac{ct}{4\beta} = [1 + \tau^2/4\beta^2]\left[1 - \frac{\sigma\tau(1 - \tau^2/4\beta^2)}{2\beta^2(1 + \tau^2/4\beta^2)^2} - \frac{\sigma^2(1 - 3\tau^2/4\beta^2)}{4\beta^2(1 + \tau^2/4\beta^2)^2}\right]\beta ct\,, \tag{4.4.7}$$

where terms of order σ^4/β^4 and $\tau\sigma^3/\beta^4$ have been neglected, while those of order $\sigma\tau/\beta^2$ and σ^2/β^2 have been retained because, for $z = ct$, they are of the same order of magnitude as the $\sigma\tau$ and σ^2 terms in the exponent $\exp[-i(\sigma^2 + 2\sigma\tau + \tau^2)z/4\beta]$. It should be noted that the binomial expansion can be used because the last two terms in (4.4.7) are smaller than unity for all values of σ and τ contributing to the integrations, as long as, $\sigma/\beta << 1$. If the photographic plate is placed at $z = L$, we seek to find the shape of the FWM pulse upon its arrival at $z = ct_L = L$. Substituting the approximate expansion (4.4.7) into equation (4.4.6) gives

$$\Psi_{\text{out}}(y, L, t_L) = \frac{A(\beta)e^{i2\beta L}}{16\pi^2\sqrt{2}\,\beta}\int_{-\infty}^{+\infty} d\sigma \int_{-\infty}^{+\infty} d\tau\, e^{-\tau^2 w^2/4}\, e^{-\sigma^2\Delta/2}\, e^{-i\tau(y - y_0)}\, e^{i\sigma(y_0 - 2L\Lambda(\tau))} \times \left[e^{i(dw^2/2b^2)\tau}\, e^{-id\sigma} + e^{-i(dw^2/2b^2)\tau}\, e^{id\sigma}\right], \tag{4.4.8}$$

where $\Delta = b^2 + i(L/\beta)(1 - \tau^2/4\beta^2)/(1 + \tau^2/4\beta^2)$ and $\Lambda(\tau) = (\tau/2\beta)/(1 + \tau^2/4\beta^2)$. Carrying out the integration over σ reduces equation (4.4.8) to

$$\Psi_{\text{out}}(y, L, t_L) = \frac{A(\beta)e^{i2\beta L}}{16\pi^{3/2}\beta}\int_{-\infty}^{+\infty} d\tau\, \frac{1}{\sqrt{\Delta}}\, e^{-\tau^2 w^2/4}\, e^{-i\tau(y - y_0)}\left[e^{-(d - y_0 + 2L\Lambda(\tau))^2/2\Delta} + e^{-(d + y_0 - 2L\Lambda(\tau))^2/2\Delta}\right], \tag{4.4.9}$$

where the exponential terms $\exp[\pm i(dw^2/2b^2)\tau]$ have been neglected because $(dw^2/2b^2)\tau < 10^{-5}$ for all values of τ contributing to the integration. Although the remaining integration is quite difficult to evaluate, general features of the solution can be obtained. First, it should be noted that the integrand has a large bandwidth ($w^{-1} \simeq 10^{11}$ m^{-1}) determined by the term $\exp(-w^2\tau^2/4)$. The rest of the terms contribute to a depression in the amplitude of the integrand that decays to zero at $\tau = 2\beta$. The center of the depression at 2β is much smaller than w^{-1} ; as a consequence, most of the contributions to the integral come from the high frequency components, while the low frequency component contributions are relatively small and are only significant at the tails. We seek to estimate the order of the error introduced when the low frequency components are neglected and only the high frequency portion is retained. In this case $\Delta \simeq \Delta' = b^2 - i(L/\beta)$ and $\Lambda(\tau) \simeq 2\beta/\tau$ So that equation (4.4.9) becomes

$$\Psi_{\text{out}}(y, L, t_L) = \frac{A(\beta)e^{i2\beta L}}{16\pi^{3/2}\beta} \int_{-\infty}^{+\infty} d\tau \, \frac{1}{\sqrt{\Delta'}} \, e^{-\tau^2 w^2/4} \, e^{-i\tau(y-y_0)} \Big[e^{-(d-y_0+4L\beta/\tau)^2/2\Delta'} + e^{-(d+y_0-4L\beta/\tau)^2/2\Delta'} \Big] . \tag{4.4.10}$$

After normalizing the bandwidth to unity by using the change of variables $q = \tau w/2$, the integration given in (4.4.10) will have the following form:

$$\Psi_{\text{out}}(y, L, t_L) = \frac{A(\beta)e^{i2\beta L}}{8\pi^{3/2}\beta w} \, \frac{1}{\sqrt{\Delta'}} \int_{-\infty}^{+\infty} dq \, e^{-q^2} \, e^{-i2(y-y_0)q/w} \Big[e^{-(d-y_0+2L\beta w/q)^2/2\Delta'} + e^{-(d+y_0-2L\beta w/q)^2/2\Delta'} \Big] . \tag{4.4.11}$$

For $q < \beta w \simeq 10^{-4}$, the integrand is exponentially small and can be taken equal to zero. As q becomes larger than βw , the amplitude of the integrand rises to a maximum value of one for $q > 4\beta^2 bw \simeq 4 \times 10^{-2}$. The amplitude stays at this value until it decays to zero for $q > 4$. Incorporating these approximations, we rewrite (4.4.11) as

$$\Psi_{out}(y, L, t_L) = \frac{A(\beta)e^{i2\beta L}}{8\pi^{3/2}\beta w} \frac{1}{\sqrt{\Delta'}} \left[\overline{\Psi}_{out}(y, L, t_L) - \delta\overline{\Psi}_{out}(y, L, t_L)\right], \qquad (4.4.12a)$$

where

$$\overline{\Psi}_{out}(y, L, t_L) = \int_{-\infty}^{+\infty} dq\, e^{-q^2} e^{-i2(y-y_0)q/w} \left[e^{-(d-y_0)^2/2\Delta'} + e^{-(d+y_0)^2/2\Delta'}\right], \qquad (4.4.12b)$$

$$\delta\overline{\Psi}_{out}(y, L, t_L) \simeq 10^{-2}. \qquad (4.4.12c)$$

The integration given in equation (4.4.12b) has a magnitude of order 1. Neglecting, therefore, the quantity $2L\beta w/q$ compared to $d \pm y_0$ introduces an error of the order 10^{-2} of the peak amplitude of the pulse around its center, and will contribute significantly only to its tails. Adopting this approximation, the integration over q can be easily carried out to give

$$\Psi_{out}(y, L, t_L) = \frac{A(\beta)e^{i2\beta L}}{8\pi\beta w} e^{-(y-y_0)^2/w^2} \frac{e^{-(d^2+y_0^2)/2(b^2-iL/\beta)}}{[b^2 - iL/\beta]^{1/2}} \times \left[e^{dy_0/(b^2-iL/\beta)} + e^{-dy_0/(b^2-iL/\beta)}\right]. \qquad (4.4.13)$$

The main results of this chapter follow from this equation. As noted earlier, what we really measure is the field's energy density which is proportional to the square of the amplitude of the pulse $|\Psi_{out}|^2$. Far from the two slit screen, where $L^2/\beta^2 >> b^4$, the scattered energy density is approximately proportional to

$$|\Psi_{out}(y, L, t_L)|^2 = \frac{A^2(\beta)}{16\pi^2 L^2 w^2} e^{-2(y-y_0)^2/w^2} e^{-b^2\beta^2(d^2+y_0^2)/L^2} \cos^2(\beta d y_0/L). \qquad (4.4.14a)$$

The field at the screen (at $t = t_L$) consists of a Gaussian pulse of width w centered around $y = y_0$ multiplied by the interference term $\cos^2(dy_0\beta/L)\ \exp(-b^2\beta^2 y_0^2/L^2)$. When the center of the pulse

does not coincide with a zero of the of the interference pattern, the energy of the central portion will be delivered to an atom (or an electron in an atom) of the photosensitive material of the plate, thus inducing a reaction that will appear as a dot on the plate. Since the field is much weaker at its tails, the energy there will be too small to be detected. When the center of the pulse ends up on a zero of the interference pattern, the amplitude of the pulse will be multiplied by zero and no atoms of the emulsion will be excited, resulting in dark fringes. In contrast, detecting the pulse just after it passes through the screen, where $b^4 >> L^2/\beta^2$, the field given in equation (4.4.13) reduces to

$$|\Psi_{\text{out}}(y, L, t_l)|^2 = \frac{A^2(\beta)}{(8\pi\beta w b)^2}\, e^{-2(y-y_0)^2/w^2}\left[e^{-(d-y_0)^2/b^2} + e^{-(d+y_0)^2/b^2}\right]^2 . \qquad (4.4.14b)$$

This expression is identical to the product of the FWM pulse at $z = ct = L$ by the slit function $S(y)$. This indicates that the pulse will only be detected if it passes through one of the two slits. Hence, detectors placed behind the screen will only detect the photons passing through either slit A or slit B.

For a large number of photons hitting the photographic plate simultaneously, tails that have been neglected in the case of a single photon might add up and disrupt the interference pattern. This is not the case, however, because not all the photons will have the same center y_0. To account for this initial distribution effect, we have to integrate the 2-D FWM given in (4.4.2) over all possible values of y_0. We assume that the centers of the photons have a Gaussian distribution of width $\Sigma > d$, viz.,

$$f(y_0) = \frac{1}{\sqrt{2\pi}\,\Sigma}\, e^{-y_0^2/2\Sigma^2} . \qquad (4.4.15)$$

Integrating the 2-D FWM over all possible values of y_0 then gives

$$\Psi(y,z,t)=\int_{-\infty}^{+\infty}dy_0\;\frac{e^{-y_0^2/2\Sigma^2}}{\sqrt{2\pi}\,\Sigma}\;\frac{A(\beta)\,e^{i\beta(z+ct)}}{4[\pi\beta\,(a_1+i(z-ct))]^{1/2}}\;e^{-\beta(y-y_0)^2/(a_1+i(z-ct))}$$
$$=\frac{1}{4\sqrt{2\pi\beta}\,\Sigma}\;\frac{A(\beta)\,e^{i\beta(z+ct)}}{[\beta+(a_1+i(z-ct))/2\Sigma^2]^{1/2}}\;e^{-y^2[(\beta/2\Sigma^2)/(\beta+(a_1+i(z-ct))/2\Sigma^2)]}. \tag{4.4.16}$$

For all possible values of $z-ct$ (e.g., $|z-ct|<1$ m), the wave number β is much larger than $(a_1+i(z-ct))/2\Sigma^2$. This gives a y dependence of the form $\exp[-y^2/2\Sigma^2]$. This indicates that the field is symmetrically distributed over the two slits; and as a result, a regular diffraction pattern will be produced. Note that this analysis is permitted solely because the FWMs are solutions to a linear partial differential equation for which a superposition of the FWMs is still a solution.

4.5 THE ENERGY AND MOMENTUM OF THE FWM PULSE

It was argued in the previous section that a photon can be represented by a bump field like the FWM solution. The quantum mechanical interference effects arose as manifestations of the nonlocal character of the tails of the FWM pulse. However, the total energy content of such a nonlocal pulse is infinite, even though its energy density is finite. As a consequence, one wonders if in this a picture, it is possible to derive the usual energy momentum relationships, i.e., $E=\hbar\omega$ and $p=\hbar\beta$. We claim that this is possible, primarily because we expect that the interactions of the FWM pulse with the fields representing other particles are most pronounced when the overlap between their fields is maximal; i.e., when the bumps of the two fields overlap. We are, therefore, mainly interested in the energy content of the central bump. The interactions with the tails are too tiny to be detected in individual processes. Nevertheless, the shape of these tails is determined from

the boundary conditions of the experimental setup and clearly (from the two slit analysis) plays a major role in the resulting physics. The effects of the tails should be felt in experiments involving very high intensities, or as we saw above, in interference experiments where the boundary conditions can produce certain nulls in the total field. When the bump of the field passes through those nulls, it disappears and the dark fringes of the diffraction patterns are produced.

It is well known that plane waves are approximations to spherical or cylindrical waves having wavefronts of very small curvatures. Along the same vein, we can regard the FWM pulse as an idealisation of a more complex physical structure of a finite total energy. One possibility is that the FWM pulse is an approximation to a solution of Maxwell's equations in curved spacetime. These equations are nonlinear and the corresponding nonlinear FWM pulse might have a finite total energy. In the limit of a flat spacetime, the nonlinear FWM pulse is expected to reduce to the linear FWM pulse used in this work. Such ideas are open to speculations and they are not the main purpose of this investigation. Since we are only capable of observing the high energy density of the central bump field, we usually acknowledge it as a light particle or a photon. We assert, then, that in all known interactions, the energy and the momentum associated with a light particle will be a reflection of the energy and momentum content of the central portion of the FWM pulse. It is our goal in this section to find such an estimate of the energy and momentum content of the central FWM bump.

Since the FWM pulse is a classical wave function, the energy and momentum densities [60] can be calculated using the formulas

$$H(\vec{r}, t) = c^{-2}\, \partial_t \Psi(\vec{r}, t)\, \partial_t \Psi^*(\vec{r}, t) + \nabla\Psi(\vec{r}, t) \cdot \nabla\Psi^*(\vec{r}, t)\,, \tag{4.5.1a}$$

$$\vec{P}(\vec{r}, t) = -\, c^{-2} \left[\partial_t \Psi(\vec{r}, t)\, \nabla\Psi^*(\vec{r}, t) + \nabla\Psi(\vec{r}, t)\, \partial_t \Psi^*(\vec{r}, t) \right]. \tag{4.5.1b}$$

Photons are created in interactions involving other particles. The fields representing these particles should also be nonlocal with an extended bump structure analogous to that of the FWM pulse. This is the case because a pure extended wave structure cannot be excited by an extremely localized point-like particle. As mentioned earlier, the interactions of such bump fields are more

pronounced when their large amplitude central portions overlap. We can assume that such overlaps take place within a certain volume. The expressions for the energy and momentum densities can be integrated over such a volume, thus, giving an estimate of the energy and the momentum of a photon represented by the FWM pulse. These ideas are rather tentative and far from being final, basically because the theory introduced here is for a free particle and the corresponding interaction schemes are not yet fully developed. Even though we are aware of the shortcomings of such crude estimates, we are willing, nevertheless, to evaluate them in order to point out some physically interesting prospects for using such pulses as models of photons.

Starting with the energy content, the 3-D FWM pulse given in equation (4.1.1) can be substituted into equation (4.5.1a) and the indicated operations carried out to obtain

$$H(\vec{r}, t) = \frac{2A^2(\beta)}{(a_1^2 + \zeta^2)^3}\left[(a_1^2 + \beta^2 a_1^4 + \beta^2\zeta^4 + 2\beta^2\zeta^2 a_1^2 + \zeta^2) + 2(\beta^2 a_1^2 - \beta a_1 + \beta^2\zeta^2)\rho^2 + \beta^2\rho^4\right] \times e^{-2\beta a_1 r^2/(a_1^2+\zeta^2)}, \tag{4.5.2a}$$

where $\zeta = z - ct$. Similarly, the z-component of the momentum density is given by

$$P_z(\vec{r}, t) = \frac{-2A^2(\beta)}{c(a_1^2 + \zeta^2)^3}\left[(\beta^2\zeta^4 + \beta^2 a_1^4 + 2\beta^2\zeta^2 a_1^2 - \zeta^2 - a_1^2) + 2\beta a_1\rho^2 - \beta^2\rho^4\right] \times e^{-2\beta a_1 r^2/(a_1^2+\zeta^2)}. \tag{4.5.2b}$$

Note that $H(\vec{r}, t)$ and $P_z(\vec{r}, t)$ are independent of $\eta = z + ct$. The energy density $H(\vec{r}, t)$ can be integrated over an ellipsoid with a transverse radius equal to R and a major axis equal to l to give the energy of the light particle buried in the extended field structure of the FWM pulse. Specifically,

$$E_y = 2\pi \int_{-l}^{+l} d\zeta \int_0^{R^2(1-\zeta^2/l^2)^{1/2}} d\rho\, \rho\, H(\vec{r}, t)\,. \tag{4.5.3}$$

Substituting the energy density (4.5.2a) into equation (4.5.3), integrating over ρ and introducing the new variable $\chi = \zeta/l$, we obtain

$$E_y = \frac{\pi A^2(\beta)}{\beta a_1^3}\, l \int_0^1 d\chi \Bigg[(1 + 2\beta a_1 + 2\beta^2 a_1^2) - e^{-2\beta a_1(1-\chi^2)R^2/l^2(\chi^2 + a_1^2/l^2)} \Bigg[1 + 2\beta a_1 (1 - \frac{R^2}{l^2}) + 2\beta^2 a_1^2 (1 - \frac{R^2}{l^2})^2 + 2\beta a_1 \frac{R^2/l^2}{(\chi^2 + a_1^2/l^2)} (1 + 3\frac{a_1^2}{l^2}) + 2\beta a_1 \frac{R^2}{l^2} \frac{(1 + a_1^2/l^2)}{(\chi^2 + a_1^2/l^2)^2} (\beta a_1 \frac{R^2}{l^2}(1 + \frac{a_1^2}{l^2}) - 2\frac{a_1^2}{l^2}) \Bigg] \Bigg]. \tag{4.5.4a}$$

A similar calculation using the momentum density given in equation (4.5.2a) yields .

$$p_z = \frac{\pi A^2(\beta)}{\beta a_1^3} \frac{l}{c} \int_0^1 d\chi \Bigg[(1 - 2\beta^2 a_1^2) - e^{-2\beta a_1(1-\chi^2)R^2/l^2(\chi^2 + a_1^2/l^2)} \Bigg[1 - 2\beta a_1 \frac{R^2}{l^2} - 2\beta^2 a_1^2 (1 - \frac{R^4}{l^4}) + 2\beta a_1 \frac{R^2/l^2}{(\chi^2 + a_1^2/l^2)} (1 + 3\frac{a_1^2}{l^2} - 2\beta a_1 (1 + \frac{a_1^2}{l^2})) + 2\beta a_1 \frac{R^2}{l^2} \frac{(1 + a_1^2/l^2)}{(\chi^2 + a_1^2/l^2)^2} (\beta a_1 \frac{R^2}{l^2} (1 + \frac{a_1^2}{l^2}) - 2\frac{a_1^2}{l^2}) \Bigg] \Bigg]. \tag{4.5.4b}$$

Since the x and y-components of the momentum density are odd functions of x and y, respectively, the integration over an ellipsoid as indicated in equation (4.5.3), gives

$$p_x = 0 \quad , \quad p_y = 0 \, . \tag{4.5.5a}$$

Therefore,

$$\vec{p} = p_z \hat{a}_z \tag{4.5.5b}$$

It should be noted that the energy and the momentum expressions given in equations (4.5.4a) and (4.5.4b), respectively, do not obey the momentum-energy relationship $|p| = E_y/c$. However,

under the conditions that $\beta a_1 << 1$, $a_1^2/l^2 << 1$ and $l \geq R$, the energy of the particle will have the following form:

$$E_\gamma = \frac{\pi A^2(\beta)}{\beta a_1^3}\, l \int_0^1 d\chi \left[1 - e^{-2\beta a_1 R^2/l^2(\chi^2 + a_1^2/l^2)} \left[1 + 2\beta a_1 \frac{R^2/l^2}{(\chi^2 + a_1^2/l^2)} + 2\beta a_1 \frac{R^2}{l^2} \frac{(1 + a_1^2/l^2)}{(\chi^2 + a_1^2/l^2)^2} \left(\beta a_1 \frac{R^2}{l^2}\left(1 + \frac{a_1^2}{l^2}\right) - 2\frac{a_1^2}{l^2}\right)\right]\right]. \tag{4.5.6a}$$

Similarly the expression for the momentum reduces to

$$p_z = \frac{\pi A^2(\beta)}{\beta a_1^3}\, \frac{l}{c} \int_0^1 d\chi \left[1 - e^{-2\beta a_1 R^2/l^2(\chi^2 + a_1^2/l^2)} \left[1 + 2\beta a_1 \frac{R^2/l^2}{(\chi^2 + a_1^2/l^2)} + 2\beta a_1 \frac{R^2}{l^2} \frac{(1 + a_1^2/l^2)}{(\chi^2 + a_1^2/l^2)^2} \left(\beta a_1 \frac{R^2}{l^2}\left(1 + \frac{a_1^2}{l^2}\right) - 2\frac{a_1^2}{l^2}\right)\right]\right]. \tag{4.5.6b}$$

The energy-momentum relationship $|p| = E_\gamma/c$ is, then, satisfied. It should be pointed out that the conditions $\beta a_1 << 1$ and $a_1^2/l^2 << 1$ follow from the need to have a_1 very small in order to guarantee that the FWM solution behaves like a localized pulse moving in the positive z-direction.

To evaluate the integration in equations (4.5.6a) and (4.5.6b), we can use the change of variables $\chi = (a_1/l)\tan\theta$; specifically,

$$E_\gamma = \frac{\pi A^2(\beta)}{\beta a_1^3}\, l \left[1 - \int_0^{\theta_c} d\theta\, \frac{a_1}{l}\, e^{-2(\beta R^2/a_1)\cos^2\theta} \left[\sec^2\theta + 2\frac{\beta}{a_1} R^2 + 2\frac{\beta}{a_1} R^2 \left(\frac{\beta}{a_1} R^2 - 2\right) \cos^2\theta \right]\right], \tag{4.5.7}$$

where $\theta_c = \arctan(l/a_1)$. Under the condition that $a_1^2/l^2 << 1$, the angle θ_c will be approximately equal to $\pi/2$. This leads to a singularity in the integration over $\sec^2\theta$. Rewriting equation (4.5.7) as

$$E_\gamma = \frac{\pi A^2(\beta)}{\beta a_1^2}\left[\frac{l}{a_1} - \int_0^{\theta_c} d\theta\ \sec^2\theta + \int_0^{\theta_c} d\theta\,(1 - e^{-2(\beta R^2/a_1)\cos^2\theta})\ \sec^2\theta \right.$$
$$\left. - \int_0^{\theta_c} d\theta\, 2\frac{\beta}{a_1} R^2\,(1 + (\frac{\beta}{a_1} R^2 - 2)\ \cos^2\theta)\, e^{-2(\beta R^2/a_1)\cos^2\theta}\right],$$

isolates the singularity in the first integral which can then be evaluated explicitly. The integrands in the last two integrations are regular over the range $\theta = 0$ to $\pi/2$. Carrying out the first integration and using $\theta_c \simeq \pi/2$, the expression of the energy reduces to

$$E_\gamma = \frac{\pi A^2(\beta)}{\beta a_1^2}\, D\,, \tag{4.5.8a}$$

where

$$D = \int_0^{\pi/2} d\theta \left[(1 - e^{-2(\beta R^2/a_1)\cos^2\theta})\ \sec^2\theta - 2\frac{\beta}{a_1} R^2 \right.$$
$$\left. \times\,(1 + (\frac{\beta}{a_1} R^2 - 2)\ \cos^2\theta)\, e^{-2(\beta R^2/a_1)\cos^2\theta}\right]. \tag{4.5.8b}$$

In the expression for the energy given in equation (4.5.8) R represents the radius of the particle interacting with the photon; the radius of the photon is of order $r_\gamma = 2(a_1/\beta)^{1/2}$. It is expected that the corpuscular character of the photon manifests itself when its transverse extension is of the same order of magnitude as that of the particle. In this case, we are primarily interested in evaluating the integral (4.5.8b) for values of $\beta > 4a_1/R^2$ for which the waist of the photon is smaller than the radius of the particle. For this range of values, a numerical evaluation of D indicates that

$$D = 1.88\sqrt{\frac{\beta R^2}{4 a_1}}\,, \tag{4.5.9}$$

and the energy of the photon can be rewritten as follows:

$$E_\gamma = \frac{0.94\pi A^2(\beta)}{\beta^{1/2}\, a_1^{5/2}}\ R\ . \tag{4.5.10}$$

To make the subsequent discussion more precise we can assume that the photon interacts with an electron of radius $R = r_e$. Choosing

$$A^2(\beta) = \frac{\beta^{3/2} a_1^{5/2} \hbar c}{0.94\pi r_e}\ , \tag{4.5.11}$$

yields

$$E_\gamma = \hbar\,\omega\ , \tag{4.5.12a}$$

where $\omega = \beta c$. A similar analysis gives the photon momentum; namely,

$$p = \hbar\,\beta\ . \tag{4.5.12b}$$

At this point we would like to find an estimate for a_1. This can be achieved by considering the photon-electron scattering cross sections. The total scattering cross section for low frequency photons (e.g., X-rays) scattered by free electrons is given by the following formula [61]:

$$\sigma_T = \frac{8\pi}{3}\left(\frac{e^2}{m_e c^2}\right)^2 . \tag{4.5.13}$$

This expression is known as the Thomson cross section. It indicates that the incident photons with $r_\gamma >> r_e$ see the electrons as localized ball-like structures whose transverse radius equals

$$r_e = \frac{e^2}{m_e\, c^2} = 2.8 \times 10^{-15}\ \text{m}\ . \tag{4.5.14}$$

This quantity is known as the classical electron radius. As the energy of the incident photon increases, the Thomson cross section is modified into [61]

$$\sigma = \frac{3}{4} \frac{m_e c^2}{\hbar\omega} \sigma_T \quad , \qquad \text{for} \quad \hbar\omega >> m_e c^2 \, . \tag{4.5.15}$$

In this case $r_\gamma \leq r_e$ and the corpuscular character of the photons becomes more pronounced. Substituting equation (4.5.13) into the total cross section given in equation (4.5.15) yields

$$\sigma = \frac{8\pi}{3} r_{\text{eff}}^2 \quad , \quad \text{for} \quad \lambda_e >> \lambda \, , \tag{4.5.16a}$$

where

$$r_{\text{eff}} = 0.866\, \alpha \sqrt{\frac{\lambda_e}{\beta}} \, . \tag{4.5.16b}$$

To arrive at these expressions, the relationship $r_e = \alpha \lambda_e$ has been used, where $\alpha = 1/137$ is the fine structure constant and λ_e is the electron's Compton wavelength divided by 2π. The total cross section (4.5.16) indicates that the photon incident on the electron will only see a circular area of radius r_{eff}, which decreases as $\beta^{-1/2}$ as the frequency increases. This idea is consistent with the picture that for $\hbar\omega >> m_e c^2$, the radius of the photon r_γ becomes smaller than r_e. As the frequency increases further the radius of the photon decreases as $\beta^{-1/2}$. Recalling that the radius of the FWM pulse is of order $2(a_1/\beta)^{1/2}$, an estimate for the parameter a_1 can be derived by equating $r_\gamma = r_{eff}$, viz.,

$$2\sqrt{\frac{a_1}{\beta}} = 0.866\, \alpha \sqrt{\frac{\lambda_e}{\beta}} \, .$$

This gives

$$a_1 = 0.1875\, \alpha^2 \lambda_e \, , \tag{4.5.17}$$

which for an electron is equal to $\sim 1.523 \times 10^{-16}$ m. Using this value for a_1, the amplitude factor $A(\beta)$ can then be given explicitly as

$$A(\beta) = 0.0714\alpha^2 \lambda_e^{3/4} \beta^{3/4} \hbar^{1/2} c^{1/2} . \tag{4.5.18}$$

From equations (4.5.17) and (4.5.18) it can be seen that the parameters a_1 and $A(\beta)$ are dependent on λ_e (or m_e). Such a dependence indicates that photons released in an interaction over a characteristic length dependent on λ_e (or m_e) carry this information along. For example, $E_\gamma = 0.5$ Mev photons released in an electron-positron annihilation will have a_1 dependent on λ_e (or m_e). If the electron and the positron each acquire a kinetic energy ~ 0.5 Mev before they collide, then their total energy ~ 1.0 Mev, and λ_e (or m_e) in expressions (4.5.17) and (4.5.18) will be replaced by $\lambda_e/2$ (or $2m_e$). Substituting these values in the energy expression

$$E_\gamma = \frac{0.94\pi A^2(\beta)}{\beta^{1/2} a_1^{5/2}} \; r_e$$

gives

$$E_\gamma = \hbar (2\beta) c ,$$

which has an effective wave number $\beta_{eff} = 2\beta$. It should be noted that r_e in the energy expression remains unaltered because this is the radius of the detector's electrons and should not be confused with the interaction length of the electron-positron pair. This analysis reflects the fact that photons emitted from interactions taking place over shorter distances acquire higher energies. At the same time, such photons are detected through their interaction with particles having $mc^2 \sim \hbar\omega$ or $r_e \sim r_\gamma$. For $r_e << r_\gamma$, the photons lose their corpuscular character and their wave properties become more prominent.

In the case of atomic photons (i.e., photons emitted in the transition of atomic electrons from one state to another), the ideas discussed earlier are still valid. It should be noted, however, that the energy eigenvalues in the case of the hydrogen atom are [62]

$$E_n = -\frac{e^2}{2r_B}\ \frac{1}{n^2}\ ,$$

where r_B is the Bohr radius. At the same time the average value of the radial extent of the wave functions representing the eigenstates of the atom is given by [62]

$$< \frac{1}{r_n} > = \frac{1}{n^2 r_B}\ .$$

The size of the wave function representing the different states of the atom increases as the states' energies increase; i.e., $E_n \propto < 1/r_n >$. Since the energy difference $E_{n_1} - E_{n_2}$ equals $\hbar\beta c$, we expect the inverse of the radius of the emitted photon $1/r_\gamma$ to be proportional to $(< 1/r_{n_1} > - < 1/r_{n_2} >)$. Consequently, the inverse of the photon's radius should be proportional to β. Recalling that the radius of the FWM pulse is equal to $2(a_1/\beta)^{1/2}$, it follows that a_1 has to behave as a_0/β, where a_0 is a constant. The energy of the photon given in equation (4.5.10) can, thus, be modified into

$$E_\gamma = 0.94\pi\, A^2(\beta)\ \frac{\beta^2}{a_0^{5/2}}\ r_B\ , \tag{4.5.19}$$

where R in equation (4.5.10) is replaced by r_B. To find an estimate for the value of a_0, we assume that the size of the photons should be of order r_B. For a photon of energy 10 ev, the wave number $\beta_B = 5 \times 10^7\ \mathrm{m}^{-1}$; hence,

$$2\frac{\sqrt{a_0}}{\beta} = r_B \tag{4.5.20}$$

gives a value of $a_0 = (\beta_B r_B)^2/4$ of order 10^{-6}. Moreover, the amplitude factor $A(\beta)$ has the following form:

$$A^2(\beta) = \frac{(10^{-6})^{5/2}}{0.94\pi\beta}\ \frac{\alpha}{\lambda_e}\ \hbar c\ . \tag{4.5.21}$$

The mental picture associated with atomic interactions is that of a photon represented by a FWM pulse incident on an atom represented by the wavefunctions of the different eigenstates of its bound electrons. It is known that the wave function of the atom's ground state has the smallest possible size. The incident photon must have enough energy to induce the transition between the discrete eigenstates of the atom. At the same time the size of the photon should be comparable to that of the eigenstate of the atom. This gives a maximal overlap between the two wavefunctions and an interaction can take place. When the photon interacts with the atom it will be absorbed, thus, enlarging the atom's wavefunction into a "fatter" excited state. If the energy of the photon is too large, its size is much smaller than that of the atomic eigenstates. The overlap between the wave function of the photon and that of the atom will then be minimal and the photon will be too thin to excite it, despite its large energy content. In such cases the photon penetrates the atom and can knock out electrons from the inner orbitals. Higher energy photons can even reach the vicinity of the nucleus where they interact with its strong field producing electron-positron pairs, or they can even penetrate the nucleus itself and interact with its nucleons.

The parameters a_1 and $A(\beta)$ given in equations (4.5.17) and (4.5.18) are quite different from those derived for the lower energy atomic photons. Both results, nevertheless, can be combined to give in the case of electrons

$$a_1 = \frac{10^{-6}}{\beta} + 1.523 \times 10^{-16} , \tag{4.5.22}$$

where the first term contributes to lower energies, while the second term dominates for higher energy ranges. A similar expression can be derived for the amplitude factor $A(\beta)$ by combining equations (4.5.18) and (4.5.21)

$$A(\beta) = \left[\frac{2.52 \times 10^{-3}}{\beta^{1/2}} + 1.88 \times 10^{-15} \beta^{3/4} \right] \hbar^{1/2} c^{1/2} . \tag{4.5.23}$$

The low and high energy contributions become comparable for $\beta \sim 10^{10}$ m^{-1}. This corresponds to energies of order .01 $m_e c^2$. For $\hbar\omega > .01\, m_e c^2$ the Compton effect starts to take over from the photoelectric effect. The latter is the dominant inelastic scattering mechanism for $\hbar\omega \leq .01\, m_e c^2$. The Compton effect continues to be the main scattering mechanism as long as $\hbar\omega \leq 2\, m_e c^2$, when pair production sets in.

4.6 THE LORENTZ TRANSFORMATION OF THE FWM PULSE

In this section we establish the fact that even though the FWM pulse is not Lorentz invariant, its energy undergoes the conventional red shift if the photon is interacting with a particle moving away from it.

Assuming that the particle is in a primed frame of reference moving away from the incident photon along the z-direction, the Lorentz transformation relations are [60]

$$t = (t' + vz'/c^2)\gamma \ , \tag{4.6.1a}$$

$$z = (z' + vt')\gamma \ , \tag{4.6.1b}$$

$$x = x' \ , \tag{4.6.1c}$$

$$y = y' \ , \tag{4.6.1d}$$

where $\gamma = [1 - v^2/c^2]^{-1/2}$. In order that

$$\beta(z - ct) = \beta'(z' - ct') \ ,$$

the wave number β should transform as follows:

$$\beta = \gamma(1 + v/c)\beta' \ . \tag{4.6.1e}$$

The low energy amplitude factor

$$A(\beta) = \frac{a_0^{5/4}}{\beta^{1/2}} \sqrt{\frac{\hbar c}{0.94\pi R}} \tag{4.6.2}$$

will transform as

$$A(\beta') = \frac{a_0^{5/4}}{\beta'^{1/2}\Upsilon^{1/4}} \sqrt{\frac{\hbar c}{0.94\pi R}} \tag{4.6.3}$$

where $\Upsilon = (1 + v/c)/(1 - v/c)$. The FWM pulse will then transform as

$$\Psi(\rho', z', t') = \frac{A(\beta')}{[(a_0/\beta'\Upsilon^{1/2}) + i\Upsilon^{-1/2}\zeta']} \, e^{-\beta'\rho'^2\Upsilon^{1/2}/[(a_0/\beta'\Upsilon^{1/2})+i\Upsilon^{-1/2}\zeta']} \, e^{i\beta'\eta'\Upsilon} \ , \tag{4.6.4}$$

an expression that can be rewritten as

$$\Psi(\rho', z', t') = \frac{A(\beta')}{\Upsilon^{-1/2}\,[(a_0\Upsilon/\beta'\Upsilon) + i\zeta']} \, e^{-\beta'\Upsilon\rho'^2/[(a_0\Upsilon/\beta'\Upsilon)+i\zeta']} \, e^{i\beta'\Upsilon\eta'} \ . \tag{4.6.5}$$

By comparing the transformed FWM pulse given in equation (4.6.4) with that given in equation (4.1.1), we see that they have the same form. Nevertheless, a_0 is replaced by $a_0\Upsilon$, the characteristic wave number β becomes $\beta'\Upsilon$ and the amplitude factor $A(\beta)$ is replaced by $A(\beta')\Upsilon^{1/2}$. Using the transformed FWM pulse given in equation (4.6.5), we can repeat exactly the same energy and momentum calculations carried out in the previous section to arrive at an equation analogous to (4.5.19); namely,

$$E'_\gamma = 0.94\pi A^2(\beta')\,\Upsilon\,\frac{\beta'^2\Upsilon^2}{a_0^{5/2}\Upsilon^{5/2}}\,R\,. \tag{4.6.6}$$

It should be noted that we have arrived at this result from the fact that R is perpendicular to the direction of motion of the electron and it does not change under a Lorentz transformation. Using the transformed amplitude factor given in equation (4.6.3) we obtain the new energy

$$E'_\gamma = \hbar\beta' c\,. \tag{4.6.7}$$

This expression shows that the energy of the photon will be red shifted as predicted by the theory of special relativity. This result should be contrasted with the fact that the FWM pulse itself is not Lorentz invariant.

4.7 SUMMARY AND CONCLUSION

In this chapter, we have established that a certain class of solutions to the wave equation can be used to represent light particles. One particular solution, the FWM, is capable of explaining the results of Young's two slit experiment. We have demonstrated that such a solution, with an appropriate choice of parameters, behaves like a bump field with a very large amplitude around its center. Its field falls rapidly to extremely low values at the tails. The FWM pulse is nondispersive for all time, it is nonsingular and it travels with the speed of light in straight lines. Besides all these interesting features, it has an unusual behavior that away from its center its field fans out in the transverse direction to cover very large distances in comparison to the waist of the pulse's central region. It is this property that allows a single FWM pulse to interfere with itself in a two slit diffraction experiment. As the FWM pulse approaches the screen containing the two slits, its very low amplitude precursor field will be symmetrically distributed over the two slits, thus, it will be

capable of forming an interference pattern. Because of its low intensity, the precursor field does not excite the atoms of the photosensitive emulsion. However, the precursor field guides the central portion of the pulse through the screen until it ends up on one of the light fringes of the interference pattern. Because of its large energy content, the central portion of the pulse can excite an atom of the emulsion, thus inducing a reaction that will appear as a dot on the photosensitive material. This behavior is in sharp contrast with other localized pulses, e.g., the transverse Gaussian pulse. The fields of such pulses remain localized in the transverse direction for all times and they are never symmetrically distributed over the two slits. Consequently, they cannot produce an interference pattern.

The idea of the precursor field guiding the central particle-like bump to its final location on a diffraction pattern resembles to a great extent similar notions in other theories attempting to explain the results of Young's experiment. One of these is Bohm's [27,28] (or de Broglie's [30]) notion of a "quantum potential" which is derived from the amplitude of the wave function. Such a potential guides the particle through the screen to its final distination on the photosensitive plate. The "quantum potential" is a sourceless entity that is determined primarily by the configuration of the experimental setup [63-65]. Moreover, the manner in which the "quantum potential" directs the particle does not depend on its strength but rather on its shape. The force it exerts on the particle does not decrease as the magnitude of the wave function decreases to very small values. This property makes such a formulation inherently nonlocal. These ideas have a very close resemblance to the notion of a weak precursor field of a FWM pulse guiding the central particle-like bump to its final destination. It should be pointed out that the FWM pulse is a nonlocal entity that covers a large portion of space. This means that the global shape of the field is determined by the boundary conditions setup by the experimental configuration under consideration. Hence, the behavior of the particle-like bump field depends to a great extent on the totality of the experimental setup, even though its dimension is much smaller than the size of the devices used and the distances between them.

The other theory that we would like to discuss is Cramer's "transactional interpretation" of quantum mechanics [29]. Following Wheeler and Feynman's time symmetric emitter-absorber

theory [66-68], Cramer hypothesized that a transaction involving an exchange of advanced and retarded waves can describe quantum events. In this theory an emitter sends out an "offer wave" Ψ in both time directions. An observer responds to the incident wave by sending an advanced "confirmation wave" echo Ψ^* to the emitter. The echo amplitude at the emitter's position has a value equal to $|\Psi|^2$ which is the same as the probability of the Copenhagen interpretation. This process continues to completion by the cancellation of the advanced components outside the range of the interaction and by the satisfaction of the quantum boundary conditions at the emitter and absorber loci. In Young's two slit experiment the advanced waves originating from the screen travel towards the source and guide the retarded particle wave to the correct location on the diffraction pattern. This picture should be contrasted with the fact that the FWM solution contains the modulation term $\exp[i\beta(z + ct)]$ that travels in a direction opposite to that of the pulse's envelope. This factor becomes more prominent as we move away from the center of the pulse. Certain portions of the tails behave, then, like advanced waves. In any case, beside having very low intensities to be detected, such dependence on $(z + ct)$ disappears completely from the energy and the momentum density expressions [cf. equations (4.5.2)].

The "transactional interpretation" is explicitly nonlocal, a property it shares with all other interpretations of the quantum theory. Such nonlocality can be accomodated by the classical FWM solution, where the nonlocal character, arising from the unusual behavior of its tails, is an indigenous property of an exact solution to the wave equation. There is no need for a collapse of the wave function, for an atemporal transaction, or a "quantum potential". Even though the process dealt with in this paper is nonlocal, it is causal in the sense that the central particle-like portion of the field can be traced starting with its initial position and going through the screen until it ends up on the photographic plate. Similar structures for massive particles will be considered in the next chapter. The nonlocality of such structures might enable us to resolve the EPR paradox [69]. Recent two photon correlation experiments [53-55] have confirmed the quantitative predictions of quantum mechanics. Such predictions are inconsistent with the EPR locality premise and they allude to the nonlocal character of the microphysical world. As a consequence, we believe that

any attempt to find a deeper objective reality, underlying the quantum theory, must resort to the use of nonlocal structures.

Under the conditions $\beta a_1 << 1$ and $a_1^2/l^2 << 1$, the FWM energy and momentum relationships satisfy the known massless particle relations $E = \hbar\omega$ and $p = \hbar\beta$. It has been pointed out that these conditions are consistent with the need to have a_1 very small, so that the FWM solution behaves as a localized pulse. The energy and the momentum content of the FWM central bump suggests that the parameter a_1 should be related to the length of interaction involved in emitting or absorbing the light particle represented by the FWM pulse. Motivated by the formula for the total cross section scattering of electromagnetic waves off electrons, we found an estimate for the parameter a_1 and the amplitude factor $A(\beta)$. More precise evaluation of these parameters, together with a verification of the results of this work, can be obtained from experiments involving high intensity light beams. This is the case because the parameter a_1 and the wave number β are related directly to the spatial volume occupied by a photon.

The notion of a photon occupying a specific volume is a classical concept that follows directly from the model advocated by this work. The volume of a photon represented by the FWM pulse decreases as the frequency increases. Subsequently, photons in a laser beam of a very high intensity will start to crowd together and at some point they will begin to overlap in such a way that having more than one photon occupying the same spot will be very probable. If such a beam interacts with matter, then the probability of having several photons contributing simultaneously to an interaction becomes reasonably high. This is a simple, alternative classical interpretation of multiphoton processes. The strong irradiation photoelectric effect [70] is an example of a multiphoton process. With the advent of high intensity laser beams, it has been observed that matter can be ionized regardless of the frequency of the photons. This phenomenon has been attributed to the simultaneous absorption of several photons. For lower intensity beams, "multiphoton ionization" could be explained by perturbation theory. The kinetic energy of the released electrons is only a fraction of the energy of the photons. With a large increase of the beam's intensity, the atoms absorb more photons than necessary and "above threshold ionization" (ATI) is observed. The excess energy is transfered to the released electrons as kinetic energy, with the peaks of the electron energy distrib-

utions separated by integral multiples of the value of the photons' energy. "Above threshold ionization" could still be explained by perturbation theory until 1983 when nonperturbative effects were first observed [71]. These effects lead to the disappearance of the lowest peaks in the electron energy spectra. Several approaches to explain such a phenomenon have been suggested; however, the problem has not been resolved and is still open to debate. One interesting prospect is to provide an explanation for these ATI effects based on the classical model of the photon presented in this chapter. An encouraging experimental result is that, for the same intensities, the suppressed peaks start to reappear if higher frequencies are used. This could be easily explained by our model, since the volume of the photons decreases with the increase of frequency. A detailed study of the applicability of our model to the results of high intensity photoelectric effect experiments is currently under investigation.

Finally it should be emphasized that unlike various interpretations of the quantum theory and their attempts to explain the results of Young's two slit experiment, our approach is radically different. It is not just a new interpretation but an entirely new path that ought to be investigated. The wave function used here is a classical entity that travels in physical space, in sharp contrast with the quantum mechanical wave function that exists only in an abstract space. The fact that we are dealing with a new structure and we are not introducing yet another interpretation of the quantum theory suggests that it might be possible to check the validity of our claims. Specifically, our model predicts high energy deviations in the expressions for the energy and momenta of photons. These possible deviations were alluded to in connection with the energy and momentum integrals given in equations (4.5.4a) and (4.5.4b). In those two expressions, we have neglected terms of order βa_l in comparison to those of order one. Even though a_l seems to depend on the energies involved, it might be possible that for extremely large frequencies, the quantity βa_l could be comparable to unity. In this case, the energy values of the photons will deviate considerably from the regular $h\nu$ value. A possible means for investigating such deviations can be carried out in connection with ultra-energetic cosmic gamma rays [72-74]. Such photons have energies of order 10 Tev (corresponding to $\beta = 10^{20}$ m^{-1}) and an anomalously large photon-hadron cross section. It is presumed that these photons generate far more muons in the upper atmosphere than the standard

electromagnetic shower theory leads us to expect. Experiments involving very high energy cosmic gamma rays are, nevertheless, very hard to perform and the possibility of using them to probe the structure of photons seems quite remote at this time.

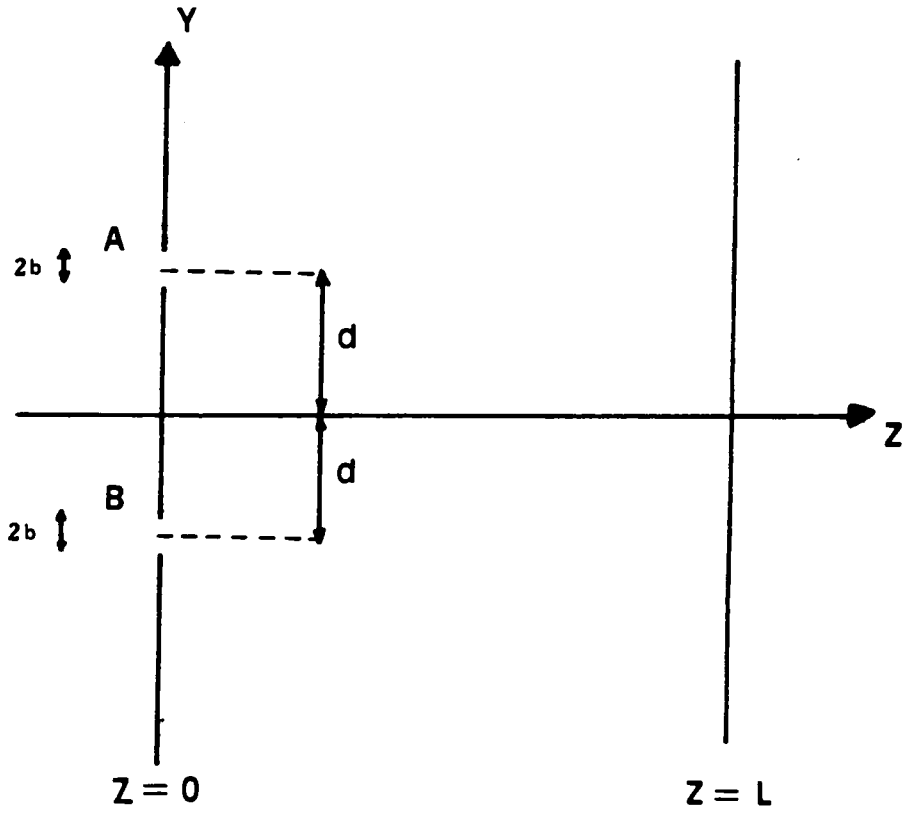

Figure 4.1 Young's two slit experiment.

5.0 NONDISPERSIVE WAVE PACKET SOLUTIONS TO THE KLEIN-GORDON EQUATION

In Chapter 2 we derived exact Brittingham-like solutions to the Klein-Gordon equation. Because of the specific type of operator decomposition that we used there, the centers of such solutions move with the speed of light c. This property makes them unattractive in modelling of massive particles, since one expects that such particles should move with a velocity $v < c$. In this chapter, we shall attempt to derive wave packet solutions to the Klein-Gordon equation that move with a velocity v smaller than the speed of light. These nondispersive solutions can be used as de Broglie wave packets representing localized massive scalar particles. The resemblance of such solutions to previously reported nondispersive wave packets will be discussed and certain subtle aspects of the latter, especially those arising in connection to the correct choice of dispersion relationships and the definition of group velocity, will be clarified. The results obtained for the Klein-Gordon equation will also used to provide nondispersive solutions to the Dirac equation which models spin 1/2 massive fermions.

5.1 NONDISPERSIVE WAVE PACKETS

The popular use of plane waves to represent moving particles defies our intuitive notion of particles as localized solutions to field equations. Other, localized solutions, e.g., Gaussian pulses, tend to spread out as they propagate in free space. In contradistinction, the FWM solutions have the attractive property of staying localized for all time. As a consequence, it was argued in the preceding chapter that they are more suitable for representing light particles (photons). The importance of this property is quite clear in view of the fact that particle localization is the only phenomenon that links us to the microphysical world. For example, a track left by a particle in a cloud chamber or a dot left by a photon on a photographic plate are just manifestations of the localization of particles, a concept that has been undermined in the orthodox interpretation of quantum mechanics.

These ideas concerning particle localization are not completely new; they reflect a position that was advocated by Einstein [77] and de Broglie [30,78,79], among others. In their view, a particle is perceived as a high concentration of a field governed by a partial differential equation, e.g., Maxwell's equations, the Klein-Gordon equation, etc. This highly concentrated field, or "bunch field", must remain localized and must not spread out as the particle travels in space-time. In this picture, the "bunch field" is incorporated in an extended wave field, thus combining the wave and the corpuscular aspects of matter. As in the case of massless particles, this interpretation of the wave-particle duality should be contrasted with Bohr's complementarity principle, whereby a particle manifests itself either in the form of a wave or in the form of a corpuscle, with both characters never being observed simultaneously.

If the idea of the "bunch field" is adopted, a representation of a particle in the form of a wave packet is one possibility. Until recently, however, it was believed that linear field equations can not support continuous nonsingular wave packets that do not spread in free motion. (This is not the case for the massless FWMs and the massive nondispersive wave packets derived by MacKinnon [75,76]. The other possibility is to use a "singularity solution" for representing the physical reality

of a localized particle. Such a singular solution to a linear field equation is an approximation to a more general solution of a corresponding nonlinear equation. The nonlinearity has a larger effect near the vicinity of the singularity, where it keeps the field amplitude large but finite. One of the first attempts to incorporate such ideas was de Broglie's in connection with his theory of the "double solution" [30]. Other attempts include Madelung's hydrodynamical model [30] and de Broglie's "pilot wave" theory [30], both of which inspired Bohm [27,28,80,81] to develop the idea of the quantum potential and to use it to give a causal interpretation of quantum mechanics. A common feature of these theories is that the particle kinematics can be derived from the information incorporated in the phase of a quantum mechanical wave function $\Psi = |\Psi| e^{i\phi}$, where both $|\Psi|$ and ϕ are real and the velocity of the particle can be given as

$$u = \frac{1}{m} \nabla \phi \,, \tag{5.1.1}$$

a relationship known as the "guidance formula" [30]. More recent developments, along the same lines, include the introduction of solitons into field theories [82], through the study of fields modelled by nonlinear equations, e.g., the cubic Schrodinger equation, the cubic Klein-Gordon equation, the sine-Gordon equation, etc. A rather broad class of such equations has been proposed for modelling localized particles. It is not very clear, however, whether a unique set of equations could be agreed upon to represent massive particles.

It is our purpose in this chapter to investigate the possibility of using Brittingham-like linear structures to represent massive particles. There are two options that we would like to examine. The first one is to think of these nondispersive wavepackets as classical billiard-like solutions. In this case the velocity of the particle is the same as the velocity of the wavepacket's envelope. The other choice is to follow de Broglie and consider such solutions as quantum mechanical objects whose kinematics can be derived from their phases as in equation (5.1.1). Since the original FWMs are solutions to the scalar wave equation or Maxwell's equations, they represent massless particles and their envelopes travel in free space with the speed of light. In the case of a massive particle, one should find for the Klein-Gordon equation or the Dirac equation solutions analogous to the FWMs, but with their envelopes travelling at some group velocity v_g smaller than the speed of light

c. A previous attempt [83] was made to find localized solutions to the Klein-Gordon equation. These solutions were approximate, with an envelope moving at a group velocity v_g very close to the speed of light c, or exact ones with an envelope travelling at the speed of light, a feature that makes them physically unattractive. A Brittingham-like solution to the massive Dirac equations has never been published before. However, Brittingham-like solutions to the massless Dirac equation and the spinor wave equation have been derived by Hillion [12,13]. Again, all these solutions have dealt with massless fields and, consequently, they have envelopes that move in straight lines with the speed of light. Our aim in the following sections is to obtain Brittingham-like solutions to massive fields, in particular the massive scalar field modelled by the Klein-Gordon equation and the massive spinor field modelled by the Dirac equation. The bidirectional representation introduced in Chapter 2 will be applied to the Klein-Gordon equation and solutions analogous to the FWMs, but moving with a group velocity v_g, will be derived. It will be shown that a special case of such solutions is the nondispersive wavepacket derived by MacKinnon [75,76].

5.2 THE KLEIN-GORDON EQUATION

In this section, we shall apply the bidirectional representation to the 3-D Klein-Gordon equation given by

$$\partial_t^2 \Psi(\vec{r}, t) - c^2 \nabla^2 \Psi(\vec{r}, t) + \mu^2 c^2 \Psi(\vec{r}, t) = 0 , \tag{5.2.1}$$

where $\mu = m_0 c/\hbar$, m_0 being the rest mass and $\hbar$ is Planck's constant divided by 2π. A comparison of this equation with (2.2.1a) shows that

$$\hat{\Omega}(-i\nabla) \equiv -c^2 \nabla^2 + \mu^2 c^2 . \tag{5.2.2}$$

In Chapter 2 the operator $\hat{\Omega}(-i\nabla)$ was split as follows:

$$\hat{\Omega}(-i\nabla) = \hat{A}(-i\partial_z) + \hat{B}(-i\nabla_T, -i\partial_z) ; \tag{5.2.3}$$

$$\hat{A}(-i\partial_z) = -c^2\partial_z^2 , \tag{5.2.4a}$$

$$\hat{B}(-i\nabla_T, -i\partial_z) = -c^2\nabla_T^2 + \mu^2 c^2 . \tag{5.2.4b}$$

This decomposition led to the characteristic variables

$$\zeta = z - ct \quad , \quad \eta = z + ct , \tag{5.2.5}$$

and, upon superposition, to a wave packet with an envelope moving with the speed of light, exactly as in the case of massless particles.

In the following, we propose to split the operator $\hat{\Omega}(-i\nabla)$ in a more physical way so that we can obtain envelopes that move with a group velocity smaller than c; specifically,

$$\hat{\Omega}(-i\nabla) = \hat{A}(-i\partial_z) + \hat{B}(-i\nabla_T, -i\partial_z) ; \tag{5.2.6}$$

$$\hat{A}(-i\partial_z) = -c^2\partial_z^2 + \mu^2 c^2 , \tag{5.2.7a}$$

$$\hat{B}(-i\nabla_T, -i\partial_z) = -c^2\nabla_T^2 . \tag{5.2.7b}$$

This choice of the operators $\hat{A}$ and $\hat{B}$ gives rise to the characteristic variables

$$\zeta = z - ct\,\frac{sgn(\alpha)}{\alpha}\,(\alpha^2 + \mu^2)^{1/2} , \tag{5.2.8a}$$

$$\eta = z + ct\,\frac{sgn(\beta)}{\beta}\,(\beta^2 + \mu^2)^{1/2}\,, \tag{5.2.8b}$$

and the constraint relationship

$$K(\alpha, \beta, \vec{\kappa}) = \kappa^2 - [\,\mu^2 + 2\alpha\beta + 2sgn(\alpha)\,(\alpha^2 + \mu^2)^{1/2}\,sgn(\beta)\,(\beta^2 + \mu^2)^{1/2}\,] = 0\,. \tag{5.2.9}$$

Following the recipe given in Chapter 2, a general solution to equation (5.2.1) can be written as follows:

$$\begin{aligned}\Psi(\vec{r}\,, t) = \frac{1}{(2\pi)^2}\int_{R^2} d\vec{\kappa}\; e^{-i\vec{\kappa}\cdot\vec{\rho}} \int_{R^1} d\alpha \int_{R^1} d\beta\; C(\alpha, \beta, \vec{\kappa})\;\delta[K(\alpha, \beta, \vec{\kappa})] \\ \times\, e^{-i\alpha(z - ct\,sgn(\alpha)\,(\alpha^2+\mu^2)^{1/2}/\alpha)}\; e^{i\beta(z + ct\,sgn(\beta)\,(\beta^2+\mu^2)^{1/2}/\beta)}\,.\end{aligned} \tag{5.2.10}$$

Analogously to the FWMs, we choose the spectrum entering into (5.2.10) as

$$C(\alpha, \beta, \vec{\kappa}) = \overline{C}(\alpha, \vec{\kappa})\,\delta(\beta - \beta_0)\,. \tag{5.2.11}$$

It follows, then, that

$$\Psi(\vec{r}\,, t) = G(\vec{\rho}\,, z, t)\; e^{i\beta_0(z + ct\,sgn(\beta_0)\,(\beta_0^2+\mu^2)^{1/2}/\beta_0)}\,, \tag{5.2.12}$$

where

$$G(\vec{\rho}\,, z, t) = \frac{1}{(2\pi)^2}\int_{R^2} d\vec{\kappa}\; e^{-i\vec{\kappa}\cdot\vec{\rho}} \int_{R^1} d\alpha\; \overline{C}(\alpha, \vec{\kappa})\;\delta[K(\alpha, \beta_0, \vec{\kappa})]\; e^{-i\alpha(z - ct\,sgn(\alpha)\,(\alpha^2+\mu^2)^{1/2}/\alpha)}\,. \tag{5.2.13}$$

We can find explicit FWM-like solutions to equation (5.2.1) by choosing a spectrum $\overline{C}(\alpha, \vec{\kappa})$ and carrying out the integrations in equation (5.2.13). This is a very tedious task, however, especially when dealing with a complicated constraint relationship such as the one given in equation

(5.2.9). Alternatively, we can find the differential equation governing $G(\vec{\rho}, z, t)$ by substituting (5.2.12) into the 3-D Klein-Gordon equation. If this procedure is implemented, we obtain

$$i\,2\beta_0(\partial_z - v_g^{-1}\partial_t)\,G(\vec{\rho}, z, t) + (\partial_z^2 - c^{-2}\partial_t^2)\,G(\vec{\rho}, z, t) + \nabla_T^2 G(\vec{\rho}, z, t) = 0\,, \tag{5.2.14}$$

where v_g is a group velocity given by

$$v_g = \frac{c\,\beta_0}{sgn(\beta_0)\,(\beta_0^2 + \mu^2)^{1/2}}\,. \tag{5.2.15}$$

It should be noted that v_g can be derived by differentiating the angular frequency characterizing the left-going plane wave with respect to the wave number β_0.

Motivated by the ansatz leading to the FWMs in the case of the scalar wave equation and by the existence of the convection term $(\partial_z - v_g^{-1}\partial_t)\,G(\vec{\rho}, z, t)$ in equation (5.2.14), we seek solutions of the form

$$G(\vec{\rho}, z, t) \equiv G(\vec{\rho}, \tau)\,; \tag{5.2.16a}$$

$$\tau = \gamma(z - v_g t)\,, \tag{5.2.16b}$$

$$\gamma = (1 - v_g^2/c^2)^{-1/2}\,. \tag{5.2.16c}$$

Equation (5.2.14) becomes, then, a hyperbolized Schrodinger-like equation, viz.,

$$i\,4\beta_0\,\gamma\partial_\tau\,G(\vec{\rho}, \tau) + \partial_\tau^2\,G(\vec{\rho}, \tau) + \nabla_T^2 G(\vec{\rho}, \tau) = 0\,. \tag{5.2.17}$$

It is now clear that v_g is the group velocity associated with a classical billiard-like particle represented by the envelope of $G(\vec{\rho}, \tau)$. In our previous work [83], we obtained solutions to (5.2.17) for $\gamma >> 1$, or, equivalently, for $v_g \simeq c$. To obtain an exact solution to equation (5.2.17), we express $G(\vec{\rho}, \tau)$ in the form

$$G(\vec{\rho}, \tau) = g(\vec{\rho}, \tau)\ e^{-i2\beta_0\gamma\tau} . \tag{5.2.18}$$

A substitution of (5.2.18) into (5.2.17) results in the Helmholtz equation

$$\nabla_T^2 g(\vec{\rho}, \tau) + \partial_\tau^2 g(\vec{\rho}, \tau) + 4\beta_0^2 \gamma^2 g(\vec{\rho}, \tau) = 0 . \tag{5.2.19}$$

The steps leading to (5.2.19) are interesting by themselves since they reduce the 3-D Klein-Gordon equation, which is hyperbolic, to a 3-D Helmholtz equation, which is elliptic. More importantly, however, a solution to equation (5.2.19) represents an envelope that travels with a velocity v_g and retains its shape for all time. As a consequence, a large class of exact nondispersive solutions to the 3-D Klein-Gordon equation can be derived from exact solutions to the Helmhotz equation. One possible solution can be expressed in terms of the spherical Bessel functions, viz.,

$$g(\vec{\rho}, \tau) = j_l(2\beta_0\gamma\ \mathrm{R})\ P_l^m(\tau/\mathrm{R})\ \cos(m\phi) ,$$

where $\mathrm{R} = \sqrt{\rho^2 + \tau^2}$, j_l is the spherical Bessel function of order l and P_l^m is the associated Legendre function. Now, exact solutions to the Klein-Gordon equation can be written as follows:

$$\Psi_{lm}(\vec{r}, t) = j_l(2\beta_0\gamma\ \mathrm{R})\ P_l^m(\tau/\mathrm{R})\ \cos(m\phi)\ e^{-i2\beta_0\gamma\tau}\ e^{i\beta_0\eta} . \tag{5.2.20}$$

For azimuthally symmetric solutions ($m = 0$), the zeroth order mode is given by

$$\Psi_{00}(\vec{r}, t) = j_0(2\beta_0\gamma\ \mathrm{R})\ e^{-i2\beta_0\gamma\tau}\ e^{i\beta_0\eta} . \tag{5.2.21}$$

Its amplitude decreases as ρ^{-1} in the transverse direction and as τ^{-1} in the direction of propagation. This is a property shared by all even modes (l = even integer .) On the other hand, odd modes are more localized in the transverse direction. To see this, consider the first order mode, viz.,

$$\Psi_{01}(\vec{r}, t) = j_1(2\beta_0\gamma\ \mathrm{R})\ \frac{\tau}{\mathrm{R}}\ e^{-i2\beta_0\gamma\tau}\ e^{i\beta_0\eta} . \tag{5.2.22}$$

For large arguments, $j_1(z) \simeq \sin(z - \pi/2)/z$; consequently, $\Psi_{01}(\vec{r}, t)$ decays as ρ^{-2} in the transverse direction, but still decays as τ^{-1} in the z-direction. These decay properties indicate that the solutions given in equation (5.2.20) have infinite total energy content, a feature they share with plane wave solutions and Brittingham's FWMs. In analogy to the FWMs, localized slowly decaying solutions to the Klein-Gordon equation, with a finite energy content, can be synthesized as a superposition of the wave packets given in equation (5.2.20).

As long as $\Psi(\vec{r}, t)$ is treated as a classical field, the kinematics of a particle represented by it can be derived from the energy and the momentum densities of a Klein-Gordon field [60], viz.,

$$H(\vec{r}, t) = c^{-2}\, \partial_t \Psi(\vec{r}, t)\, \partial_t \Psi^*(\vec{r}, t) + \nabla\Psi(\vec{r}, t) \cdot \nabla\Psi^*(\vec{r}, t) + \mu^2\, \Psi(\vec{r}, t)\, \Psi^*(\vec{r}, t) ,$$

$$\vec{P}(\vec{r}, t) = -\, c^{-2} \left[\partial_t \Psi(\vec{r}, t)\, \nabla\Psi^*(\vec{r}, t) + \partial_t \Psi^*(\vec{r}, t)\, \nabla\Psi(\vec{r}, t) \right] .$$

As mentioned earlier, solutions of infinite energy content, such as those given in equation (5.2.20), can be superimposed to obtain finite energy ones. In this case, the integration of $H(\vec{r}, t)$ and $\vec{P}(\vec{r}, t)$ over all space will give the energy and the momentum of the particle represented by such solutions. Another possibility is to search for nondispersive bump solutions of finite energy densities. For a solution of this kind the central portion of the field has a larger energy content and small oscillations compared to the tails. The relatively large oscillations of the tails cancel out on the average when such a field interacts with a large scale measuring instrument. Space will appear to be empty except for the large amplitude, oscillation-free central portion. In this case the energy and the momentum of the particle can be calculated by integrating the energy and momentum densities over the central part of the field. A crude example of what we mean is the integration of the one-dimensional function $\sin(x)/x$ over all values of x from $-\infty$ to $+\infty$. This will give a value of π which is approximately equal to the area under the first lobe of the function between its first two zeroes. In an interaction of such a field with another bump field (e.g., the FWM pulse), the interaction will be very large when the central parts of both fields overlap; at the same time the tails will be averaged out. In such a case the large amplitude central portions of the fields are the only

parts which really contribute to the interaction and can be measured. An interaction theory is needed to provide a more rigorous and complete discussion of this possibility; the developement of such a theory is out of the scope of this work.

Solutions describing nondispersive wave packets are not restricted to the form given in equation (5.2.20); as mentioned earlier, any solution to equation (5.2.17) will give a wavepacket that will keep its form as it travels in free space. A special case of these solutions has been derived by MacKinnon [75,76], who demonstrated that a de Broglie wavepacket can be formed by assuming that the phase of a particle's internal vibration is independent of the choice of a reference frame. MacKinnon's solution is almost identical to the Ψ_{00} mode, especially when the terms in the exponent are rearranged so that

$$\Psi_{00}(\vec{r}, t) = j_0(2\beta_0\gamma \, \mathrm{R}) \, e^{-i\beta_0\gamma^2(1+v_g^2/c^2)(z-(c^2/v_g)t)} . \tag{5.2.23}$$

Because of the close resemblance of the two solutions, it is of interest to compare more closely the methods leading to them. This comparison will be carried out in the next section, where the difference between the interpretations of the solution in (5.2.20) as a classical wave function and as a quantum mechanical wavepacket will be investigated. A discussion will also be provided of the dispersion relationships involved and their effect on the kinematics of a free particle represented by a wave packet such as the one in equation (5.2.23).

Before we proceed to the next section, it is worthwhile to point out that the de Broglie relationship between the group velocity v_g of the envelope and the phase velocity v_{ph} of the associated plane wave (i.e., $v_{ph}v_g = c^2$) is embodied automatically in equation (5.2.23) by simply imposing the requirement that $\Psi(\vec{r}, t)$ should be a nonsingular continuous wavepacket that does not disperse with time. It is quite interesting that the localization requirement alone can lead to such a relationship, without any reference to an "internal clock" of the particle, or the need for the assumption that the phase of the internal clock of the particle be equal to the phase of the associated wave, two concepts utilized by de Broglie to derive the relationship $v_{ph}v_g = c^2$ in his attempt to maintain the invariance of the relationship $mc^2 = h\nu$ for all frames of reference. The particle-wave velocity equation

$v_{ph}v_g = c^2$ has been considered [84] to be a generalization of the more limited velocity relation $v_g = v_{ph} = c^2$, which is true for massles particles only. Moreover, it has been argued by MacGregor [84] that the relationship $v_{ph}v_g = c^2$ should be taken as a basic postulate of special relativity, replacing the popular postulate that the speed of light in free space has the value c in all inertial frames.

5.3 NONDISPERSIVE WAVE PACKETS AND DISPERSION RELATIONSHIPS

The similarity between MacKinnon's solution and the Ψ_{00} mode is very clear when we recall that $j_0(x) = \sin(x)/x$. In order to examine these two results more carefully, we first write MacKinnon's 3-D wave packet [76] as

$$\Psi_M(\vec{r}, t) = \frac{\sin(k\mathrm{R})}{k\mathrm{R}} \; e^{i(\omega(k_0)t - k_0 z)} , \tag{5.3.1}$$

where

$$k = \mu , \tag{5.3.2}$$

$$\mathrm{R} = \sqrt{\rho^2 + \gamma^2 (z - vt)^2} . \tag{5.3.3}$$

The parameter k_0 was defined by MacKinnon in the case of the 1-D solution [75] as

$$k_0 = \gamma\mu \frac{v}{c} . \tag{5.3.4}$$

In the 3-D case, it is only correct up to a numerical factor of $\sqrt{2}$, as will be shown later. The frequency $\omega(k_0)$ entering into equation (5.3.1) was defined as

$$\omega(k_1) - \omega(k_0) = v\,(k_1 - k_0)\,, \tag{5.3.5}$$

with the provision that

$$\partial_{k_0}\,\omega(k_0) = v \quad \text{and} \quad \partial^2_{k_0}\,\omega(k_0) = 0\,, \tag{5.3.6}$$

These conditions were claimed by MacKinnon to be necessary for the wave packet to retain its form for all time. The velocity v of the particle is derived from the derivative of $\omega(k_0)$ with respect to k_0. However, the explicit dependence of $\omega(k_0)$ on k_0 is not very obvious, and the adequacy of the definition given by (5.3.5) is questionable.

Our aim in this section is to clarify these issues through a detailed analysis of the properties of the solutions given in equations (5.2.23) and (5.3.1). The main difference between the two solutions is that Ψ_{00} has been treated, until now, as a classical nondispersive wavepacket with an envelope that moves with a velocity v_g defined in equation (5.2.15). This is not, however, a unique velocity as will be shown in this section. The wave function Ψ_M, on the other hand, is considered to be a quantum mechanical entity moving with a velocity v derived from a dispersion relationship as in equation (5.3.6). In order to compare the two wave functions, we will consider Ψ_{00}, for the rest of this section, to be a quantum mechanical wave packet. In this case, the group velocity v_g might not be consistent with the fact that the kinematics of a particle should be derived from its phase factor. To check such an inconsistency we can refer to the particle's energy and momentum relationships. As stated earlier, the energy and the momentum can be calculated by taking the derivatives of the phase of Ψ_{00} with respect to time and space, respectively, viz.,

$$E = \hbar\,\partial_t\phi \quad , \quad p = -\hbar\,\nabla\,\phi\,. \tag{5.3.7}$$

Using $\Psi_{00}(\vec{r}, t)$ in equation (5.2.23) together with definition of v_g given by equation (5.2.15), we obtain the following expressions for the energy and the z-component of the momentum:

$$E = \frac{c^2}{[1 - v_g^2/c^2]^{1/2}} \, m_0 \, \frac{[1 + v_g^2/c^2]}{[1 - v_g^2/c^2]} \, , \tag{5.3.8a}$$

$$p_z = \frac{v_g}{[1 - v_g^2/c^2]^{1/2}} \, m_0 \, \frac{[1 + v_g^2/c^2]}{[1 - v_g^2/c^2]} \, . \tag{5.3.8b}$$

These are incorrect expressions unless we use an apparent rest mass

$$M_0 = m_0 \, \frac{[1 + v_g^2/c^2]}{[1 - v_g^2/c^2]} \, , \tag{5.3.9}$$

which is identical to the "apparent mass" introduced by de Broglie [30] in order to guarantee the consistency of the equations of motion of particles represented by such wave packets. The "apparent mass" is defined as

$$M_0 = \sqrt{m_0^2 + \delta m_0^2} \, , \tag{5.3.10a}$$

$$\delta m_0^2 = \frac{\hbar^2}{c^2} \, \frac{1}{|\Psi|} \, (c^{-2} \partial_t^2 - \nabla^2) \, |\Psi| \, . \tag{5.3.10b}$$

The redefinition of the mass M_0, as given in (5.3.9), produces the expected energy and momentum relations. The results are physically unattractive, however, because of the dependence of M_0 on v_g. On the other hand, MacKinnon [76] has indicated that his solution can not suffer from such a problem because, for $|\Psi| = \sin(\mu R)/\mu R$, it follows that $\delta m_0 = \mu\hbar/c$ and the apparent mass reduces to

$$M_0 = \sqrt{2} \, m_0 \, . \tag{5.3.11}$$

To overcome the difficulty associated with the solution $\Psi_{00}(\vec{r}, t)$ obtained by utilizing the bidirectional representation, we can start with the ansatz

$$\Psi(\vec{r}, t) = G(\vec{\rho}, z, t)\, e^{i\beta_0(z+(c^2/v)t)}\,, \tag{5.3.12}$$

where, now, the particle velocity, designated by v, is left undefined. Substitution of (5.3.12) into equation (5.2.1) gives a generalization of the partial differential equation (5.2.14), viz.,

$$\begin{aligned} i\,2\beta_0(\partial_z - v^{-1}\partial_t)\, G(\vec{\rho}, z, t) + (\partial_z^2 - c^{-2}\partial_t^2)\, G(\vec{\rho}, z, t) + \nabla_T^2 G(\vec{\rho}, z, t) \\ + (\beta_0^2\gamma^{-2}\,(c^2/v^2) - \mu^2)\, G(\vec{\rho}, z, t) = 0\,, \end{aligned} \tag{5.3.13}$$

where

$$\gamma = (1 - v^2/c^2)^{-1/2}\,.$$

Motivated by the convection term on the left hand side of equation (5.3.13), we can choose

$$G(\vec{\rho}, z, t) = g(\vec{\rho}, \tau)\, e^{-i2\beta_0\gamma\tau}\,, \qquad \tau = \gamma(z - vt)\,, \tag{5.3.14}$$

which reduces (5.3.13) into a Helmholtz equation; specifically,

$$\nabla_T^2 g(\vec{\rho}, \tau) + \partial_\tau^2 g(\vec{\rho}, \tau) + \chi^2 g(\vec{\rho}, \tau) = 0\,; \tag{5.3.15a}$$

$$\chi^2 = 4\beta_0^2\gamma^2 + \frac{\beta_0^2}{\gamma^2}\,\frac{c^2}{v^2} - \mu^2\,. \tag{5.3.15b}$$

A solution to the Klein-Gordon equation can be written now as follows:

$$\Psi(\vec{r}, t) = \frac{\sin(\chi \mathrm{R})}{\chi \mathrm{R}}\; e^{i\beta_0(1+v^2/c^2)\gamma^2(z-(c^2/v)t)}\,. \tag{5.3.16}$$

It should be noted that χ is identical to MacKinnon's k. The value of $v = v(\beta_0)$ can be deduced from the algebraic relationship (5.3.15b). Instead, we introduce the change of variables

$$k_0 = \beta_0 \gamma^2 \left(1 + v^2/c^2\right) , \tag{5.3.17}$$

which yields, upon substitution into equation (5.3.15b), the following expression for the velocity:

$$u = \pm \frac{c\, k_0}{\sqrt{k_0^2 + \chi^2 + \mu^2}} . \tag{5.3.18}$$

In the case of MacKinnon's wave packet, v was treated as a parameter independent of k_0. However, such an assumption does not make sense because the relationship $p_z = \hbar k_0$ for the momentum implies that p_z depends on k_0, and one expects the velocity to change as the momentum varies.

The definition of k_0 given in (5.3.17) changes the wave packet into the form

$$\Psi(\vec{r}, t) = \frac{\sin(\chi R)}{\chi R}\; e^{i(\omega(k_0)t - k_0 z)} , \tag{5.3.19}$$

where

$$\omega(k_0) = \frac{c^2}{v}\, k_0 . \tag{5.3.20}$$

An explicit dispersion relationship for $\omega(k_0)$ can be found by combining equations (5.3.18) and (5.3.20); specifically,

$$\omega(k_0) = \pm\, c \sqrt{k_0^2 + \chi^2 + \mu^2} . \tag{5.3.21}$$

The positive and negative signs correspond to positive and negative energies, respectively. It is tempting to think of χ and k_0 as transverse and longitudinal wavenumbers, respectively. This is not the case, however, and for the wave packet to represent a quantum mechanical particle moving in free space, we need to introduce the notion of an apparent mass M_0, as defined in equation (5.3.10).

It is straightforward to show that $M_0 = (\chi^2 + \mu^2)^{1/2}\hbar/c$, and using equation (5.3.21) we arrive at the familiar energy momentum relationship

$$E = \pm c\sqrt{p^2 + M_0^2 c^2} \ , \tag{5.3.22}$$

where we have made use of the relationships $p = \hbar k_0$ and $E = \hbar\omega(k_0)$.

If we choose $\chi = \mu$, the velocity relationship reduces to

$$u = \frac{c\,k_0}{\sqrt{k_0^2 + 2\mu^2}} \tag{5.3.23}$$

which resembles the group velocity of a 1-D wave packet with an "apparent mass" $M_0 = \sqrt{2}\ \mu\hbar/c$. Furthermore, using equation (5.3.23), an expression for k_0 can be easily derived, viz.,

$$k_0 = \sqrt{2}\ \gamma\mu\ \frac{v}{c} \ , \tag{5.3.24}$$

which is the correct definition of k_0 for the 3-D wave packet.

It should be pointed out that the velocity expression given in equation (5.3.18) satisfies neither (5.3.5) nor the second provision in equation (5.3.6), i.e., the conditions claimed by MacKinnon as necessary for the construction of nondispersive wave packets. The similarity between the definitions of v and v_g should, also, be noted. Beside the apparent mass factor of $\sqrt{2}$, the main difference between the expresions (5.2.15) and (5.3.23) is that β_0 is replaced by k_0. The velocity v, on the other hand, leads to the correct kinematics only because the momentum and energy operators are specified as in equation (5.3.7). If these operators are defined differently, we need a velocity different from v to get the correct kinematics.

5.4 A UNIDIRECTIONAL SUPERPOSITION

Before we deal with the Dirac equation we would like to comment on the bidirectional derivation of the wave packet solutions given in equations (5.2.20) and (5.3.19). Even though the bidirectional representation provided a systematic way to arrive at such solutions, the same results could be derived in a slightly different fashion. In particular, one can see that the final results are not bidirectional but rather unidirectional, in the sense that the envelopes and the phase modulation move in the same direction but at different speeds.

In retrospect, one could have started with the ansatz

$$\Psi(\vec{r}, t) = G(\vec{\rho}, z, t)\, e^{-i\alpha_0(z - t\,c^2/v_g)} \tag{5.4.1}$$

instead of equation (5.2.12). Substituting this new ansatz into the Klein-Gordon equation (5.2.1) gives

$$\begin{aligned} -i\,2\alpha_0(\partial_z + v_g^{-1}\partial_t)\, G(\vec{\rho}, z, t) + (\partial_z^2 - c^{-2}\partial_t^2)\, G(\vec{\rho}, z, t) + \nabla_T^2\, G(\vec{\rho}, z, t) - \mu^2\, G(\vec{\rho}, z, t) \\ + \alpha_0^2(c^2 v_g^{-1} - 1)\, G(\vec{\rho}, z, t) = 0\,, \end{aligned} \tag{5.4.2}$$

where v_g has been left undefined, as in Section 5.3. Again, motivated by the convection term in equation (5.4.2), we assume that

$$G(\vec{\rho}, z, t) = G(\vec{\rho}, \gamma(z - v_g t))\,.$$

This assumption reduces equation (5.4.2) to the Helmholtz equation

$$\nabla_T^2\, G(\vec{\rho}, \tau) + \partial_\tau^2\, G(\vec{\rho}, \tau) + \chi^2\, G(\vec{\rho}, \tau) = 0\,, \tag{5.4.3}$$

where $\tau = \gamma(z - v_g t)$ and χ obeys the same dispersion relationship as that given in Section 5.3; namely,

$$\chi^2 + \mu^2 + \alpha_0^2 = \alpha_0^2 c^2 / v_g^2 \,. \tag{5.4.4}$$

This dispersion relationship leads a definition of the group velocity, viz.,

$$v_g = \pm \frac{\alpha_0 \, c}{\sqrt{\alpha_0^2 + \mu^2 + \chi^2}} \,,$$

which is identical to that given in equation (5.3.18).

In the ansatz given in equation (5.4.1), we have used the specific "characteristic" variable

$$\zeta = z - \frac{c^2}{v_g} \, t \,, \tag{5.4.5a}$$

and it has been shown that its natural companion is

$$\eta = z - v_g t \,. \tag{5.4.5b}$$

This choice of "characteristics" changes the constraint relationship to

$$\mathrm{K}(\alpha, \beta, \vec{\kappa}) = [\kappa^2 + \mu^2 + \beta^2 \gamma^{-2} - \alpha^2 \gamma^{-2} \, (c^2 / v_g^2)] = 0 \,, \tag{5.4.6}$$

and a *unidirectional superposition* can be used to synthesize azimuthally symmetric solutions, viz.,

$$\begin{aligned} \Psi(\rho, \zeta, \eta) = \frac{1}{(2\pi)^2} \int_0^{\infty} d\kappa \int_{-\infty}^{+\infty} d\alpha \int_{-\infty}^{+\infty} d\beta \; \kappa \, J_0(\kappa\rho) \, e^{-i\alpha\zeta} \, e^{i\beta\eta} \, C(\alpha, \beta, \kappa) \\ \times \delta[\kappa^2 + \mu^2 + \beta^2 \gamma^{-2} - \alpha^2 \gamma^{-2} \, (c^2 / v_g^2)] \,. \end{aligned} \tag{5.4.7}$$

If we choose the spectrum as

$$C(\alpha, \beta, \kappa) = \overline{C}(\beta, \kappa)\, \delta(\alpha - \alpha_0)\ , \tag{5.4.8}$$

equation (5.4.7) reduces to

$$\Psi(\rho, \zeta, \eta) = \frac{e^{-i\alpha_0\zeta}}{(2\pi)^2} \int_0^{\infty} d\kappa \int_{-\infty}^{+\infty} d\beta\, \kappa\, J_0(\kappa\rho)\, e^{i\beta\eta}\, \overline{C}(\beta, \kappa)\, \delta[\kappa^2 + \mu^2 + \beta^2\gamma^{-2} - \alpha_0^2\gamma^{-2}\,(c^2/v_g^2)] \tag{5.4.9}$$

Using the dispersion relationship given in equation (5.4.4) and rearranging the argument of the delta function, we obtain

$$\Psi(\rho, \zeta, \eta) = \frac{e^{-i\alpha_0\zeta}}{(2\pi)^2} \int_0^{\infty} d\kappa \int_{-\infty}^{+\infty} d\beta\, \kappa\, J_0(\kappa\rho)\, e^{i\beta\eta}\, \overline{C}(\beta, \kappa)\, \delta[\kappa^2 - (\chi^2 - \beta^2\gamma^{-2})]\ . \tag{5.4.10}$$

Assuming that $|\beta| < \chi\gamma$, the integration over κ can be carried out; as a result,

$$\Psi(\rho, \zeta, \eta) = \frac{e^{-i\alpha_0\zeta}}{(2\pi)^2} \int_{-\chi\gamma}^{+\chi\gamma} d\beta\, \frac{1}{2}\, J_0\left[\frac{\rho}{\gamma}\sqrt{\gamma^2\chi^2 - \beta^2}\right] e^{i\beta\eta}\, \overline{C}\left(\beta, \sqrt{\gamma^2\chi^2 - \beta^2}\right)\ . \tag{5.4.11}$$

The following choice for the spectrum

$$\begin{aligned} \overline{C}(\beta, \kappa) &= (2\pi)^2 \quad , \quad |\beta| < \chi\gamma, \\ &= 0 \quad , \quad |\beta| > \chi\gamma \end{aligned} \tag{5.4.12}$$

will produce the wave packet solution given in equation (5.3.19).

Other solutions can be derived by choosing different spectra. For example, we can assume that $\kappa < \chi$ and carry out the integration over β first. Under this assumption we obtain

$$\Psi(\rho,\zeta,\eta)=\frac{e^{-i\alpha_0\zeta}}{(2\pi)^2}\int_0^{\chi}d\kappa\,J_0(\kappa\rho)\,\frac{\kappa\gamma}{\sqrt{\gamma^2\chi^2-\kappa^2}}\,\cos\left[\eta\gamma\sqrt{\chi^2-\kappa^2}\,\right]\overline{C}\left(\sqrt{\chi^2-\kappa^2}\,,\kappa\right). \tag{5.4.13}$$

We can choose the following spectrum:

$$\begin{aligned}\overline{C}(\beta,\kappa)&=\frac{(2\pi)^2}{\kappa\gamma}\quad,\quad 0<\kappa<\chi,\\ &=0\qquad,\quad \kappa>\chi\,.\end{aligned} \tag{5.4.14}$$

The integration over κ can be carried out by utilizing formula (6.737.3) in Gradshteyn and Ryzhik [47]. This results in the wave function

$$\Psi(\rho,\zeta,\eta)=\frac{\pi}{2}\,e^{-i\alpha_0\zeta}\,J_0\left[\frac{\chi}{2}\{\sqrt{\rho^2+\gamma^2\eta^2}-\gamma\eta\}\right]J_0\left[\frac{\chi}{2}\{\sqrt{\rho^2+\gamma^2\eta^2}+\gamma\eta\}\right]. \tag{5.4.15}$$

It is seen that choosing a natural combination of "characteristic" variables facilitates the evaluation of the superposition integrals and provides a great flexibility in deriving wave packet solutions to the Klein-Gordon equation.

The "double Bessel" solution given in equation (5.4.15) is more localized in the transverse direction than MacKinnon's wave packet. At the plane $\eta=0$, we have

$$\Psi(\rho,\zeta,0)=\frac{\pi}{2}\,e^{-i\alpha_0\zeta}\,J_0^2(\chi\rho/2)\,. \tag{5.4.16}$$

For large arguments, the Bessel function can be approximated by [49]

$$J_o(x)\sim\sqrt{\frac{2}{\pi x}}\,\cos(x-\frac{\pi}{4})\,. \tag{5.4.17}$$

When this property is used in conjunction with (5.4.16), it is seen that the "double Bessel" falls off as ρ^{-1} on the plane $\eta=0$; on the other hand, MacKinnon's wave packet decays as $\rho^{-1/2}$.

We shall consider, next, the behavior of the solution given in (5.4.15) for $\gamma\eta >> \rho$. The large argument approximation given in (5.4.19) yields

$$\Psi(\rho,\zeta,\eta) = \frac{2}{\chi\rho}\, e^{-i\alpha_0\zeta} \cos\left[\frac{\chi}{2}\{\sqrt{\rho^2+\gamma^2\eta^2} - \gamma\eta\} - \frac{\pi}{4}\right] \cos\left[\frac{\chi}{2}\{\sqrt{\rho^2+\gamma^2\eta^2} + \gamma\eta\} - \frac{\pi}{4}\right]. \tag{5.4.18}$$

It is clear that apart from the oscillatory terms in equation (5.4.18), the magnitude of $\Psi(\rho,\zeta,\eta)$ is independent of η. The amplitude of the packet solution (5.4.15) thus stays constant and does not fall off along the direction of propagation as long as $1 << \chi[(\rho^2+\gamma^2\eta^2)^{1/2} - \gamma\eta]/2$. Using a binomial expansion for $\gamma\eta >> \rho$, this condition can be approximated by $1 << \chi\rho^2/4\gamma\eta$. Hence, as long as $\gamma\eta << \chi\rho^2/4$, the solution does not fall off in the z-direction. As η increases, such that $\gamma\eta > \chi\rho^2/4$, the Bessel function $J_0[\chi\{(\rho^2+\gamma^2\eta^2)^{1/2} - \gamma\eta\}/2]$ approaches 1, while the other Bessel function in (5.4.15) falls off as $(\gamma\eta)^{-1/2}$. The "double Bessel" solution is thus less localized along the direction of propagation than MacKinnon's packet that falls off as $(\gamma\eta)^{-1}$. At the same time, the "double Bessel" wave packet is more localized in the transverse direction, where its amplitude decreases as ρ^{-2} instead of the ρ^{-1} characterizing MacKinnon's solution.

It is of interest to point out that the solution given in equation (5.4.15) provides us with new solutions to the Helmholtz equation

$$\nabla^2 \Psi_H(\rho,z) + \chi^2 \Psi_H(\rho,z) = 0\,. \tag{5.4.19}$$

In particular, an exact solution to equation (5.4.16) can be written as follows:

$$\Psi_H(\rho,z) = \frac{\pi}{2}\, J_0\left[\frac{\chi}{2}\{\sqrt{\rho^2+z^2} - z\}\right] J_0\left[\frac{\chi}{2}\{\sqrt{\rho^2+z^2} + z\}\right]. \tag{5.4.20}$$

This "double Bessel" solution has an infinite energy content, and it represents a standing wave.

5.5 THE DIRAC EQUATION

The exposition given in Chapter 2 might give one the impression that the bidirectional representation is only applicable to second-order equations which are quadratic in the time derivative. This is not the case, since it can be applied to the Schrodinger equation as well as the Dirac equation. In this section the de Broglie wave packet derived in the case of a scalar Klein-Gordon field will be used to find nondispersive wave packets for the vector fields representing massive spin 1/2 fermions. Such particles are naturally represented by the Dirac equation. It is well known, however, that fermions can be represented rather satisfactorily by a spinorial form of the Klein-Gordon equation [85].

We begin with the second order equation

$$(ic^{-1}\,\partial_t + \vec{\sigma}.\nabla)\,(ic^{-1}\,\partial_t - \vec{\sigma}.\nabla)\,\phi(\vec{r}\,,t) = \mu^2\,\phi(\vec{r}\,,t)\,, \tag{5.5.1}$$

where $\vec{\sigma}$ are Pauli matrices, viz.,

$$\sigma_x = \begin{bmatrix} 0 & 1 \\ 1 & 0 \end{bmatrix}\,,\quad \sigma_y = \begin{bmatrix} 0 & -i \\ i & 0 \end{bmatrix}\,,\quad \sigma_z = \begin{bmatrix} 1 & 0 \\ 0 & -1 \end{bmatrix}, \tag{5.5.2}$$

and $\phi(\vec{r}\,,t)$ is a two-component spinor. Making use of the properties of the Pauli matrices it can be shown that equation (5.5.1) can be reduced to the two-component spinorial Klein-Gordon equation

$$(c^{-2}\partial_t^2 - \nabla^2)\,\phi(\vec{r}\,,t) + \mu^2\,\phi(\vec{r}\,,t) = 0\,. \tag{5.5.3}$$

To find a nondispersive packet solution representing a massive spin 1/2 field, we can choose a solution to equation (5.5.3) similar to that given in equation (5.3.19); namely,

$$\phi(\vec{r}, t) = \begin{bmatrix} \phi_a \\ \phi_b \end{bmatrix} j_0(\chi R)\, e^{i(\omega(k_0)t - k_0 z)} . \tag{5.5.4}$$

This spinor field can be used to derive solutions to the Dirac equation

$$(\gamma_\mu \frac{\partial}{\partial x_\mu} + \mu)\, \Psi_D(\vec{r}, t) = 0 , \tag{5.5.5}$$

The definitions of the gamma matrices entering into this equation are given in Ref. 85. $\Psi_D(\vec{r}, t)$ is a four-component spinor defined as follows:

$$\Psi_D(\vec{r}, t) = \begin{bmatrix} \phi^R(\vec{r}, t) + \phi^L(\vec{r}, t) \\ \phi^R(\vec{r}, t) - \phi^L(\vec{r}, t) \end{bmatrix} . \tag{5.5.6}$$

The two-component spinors $\phi^L(\vec{r}, t)$ and $\phi^R(\vec{r}, t)$ are related to $\phi(\vec{r}, t)$ given in equation (5.5.4) as follows:

$$\phi^L(\vec{r}, t) = \phi(\vec{r}, t) , \tag{5.5.7a}$$

$$\phi^R(\vec{r}, t) = \frac{i}{\mu} (c^{-1}\partial_t - \vec{\sigma}.\nabla)\, \phi(\vec{r}, t) . \tag{5.5.7b}$$

Carrying out the operations indicated in (5.5.7b), we find that

$$\Psi_D(\vec{r}, t) = \begin{bmatrix} \psi_1 \\ \psi_2 \\ \psi_3 \\ \psi_4 \end{bmatrix} e^{i(\omega t - k_0 z)} , \tag{5.5.8}$$

where

$$\psi_1 = \phi_a \left\{ i(1+\tfrac{v}{c})\,\chi j_1(\chi R)\,\gamma^2 \frac{(z-vt)}{\mu R} + (1-\frac{\omega}{\mu c}-\frac{k_0}{\mu})\,j_0(\chi R) \right\} + i\phi_b\,\chi j_1(\chi R)\frac{(x-iy)}{\mu R} \quad ,(5.5.8a)$$

$$\psi_2 = i\phi_a\,\chi j_1(\chi R)\frac{(x+iy)}{\mu R} - \phi_b \left\{ i(1-\tfrac{v}{c})\,\chi j_1(\chi R)\,\gamma^2 \frac{(z-vt)}{\mu R} - (1-\frac{\omega}{\mu c}+\frac{k_0}{\mu})\,j_0(\chi R) \right\} , \quad (5.5.8b)$$

$$\psi_3 = \phi_a \left\{ i(1+\tfrac{v}{c})\,\chi j_1(\chi R)\,\gamma^2 \frac{(z-vt)}{\mu R} - (1+\frac{\omega}{\mu c}+\frac{k_0}{\mu})\,j_0(\chi R) \right\} + i\phi_b\,\chi j_1(\chi R)\frac{(x-iy)}{\mu R} \quad ,(5.5.8c)$$

$$\psi_4 = i\phi_a\,\chi j_1(\chi R)\frac{(x+iy)}{\mu R} - \phi_b \left\{ i(1-\tfrac{v}{c})\,\chi j_1(\chi R)\,\gamma^2 \frac{(z-vt)}{\mu R} + (1+\frac{\omega}{\mu c}-\frac{k_0}{\mu})\,j_0(\chi R) \right\} . \quad (5.5.8d)$$

The four independent solutions to the Dirac equation can be directly obtained from equation (5.5.8) using the negative and positive energy values of $\omega(k_0)$, in addition to choosing ϕ_a and ϕ_b so that two independent solutions for $\phi(\vec{r},t)$ can be obtained, e.g., $\phi_a = 0$, $\phi_b = 1$ and $\phi_a = 1$, $\phi_b = 0$. These solutions seem to be quite complicated; nevertheless, they represent a field peaked around the origin that travels in a straight line in free space and does not disperse for all time. Despite the complicated form of the solutions, still some physical results can be obtained. For example, the four independent solutions given in equation (5.5.8) are not eigenspinors of the helicity operator Σ_z defined as

$$\Sigma_z = \begin{bmatrix} \sigma_z & 0 \\ 0 & \sigma_z \end{bmatrix} . \quad (5.5.9)$$

Moreover, if we choose $\phi_a = 1$ and $\phi_b = 0$, the solution given in (5.5.8) is still not an eigenstate. We are mainly interested, however, in the large amplitude portion of the field around the center of the pulse ($x = 0$, $y = 0$, $z = vt$). In this portion, $j_1(\chi R) \simeq 0$, while $j_0(\chi R) \simeq 1$. Therefore, the components of the spinor given in equation (5.5.8) can be approximated around the center of the pulse as

$$\psi_1 \simeq 1 - \frac{\omega}{\mu c} - \frac{k_0}{\mu} \ ,$$

$$\psi_2 \simeq 0 \ ,$$

$$\psi_3 \simeq 1 + \frac{\omega}{\mu c} + \frac{k_0}{\mu} \ ,$$

$$\psi_4 \simeq 0 \ ,$$

and $\Psi_D(\vec{r}, t)$ becomes an eigenspinor of the helicity operator with an eigenvalue + 1. The same argument can be repeated for $\phi_a = 0$ and $\phi_b = 1$ in order to obtain an eigenspinor with an eigenvalue equal to -1. Similarly, we can get two independent eigenspinors for negative energies with eigenvalues + 1 and -1.

5.6 *SUMMARY AND CONCLUSION*

The bidirectional representation has been used to derive localized, nondispersive solutions to the Klein-Gordon equation by reducing it to a Helmholtz equation with its z coordinate replaced by the translational variable $\tau = \gamma(z - vt)$. The ansatz leading to such a reduction allows one to derive systematically a large class of nondispersive wavepackets, representing massive particles, by making use of the known solutions to the Helmholtz equation. In seeking solutions of this type the particle-wave velocity relationship $v_{ph}v_g = c^2$ follows automatically from the sole requirement of particle localization. The importance of this result need not be emphasized. It is quite intriguing, however, that in order to derive a nondispersive localized solution to the Klein-Gordon equation we arrive at a relationship that guarantees the Lorentz invariance of the formula $h\nu = mc^2$ and which can be used to generalize the postulates of spectial relativity [84].

A special case of the solutions derived in connection with the Klein-Gordon equation was MacKinnon's nondispersive wave packet. A comparison of this packet to our results helped in clarifying some of the subtleties in MacKinnon's solution; his parameters k, k_0 are now well defined and an explicit form of the dispersion relationship $\omega(k_0)$ has been derived. The derivative of $\omega(k_0)$ with respect to k_0 gives an expression of the velocity which does not satisfy equation (5.3.5); furthemore, $\omega(k_0)$ is a nonlinear function of k_0, thus violating MacKinnon's condition $\partial^2_{k_0}\,\omega(k_0) = 0$. The dependence of the velocity on k_0 is expected if one recalls the momentum relationship $p_z = \hbar k_0$; as the momentum of the particle increases, one expects the group velocity of the wave packet representing the particle to increase also.

It has been shown that the "apparent mass" introduced by de Broglie has to be used in order to obtain the correct energy and momentum describing the motion of massive particles. For the specific wave packet given in equation (5.3.16) the "apparent mass" has the value $\hbar c^{-1}(\chi^2 + \mu^2)^{1/2}$. Choosing χ to be proportional to μ through a numerical factor independent of v_g, it follows that M_0 is proportional to the rest mass m_0. On the other hand, if χ is chosen to depend on v_g, the "apparent mass" M_0 depends on the velocity of the particle, a property which is not very attractive.

Although the bidirectional representation provided a systematic way to arrive at the Klein-Gordon wave packets [cf. equation (5.3.19)], the same results can be obtained through a unidirectional superposition. The latter representation uses the natural "characteristic" variables of the Klein-Gordon equation, namely, $\zeta = z - t\,c^2/v_g$ and $\eta = z - v_g t$. The use of these "characteristic" variables leads to a class of new solutions which could be easily related to solutions of the Helmholtz equation.

The results obtained for the case of the scalar massive Klein-Gordon fields were extended to the spinor massive fields governed by the Dirac equation giving de Broglie nondispersive wave packets representing free massive fermions. This particular application demonstrates that bidirectional solutions can also be derived for field equations characterized by first order time derivatives. Similar solutions can be obtained for the Schrodinger equation and will be derived in the next chapter because of their relevance to an interesting class of nondispersive solutions to the Schrodinger equation introduced by Berry and Balazs [86].

In summary, localized, nonsingular and nondispersive solutions have been derived to linear equations governing the motion of massive particles; specifically, the Klein-Gordon equation and the Dirac equation. Unlike soliton solutions to nonlinear equations, these are solutions to linear equations that can explain the localization properties of particles, at least in free motion. If $\Psi(\vec{r}, t)$ is treated as a quantum mechanical wave packet, the kinematics of a particle represented by such a field are derived from its phase. On the other hand, if we consider $\Psi(\vec{r}, t)$ to be a classical field, the kinematics are derived from the energy and momentum densities. A linear superposition can be used to construct finite energy, slowly spreading wave packets. As a consequence, an integration over all space of the field's energy and momentum densities will give the particle's energy and momentum. Another possibility is to derive nonsingular bump field solutions (not neccessarily of finite total energy content) of a large amplitude at the center and much smaller amplitudes but highly oscillatory tails. During an interaction these tails are averaged out and only the central portion of the field can be felt. The kinematics of a particle are, thus, related to the momentum and energy content of the central field.

6.0 NONDISPERSIVE WAVE PACKET SOLUTIONS TO THE SCHRODINGER EQUATION

In this chapter we would like to demonstrate that the bidirectional representation can be used to derive exact, nonspreading, bump-like solutions to the Schrodinger equation. This equation is characterized by a single time derivative, in contradistinction to the quadratic time derivatives characterizing the scalar wave and Klein-Gordon equations. Maxwell's and Dirac's equations contain only first order derivatives in time, however, bump solutions for such equations were derived by making use of bidirectional solutions to the scalar wave and Klein-Gordon equations. In the nonrelativistic limit, the Klein-Gordon equation reduces to the Schrodinger equation. The latter is inherently linear with respect to time derivatives. It is of interest to see if bidirectional solutions can be derived for such a structure.

An interesting nonspreading solution to the 1-D force free Schrodinger equation was derived by Berry and Balazs [86]. Inspite of the absence of forces, the wave packet reported by Berry and Balazs moves with a uniform acceleration. It was argued by the authors that the "Airy packet" represents an ensemble of an infinite number of particles. That interpretation was inspired, basically,

by an analogy with semiclassical ray theory. They demonstrated that the particles' trajectories on a spacetime diagram form a caustic which corresponds to the classical boundary describing the motion of the largest amplitude of the wave function. Berry and Balazs demonstrated, also, that the tendency of the wave packet to accelerate is counterbalanced by the action of a constant force. This result stimulated another interpretation due to Greenberger [87] who demonstrated that such a solution can represent a free falling particle in a gravitational field.

It is our intent in this section to extend the ideas of Berry, Balazs and Greenberger to the 3-D Schrodinger equation. This work will lead us also to a class of unusual solutions to the 3-D scalar wave equation.

6.1 NONDISPERSIVE WAVE PACKETS OF UNIFORM VELOCITY

The force-free 3-D Schrodinger equation

$$i\hbar\partial_t \Psi(\vec{r}, t) + \frac{\hbar^2}{2m}\,\partial_z^2 \Psi(\vec{r}, t) + \frac{\hbar^2}{2m}\,\nabla_T^2 \Psi(\vec{r}, t) = 0 \tag{6.1.1}$$

is usually used to represent nonrelativistic massive particles. The wave function $\Psi(\vec{r}, t)$ is considered to be an abstract quantity that does not have any direct physical significance. Only $|\Psi(\vec{r}, t)|^2$ is interpreted as the probability of finding the particle at a certain point $\vec{r}$ and time t. At the time of the inception of equation (6.1.1), Schrodinger attempted to attach real physical significance to the wave function Ψ. Specifically, he tried to use it as a representation of the distribution of the particle's charge. That attempt was met with severe opposition, mainly because of the dispersive character of any finite energy solutions to equation (6.1.1). Nevertheless, Schrodinger, together

with Einstein and de Broglie, remained skceptical of the probabilistic interpretation of the quantum theory.

Following ideas that are essentially the same as those advocated in the preceding chapters, we shall attempt to derive exact bump solutions to the Schrodinger equation (6.1.1). We begin by taking the Fourier transform with respect to the transverse component [cf. equation (2.2.6)]. This operation reduces equation (6.1.1) to

$$i\hbar\partial_t \tilde{\psi}(\vec{\kappa}, z, t) + \frac{\hbar^2}{2m}\,\partial_z^2 \tilde{\psi}(\vec{\kappa}, z, t) + \frac{\hbar^2}{2m}\,\kappa^2 \tilde{\psi}(\vec{\kappa}, z, t) = 0\,. \tag{6.1.2}$$

Motivated by the bidirectional solutions to the Klein-Gordon equation, we use the function

$$\psi_e(z, t;\beta, \alpha) = e^{-i\beta\eta}\, e^{i\alpha\zeta}\,, \tag{6.1.3}$$

as a an elementary solution to equation (6.1.2). It should be noted that the arguments of the exponential functions entering into (6.1.3) have signs opposite to those used in previous chapters. This particular use of signs is a consequence of the sign of the time derivative appearing in equation (6.1.1). The choice made in equation (6.1.3) will yield only positive energy solutions, as expected for a nonrelativistic particle. The characteristics given in equations (5.2.8a) and (5.2.8b) can be used to derive the corresponding nonrelativisitic characteristic variables associated with the Schrodinger equation. For the former we have

$$\zeta = z - ct\,\frac{sgn(\alpha)}{\alpha}\,\mu(1 + \alpha^2/\mu^2)^{1/2}\,.$$

For $\alpha << \mu$ we get

$$\zeta = z - ct\,\frac{sgn(\alpha)}{\alpha}\,\frac{\alpha^2\hbar}{2m} - t\,sgn(\alpha)\,\frac{mc^2}{\hbar\alpha}\;; \tag{6.1.4a}$$

similarly, for $\beta << \mu$,

$$\eta = z + ct\,\frac{sgn(\beta)}{\beta}\,\frac{\beta^2\hbar}{2m} + t\,sgn(\beta)\,\frac{mc^2}{\hbar\beta}\ . \tag{6.1.4b}$$

In the last two expressions, the relation $\mu = mc/\hbar$ has been used.

The elementary function given in equation (6.1.3) is a solution to the Schrodinger equation if the constraint relationship

$$K(\alpha, \beta, \vec{\kappa}) = (\,sgn(\alpha) + sgn(\beta)\,)\,\frac{mc^2}{\hbar} + sgn(\alpha)\,\alpha^2 + sgn(\beta)\,\beta^2 - (\alpha - \beta)^2 - \kappa^2 = 0 \tag{6.1.5}$$

is satisfied. If we choose to work on the positive branch of α and β, it follows that

$$K(\alpha, \beta, \vec{\kappa}) = 2\,\frac{mc^2}{\hbar} + 2\alpha\,\beta - \kappa^2 = 0\ . \tag{6.1.6}$$

A linear superposition of the type used in Chapter 5 leads to the general solution

$$\Psi(\vec{r}\,, t) = \frac{e^{-i2mc^2\,t/\hbar}}{(2\pi)^2}\int_{R^2} d\vec{\kappa}\; e^{-i\vec{\kappa}\cdot\vec{\rho}}\int_0^\infty d\alpha\int_0^\infty d\beta\; C(\alpha, \beta, \vec{\kappa})\;\delta[K(\alpha, \beta, \vec{\kappa})] \times e^{i\alpha(z - t\,\alpha\hbar/2m)}\,e^{-i\beta(z + t\,\beta\hbar/2m)}\ . \tag{6.1.7}$$

It should be pointed out that the rest energy terms $t\,sgn(\alpha)mc^2/\hbar\alpha$ and $t\,sgn(\beta)mc^2/\hbar\beta$ introduced via the characteristic variables (6.1.4a) and (6.1.4b) contribute only to the oscillatory phase $\exp(-i2mc^2\,t/\hbar)$. Apart from a factor of 2, this term reminds us of the particle's internal oscillation associated with a de Broglie wave [30].

Choosing the spectrum entering into equation (6.1.7) as

$$C(\alpha, \beta, \vec{\kappa}) = \overline{C}(\beta, \vec{\kappa})\;\delta(\alpha - \alpha_0)\ , \tag{6.1.8}$$

yields a wave function of the form

$$\Psi(\vec{r}, t) = G(\vec{\rho}, z, t)\, e^{i\alpha_0(z - t\,\alpha_0\hbar/2m)} e^{-imc^2 t/\hbar}, \tag{6.1.9a}$$

where

$$G(\vec{\rho}, z, t) = \frac{e^{-imc^2 t/\hbar}}{(2\pi)^2} \int_{R^2} d\vec{\kappa}\, e^{-i\vec{\kappa}\cdot\vec{\rho}} \int_0^\infty d\beta\, \overline{C}(\beta, \vec{\kappa})\; \delta[\mathrm{K}(\alpha, \beta_0, \vec{\kappa})]\, e^{-i\beta(z + t\,\beta\hbar/2m)}\,. \tag{6.1.9b}$$

Further progress depends on the choice of the spectrum $\overline{C}(\beta, \vec{\kappa})$. Instead of following this path, we shall adopt the procedure developed in Chapter 5 and substitute the expression (6.1.9a) directly into equation (6.1.1) to obtain

$$mc^2\, G(\vec{\rho}, z, t) + i\hbar\, v_g(\partial_z + v_g^{-1}\partial_t)\, G(\vec{\rho}, z, t) + \frac{\hbar^2}{2m}\, \partial_z^2\, G(\vec{\rho}, z, t) + \frac{\hbar^2}{2m}\, \nabla_T^2\, G(\vec{\rho}, z, t) = 0\,, \tag{6.1.10}$$

where the group velocity v_g is chosen as

$$v_g = \frac{\alpha_0 \hbar}{m}\,. \tag{6.1.11}$$

Motivated by the convection term $(\partial_z + v_g^{-1}\partial_t)\, G(\vec{\rho}, z, t)$, we assume that $G(\vec{\rho}, z, t)$ depends on z and t through the new variable $\tau = z - v_g t$; specifically,

$$\Psi(\vec{r}, t) = G(\vec{\rho}, z - v_g t)\, e^{i(mv_g/\hbar)(z - v_g t/2)}\, e^{-i(mc^2/\hbar)t}\,. \tag{6.1.12}$$

In this case, equation (6.1.10) reduces to the Helmholtz equation

$$\nabla_T^2\, G(\vec{\rho}, \tau) + \partial_\tau^2\, G(\vec{\rho}, \tau) + 2\mu^2\, G(\vec{\rho}, \tau) = 0\,. \tag{6.1.13}$$

By analogy to the solutions obtained for the Klein-Gordon equation, one can choose a solution to equation (6.1.13) of the form

$$G(\vec{\rho}, \tau) = j_l(\sqrt{2}\,\mu\,\mathrm{R})\, P_l^m(\tau/\mathrm{R})\, \cos(m\phi)\,, \tag{6.1.14}$$

where $\mathrm{R} = [\rho^2 + \tau^2]^{1/2}$ and $\mu = mc/\hbar$. Invoking azimuthal symmetry we arrive, finally, at the following nondispersive wavepacket solution to the Schrodinger equation:

$$\Psi(\vec{r}, t) = j_0\left[\sqrt{2}\,\mu(\rho^2 + (z - pt/m)^2)^{1/2}\right] e^{ipz/\hbar}\, e^{-i(p^2/2m)t/\hbar}\, e^{-i(mc^2)t/\hbar}\,. \tag{6.1.15}$$

In equation (6.1.15) we have used the nonrelativistic definition of momentum; namely, $p = mv_g$. It is of great interest to point out that if the wave function (6.1.15) is used as a classical entity, the center of its envelope will move with a velocity equal to p/m. On the other hand, if it is treated as a quantum mechanical object, its momentum can be obtained from the derivative of the phase with respect to z. This operation will give a momentum equal to p, which is exactly equal to the product of the mass m and the velocity v_g of the classical envelope. It is seen, then, that the kinematics of a free particle represented by the wavepacket (6.1.15) are the same, both in the classical or the quantum mechanical interpretation. As far as the energy is concerned, it can be seen that the kinetic energy $p^2/2m$ is added to the rest energy mc^2. It seems that the rest energy term is retained just for convenience; nevertheless, if such a term had not been taken into consideration, equation (6.1.13) would have degenerated into a Laplace equation and no localized solutions could have been derived. Solutions to the Schrodinger equation are derived up to a phase factor dependent on t. This corresponds to the choice of the reference zero energy. Choosing the nonrelativistic reference point at mc^2 will not yield a packet solution. Allowing, on the other hand, the reference energy to be equal to zero (i.e., the total energy is equal to the kinetic energy plus the rest energy) will produce a packet solution to the Schrodinger equation. It is quite interesting to note, also, that the γ factor appearing naturally in the packet solution to the relativistic Klein-Gordon equation is absent from the corresponding solution to the nonrelativistic Schrodinger equation. As a consequence, the central portion of the Schrodinger wave packet does not undergo any length shrinking, as it is the case for the Klein-Gordon wave packet; and all the relativistic effects disappear.

6.2 NONDISPERSIVE ACCELERATING WAVE PACKETS

It was realized by Berry and Balazs [86] that the force-free 1-D Schrodinger equation

$$i\hbar\partial_t \psi(x, t) + \frac{\hbar^2}{2m}\,\partial_x^2 \psi(x, t) = 0 \tag{6.2.1}$$

has a unique nonspreading packet solution expressed in terms of the Airy function [49], viz.,

$$\psi(x, t) = \mathrm{Ai}\left[\frac{B}{\hbar^{2/3}}\left(x - \frac{B^3 t^2}{4m^2}\right)\right] e^{i(B^3 t/2m\hbar)[x - (B^3 t^2/6m^2)]}\,. \tag{6.2.2}$$

The square of the envelope $|\psi|^2$ of this wave packet travels in free space without any spreading. It is interesting, also, to note that it is moving with a velocity equal to $B^3t/2m^2$ which increases linearly with time. This means that the Airy packet (6.2.2) is moving with a uniform acceleration even though the Schrodinger equation (6.2.1) is force-free. Berry and Balazs provided an explanation of this unusual behavior by resorting to an integral representation of (6.2.2) which is composed of a superposition of plane waves. Assigning a particle to each plane wave and using an analogy to ray theory, they argued that the Airy packet corresponds to an ensemble of an infinite number of particles. The straight trajectories of these particles in a spacetime diagram are enveloped by a parabolic caustic. The curvature of the caustic embodies the acceleration of the classically allowed region, which corresponds to the point where $x = B^3t^2/4m^2$. Berry and Balazs illustrated, furthermore, that if the Airy packet is allowed to evolve not in free space, but in a linear potential

$$V(x, t) = \frac{B^3}{2m}\,x\,, \tag{6.2.3}$$

the resulting force will be just enough to overcome the packet's natural tendency to accelerate and will bring its center to rest.

An alternative interpretation was provided by Greenberger [87] who argued that the Airy packet can be used to represent a free nonrelativistic particle falling in a constant gravitational field. Using the generalized Galilean transformation

$$x' = x + \xi(t) \quad \text{and} \quad t = t' , \tag{6.2.4}$$

Greenberger was able to change the forced Schrodinger equation

$$i\hbar\partial_t \chi(x, t) + \frac{\hbar^2}{2m} \partial_x^2 \chi(x, t) + \frac{B^3 x}{2m} \chi(x, t) = 0 , \tag{6.2.5}$$

to the force-free equation

$$i\hbar\partial_t \psi(x', t) + \frac{\hbar^2}{2m} \partial_{x'}^2 \psi(x', t) = 0 . \tag{6.2.6}$$

The new function $\psi(x', t)$ being related to the wave function $\chi(x, t)$ through the transformation

$$\chi(x, t) = \psi(x', t)\, e^{-i(m/\hbar)[\dot{\xi}(t)x' - \int dt\, \dot{\xi}^2(t)/2]} . \tag{6.2.7}$$

In the last expression $\dot{\xi}(t)$ denotes the time derivative of the function $\xi(t)$; the latter is governed by the equation of motion

$$m \frac{d^2\xi(t)}{dt^2} = -\frac{B^3}{2m} . \tag{6.2.8}$$

The wave function $\psi(x', t)$ representing a free particle is just the Airy packet given in equation (6.2.2); however, it has been transformed from the initial uniformly gravitating frame of reference x to a free falling frame denoted by x'. The equivalence principle states that all forces disappear in

a free falling system. This explains how Berry and Balazs were able to derive an accelerating wave packet solution to a force-free equation. It was, thus, concluded by Greenberger that the Airy packet does not spread out because it is a stationary state in a uniform gravitational field.

6.3 3-D NONSPREADING WAVE PACKETS

The Airy packet given in equation (6.2.2) can be directly generalized to obtain nonspreading 3-D solutions. This can be carried out by making use of the integral representation of the Airy packet [86], viz.,

$$\psi(x, t) = \frac{\hbar^{2/3}}{2\pi B} \int_{-\infty}^{+\infty} dk\, e^{i[kx - (\hbar k^2 t/2m) + (\hbar^2 k^3/3B^3)]} . \tag{6.3.1}$$

This result is based on a Fourier decomposition of the 1-D Schrodinger equation (6.2.1). For the 3-D case we have the integral representation

$$\Psi(\vec{r}, t) = \frac{\hbar^2}{(2\pi)^3 B^3} \int_{-\infty}^{+\infty} dk_x \int_{-\infty}^{+\infty} dk_y \int_{-\infty}^{+\infty} dk_z\, F(\vec{k})\, e^{i(\vec{k}\cdot\vec{r} - \hbar|k|^2 t/2m)} , \tag{6.3.2}$$

where $|k|^2 = k_x^2 + k_y^2 + k_z^2$. A choice for the spectrum equivalent to that given in equation (6.3.1), namely,

$$F(\vec{k}) = e^{i\hbar^2(k_x^3 + k_y^3 + k_z^3)/3B^3} , \tag{6.3.3}$$

yields the following accelerating 3-D wave packet:

$$\Psi(\vec{r},t)=\mathrm{Ai}\left[\frac{B}{\hbar^{2/3}}\left(x-\frac{B^3t^2}{4m^2}\right)\right]\mathrm{Ai}\left[\frac{B}{\hbar^{2/3}}\left(y-\frac{B^3t^2}{4m^2}\right)\right]\mathrm{Ai}\left[\frac{B}{\hbar^{2/3}}\left(z-\frac{B^3t^2}{4m^2}\right)\right] \times e^{i(B^3t/2m\hbar)[x+y+z-(B^3t^2/2m^2)]}. \tag{6.3.4}$$

Another type of solution to the 3-D Schrodinger equation can be derived directly from equation (6.3.1); specifically

$$\Psi(\vec{r},t)=\frac{\hbar^{2/3}}{2\pi B}\int_{-\infty}^{+\infty}dk\, e^{i[kx+ky+kz-(3\hbar k^2t/2m)+(\hbar^2k^3/3B^3)]}. \tag{6.3.5}$$

Carrying out the integration over k, we get

$$\Psi(\vec{r},t)=\mathrm{Ai}\left[\frac{B}{\hbar^{2/3}}\left(x+y+z-\frac{9B^3t^2}{4m^2}\right)\right]e^{i(3B^3t/2m\hbar)[x+y+z-(3B^3t^2/2m^2)]}. \tag{6.3.6}$$

The solutions given in equations (6.3.4) and (6.3.6) are characterized by an oscillatory behavior for negative envelope arguments. They rise to their maxima at points very close to the zeros of the envelope arguments and fall off exponentially to zero for positive arguments. For example, the solution given in equation (6.3.4) has its greatest value at a point very close to $x=y=z=B^3t^2/4m^2$, while its field extends out behind it in a direction opposite to the direction of propagation.

Our results in connection to the Schrodinger equation have motivated us to search for analogous solutions to the wave equation (2.2.1). The Brittingham ansatz [7]

$$\Psi(\vec{r},t)=G(\rho,\zeta)\,e^{i\beta\eta} \tag{6.3.7}$$

reduces the 3-D scalar wave equation to the 2-D Schrodinger equation

$$i4\beta\,\partial_\zeta G(\rho,\zeta)+\nabla_T^2 G(\rho,\zeta)=0, \tag{6.3.8}$$

where $\zeta = z - ct$. For the 2-D Schrodinger equation one can derive an Airy packet solution analogous to that given in equation (6.3.4); specifically,

$$G(\rho, \zeta) = \text{Ai}\left[2\beta(x - 3\beta\zeta^2/4)\right] \text{Ai}\left[2\beta(y - 3\beta\zeta^2/4)\right] e^{i2\beta^2\zeta(x+y-2\beta\zeta^2/3)} . \qquad (6.3.9)$$

Using this result, in conjunction with the Brittingham asnatz (6.3.7), we arrive at the following Airy packet solution to the 3-D scalar wave equation:

$$\Psi(\vec{r}, t) = \text{Ai}\left[2\beta(x - 3\beta\zeta^2/4)\right] \text{Ai}\left[2\beta(y - 3\beta\zeta^2/4)\right] e^{i2\beta^2\zeta(x+y-2\beta\zeta^2/3)} e^{i\beta\eta} , \qquad (6.3.10)$$

This wave packet moves with speed c in the z-direction and remains invariant under translations along this axis.

6.4 *SUMMARY AND CONCLUSION*

An interesting set of nondispersive wave packet solutions to the Schrodinger equation were derived in this chapter. This was facilitated by an appropriate choice of characteristic variables. The wave packet given in equation (6.1.12) was found to possess an interesting property; namely, that the group velocity associated with its envelope is equal to that obtained from the derivative of its phase with respect to z. This means that for a free particle represented by such a wave packet, the classical envelope will have the same kinematics as those obtained from the action of the quantum energy and momentum operators acting on the phase of the wave function.

Motivated by the work of Berry and Balazs [86] and Greenberger [87], we investigated a class of nonspreading solutions to the 3-D Schrodinger equation involving accelerating Airy envelopes. They are characterized by an asymmetric structure, in contrast to spherically symmetric packets moving with constant velocities. The field of a characteristic Airy packet extends in an oscillatory

fashion behind its peak amplitude, while it quickly disappears in front of the packet's center. It seems that a particle modelled by such a packet leaves a wake of its field behind as it accelerates in a certain direction. On the other hand, a wave packet moving with a constant velocity has a field which is symmetrically distributed in all directions.

Our work on Airy type solutions to the Schrodinger equation led us to analogous solutions to the 3-D scalar wave equation.

7.0 SUMMARY AND CONCLUSION

In this work we have investigated the different aspects of an interesting class of solutions to linear partial differential equations, namely, nondispersive wave packets. Such solutions have been considered to be uninteresting by a large section of the current literature, mainly because of their infinite energy content. We, nevertheless, think that this property is not a drawback *per se* . On the contrary, there seems to be some kind of a trade off between the nondispersive character of wave packet solutions and the finiteness of their energy content. For an example, a photon travelling for millions of years between a distant galaxy and our own does seem to have a finite energy content and at the same time is not expected to spread out. Such a photon is governed basically by linear equations and nonlinear effects can only come into the picture through the curvature of space-time. Nevertheless, in the limit of flat space-time (i.e., far away from any significant masses) light is mainly governed by linear equations. It would be a great relief if the solutions of the nonlinear equations could go in the limit of flat space-time into regular, well behaved, nondispersive solutions to the corresponding linear ones. It has always been assumed that localized, nondispersive, solutions to nonlinear equations (e.g., solitons) will degenerate into singular solutions if the nonlinearity is neglected (e.g., de Broglie's [30] "double solution" theory). It is our opinion that nonsingular, nondispersive packet solutions can provide a more reasonable alternative, even if their total energies are infinite.

The use of nondispersive wave packets in modelling particles (e.g., photons) emphasizes the importance of their localization over the finiteness of their total energy content. In this work, it has been demonstrated that if the localization of particles is given more priority, one can circumvent the infinite energy problems by utilizing the energy content of the central portions of the wave packets. Such packets are bump-like fields and with an appropriate choice of parameters, they can have very large amplitudes around their centers compared to their tails. Thus, one can assume that the energies usually observed in experiments result mainly from interactions of these bumps. A photon model based on Brittingham's FWMs provided a good example of the procedure for estimating the energy content of the bump field when it interacts with other particles. It was shown that such an energy content depends on the length of interaction, in such a way that photons emitted in interactions taking place over shorter lengths acquire higher energies. The mental picture, thus associated with our photon, is that of a localized bump that does not spread out as it travels in free space with the speed of light. The energy density of this bump is much larger than that of the tails. An estimate of the energy and momentum content of the bump can be related to the all familiar formula $E_\gamma = pc = \hbar\omega$. Our localized packet representation of the photon is closer to what Einstein had originally advocated [77]. The proposed model has a clear mental picture associated with it, in contrast to a plane wave representation for which it is not known exactly where the photon is coming from, where it is going or where it is. Even in quantum field theory, where photons are represented by propagators, the position of a photon has lost any meaning since $\vec{r}$ and t are treated as parameters that are integrated out in the final results. These ideas echo the same difficulties that have been extensively dealt with in the literature. The body of this work is known as the photon localization problem [88-91].

The use of the bump field of the FWM to represent a light particle was motivated primarily by the fact that the FWM pulse is capable of explaining the results of Young's two slit interference experiment. This experiment is considered to lie close to the heart of the quantum theory and it has been argued that no classical model could explain the interference results for individual events. In this work, it has been shown that the FWM pulse can interfere with itself, so that the bump field will impart its energy to one of the light fringes of the resulting diffraction pattern. This occurs be-

cause the FWM field is not a local structure but exists everywhere, with the shape of the total field determined by the boundary conditions setup by the configuration of the experiment. In interference experiments, the total field forms null regions, wherein the field is extremely small. If the center of the bump of the field ends up on one of these nulls, its amplitude becomes so small that it cannot be detected. This nonlocal character of the totality of the field of the FWM might provide a way of resolving the EPR paradox within the premise of a nonlocal classical theory. It is of great interest to investigate the possibility of using the vector form of the FWMs to explain the results of the two photon correlation experiments. Another interesting aspect of our model is that a photon is a classical entity that occupies a certain volume in space. This property might enable us to explain the unusual results of high intensity photoelectric effect experiments. This is another direction that should be investigated in the future, together with the possible occurence of deviations from the usual energy-momentum relationships in the case of ultra-energetic photons.

In order to understand the unusual structure associated with the FWM, we have developed a new superposition technique, namely, the bidirectional representation. This representation makes use of a superposition of products of two plane waves, one moving in the positive z-direction and the other travelling in the negative z-direction. This reflects the fact that the "natural" characteristic variables associated with packet solutions to the scalar wave equation are $\zeta = z - ct$ and $\eta = z + ct$. A nondispersive solution will thus be comprised of a nondispersive envelope that is a function of ζ only, multiplied by a modulation depending on η.

A naive extention of the bidirectional representation to other classes of equations, e.g., the Klein-Gordon and the dissipative wave equations, leads to new exact packet solutions that have centers moving with the speed of light. This behavior is unattractive, however, because one expects that a packet solution to the Klein-Gordon equation should propagate with a speed $v_g < c$. Using a new decomposition of the operator of the Klein-Gordon equation we arrived in a systematic way at the result that the natural characteristics associated with a nondispersive packet solution are $\zeta = \gamma(z - v_g t)$ and $\eta = z - t\,c^2/v_g$, with the relativistic quantity γ appearing naturally. Working with the new characteristic variables facilitates the derivation of a class of nondispersive packet solutions to the Klein-Gordon equation. These solutions have envelopes that move with a speed v_g multi-

plied by a modulation that moves with a phase velocity equal to c^2/v_g. It should be pointed out that in this case the envelope and the modulation are moving in the same direction, while in the case of the FWM the envelope moves in a direction opposite to that of the modulation. As a consequence, we cannot reduce the Klein-Gordon wave packets to packet solutions to the scalar wave equation in the limit $v_g \rightarrow c$. The wave packet solutions to the Klein-Gordon equation derived in this work are generalizations to MacKinnon's wave packet. A comparison between these two classes of solutions has cleared up some of the subtle issues concerning dispersionrelationships and definitions of the group velocities. In this work we have investigated the possibility of using a Klein-Gordon wave packet as a classical entity with a center moving with a velocity equal to v_g. On the other hand, we have treated this wave function as a quantum mechanical de Broglie wave packet. In the latter case, the kinematics of the particle can be derived from the action of the energy and momentum operators on the phase of the wave function. The Klein-Gordon wave packet has, also, been used to derive exact packet soultions to the Dirac equation. Similarly, wave packet solutions to the Schrodinger equation have been derived and it has been shown that the momentum and energy operators acting on the phase of these wave functions give momenta and energies equal to mv_g and $mc^2 + mv_g^2/2$, respectively. It is of interest in this case to note that the velocity of a free particle derived using a quantum procedure is identical with the velocity of the center of the packet's envelope. Wave packet solutions moving with constant velocities have been compared to an unusual class of accelerating Airy packet solutions to the Schrodinger equation. The latter have led to a new set of exact packet solutions to the 3-D scalar wave equation.

The bidirectional representation has, also, been used to provide a natural basis to the synthesis of all known Brittingham-like solutions. The relation between the Fourier synthesis and the bidirectional superposition has been utilized to study the Fourier structure of these unusual solutions. This demonstrated the fact that very simple spectra used in the case of the bidirectional representation lead to new solutions for which the corresponding Fourier spectra are very hard to guess. The sufficient and necessary conditions that should be imposed on the bidirectional spectra in order to ensure square integrability have been derived. Because of the general form of the bidirectional representation, it has been shown that it can be used to derive new solutions that can

not be easily obtained otherwise. Some of these new solutions [cf. equations (2.5.5) and (2.5.9)] are direct generalizations of Brittingham's FWM. This emphasizes the fact that the FWM bump solution used in Chapter 4 to represent light particles is not unique but belongs to a large class of solutions. This means that the photon model we have presented is just a tentative one that can capture some of the general features of a bump field representation of light particles. This work calls upon a more thorough theoretical investigation accompanied, if possible, by experimental verification to be undertaken.

The efficacy of the bidirectional representation has been demonstrated in connection to problems with boundaries. It has been shown that a localized pulse can be launched in an infinite, acoustic waveguide. Such a pulse behaves differently as it propagates through three distinct sections of the waveguide. In the first one, the center of the pulse does not decay at all, in the second region the center decays logarithmically, while in the third portion it decays exponentially. As a natural extension, the case of a semi-infinite waveguide excited by a similar pulse has been studied. Upon reaching the open end of the waveguide, such a pulse is launched into free space. The far field outside the waveguide was computed using a time-retarded Green's function. The results obtained demonstrated that the decay behavior of time-limited pulses of large bandwidths can vary from one pulse to another. For CW signals of very narrow bandwidths, one can easily distinguish between a far and a near field. In the case of time-limited pulses, however, the distinction between the far and near field becomes too fuzzy. Such pulses have eventually to decay to zero; nevertheless, some pulses can decay at a slower rate than others.

In Summary, we hope that the vitality of nondispersive wave packet solutions has been restored by this work. We have demonstrated that such solutions can be utilized in a large number of diverse problems and that their infinite energy content is not an insurmountable obstacle, as it is usually perceived. We have, also, illustrated that using such wave packets as basic entities instead of thinking in terms of their plane wave decomposition, can lead to a significantly different perspective, especially when applied to the realm of localized objects or time-limited pulses. Finally, we wish that this thesis could stimulate more work that would restore the long due respect to the linear nondispersive wave packets.

REFERENCES

1. J. N. Brittingham, "Focus Wave Modes in Homogeneous Maxwell's Equations: Transverse Electric Mode," J. Appl. Phys. **54,** 1179 (1983).

2. C. K. Hong and L. Mandel, "Experimental Realization of a Localized One-Photon State," Phys. Rev. Lett. **56,** 58 (1986).

3. A. Messiah, *Quantum Mechanics*, Vol. 1 (North-Holland, Amsterdam, 1961).

4. T. T. Wu and R. W. P. King, "Comments on 'Focus Wave Modes in Homogeneous Maxwell's Equations: Transverse Electric Mode'," J. Appl. Phys. **56,** 2587 (1984).

5. A. Sezginer, "A General Formulation of Focus Wave Modes," J. Appl. Phys. **57,** 678 (1985).

6. T. T. Wu and H. Lehman, "Spreading of Electromagnetic Pulses," J. Appl. Phys. **58,** 2064 (1985).

7. P. A. Belanger, "Packetlike Solutions of the Homogeneous-Wave Equation," J. Opt. Soc. Am. A **1,** 723 (1984).

8. P. A. Belanger, "Lorentz Transformation of the Packetlike Solutions of the Homogeneous-Wave Equations," J. Opt. Soc. Am. A **3,** 541 (1986).

9. R. W. Ziolkowski, "Exact Solutions of the Wave Equation with Complex Source Locations," J. Math. Phys. **26,** 861 (1985).

10. G. A. Deschamps, "Gaussian Beam as a Bundle of Complex Rays," Electron Lett. **7,** 684 (1971).

11. L. B. Felsen, "Complex Source-Point Solutions of the Field Equations and Their Relation to the Propagation and Scattering of Gaussian Beams," Symp. Math. **18,** 39 (1976).

12. P. Hillion, "Spinor Focus Wave Modes," J. Math. Phys. **28,** 1743 (1987).

13. P. Hillion, "Spinor Fields with Zero Mass in Unbounded Isotropic Media," Int. J. Theor. Phys. **27,** 57 (1988).

14. P. Hillion, "Solution of the Wave Equations with Boundary Conditions on the Hyperplane $z - ct = 0$," J. Math. Phys. **29**, 1771 (1988).

15. M. E. Sockell, *Similarity Solutions of Stochastic Nonlinear Parabolic Equations* , Ph.D. Dissertation, Virginia Polytechnic Inst. and State Univ. (1987).

16 R. W. Ziolkowski, "Localized Transmission of Electromagnetic Energy," Phys. Rev. A **39**, 2005 (1989).

17. T. T. Wu, "Electomagnetic Missiles," J. Appl. Phys. **57**, 2370 (1985).

18. H. M. Lee, "Field from a Uniform Current Source: Instantaneous Switch-on," J. Appl. Phys. **60**, 514 (1986).

19. H. M. Lee, "Rise and Fall of Directed Transient: Use of Mellin Transformation in Time Domain Problems," Radio Sci. **22**, 1102 (1987).

20. T. T. Wu, R. W. P. King and H. M. Shen, "Spherical Lens as a Launcher of Electromagnetic Missiles," J. Appl. Phys. **62**, 4036 (1987).

21. T. T. Wu, R. W. P. King and H. M. Shen, "Circular Cylindrical Lens as a Line Source Electromagnetic-Missile Launcher," IEEE Trans. Antennas Propagat. **AP-37**, 39 (1989).

22. R. W. Ziolkowski, D. K. Lewis and B. D. Cook, "Evidence of Localized Wave Transmission," Phys. Rev. Lett. **62**, 147 (1989).

23. H. M. Shen, "Experimental Study of Electromagnetic Missiles," Proc. SPIE Conference 873, Los Angeles, CA, January (1988).

24. J. Durnin, "Exact Solutions for Nondiffracting Beams. I. The Scalar Theory," J. Opt. Soc. Am. A **4**, 651 (1987).

25. J. Durnin, J. J. Miceli, Jr. and J. H. Eberly, "Comparison of Bessel and Gaussian Beams," Optics Lett. **13**, 79 (1988).

26. J. Durnin, J. J. Miceli, Jr. and J. H. Eberly, "Diffraction-Free Beams," Phys. Rev. Lett. **58**, 1499 (1987).

27. D. Bohm, "A Suggested Interpretation of the Quantum Theory in Terms of 'Hidden' Variables. I," Phys. Rev. **85**, 166 (1952).

28. D. Bohm, "A Suggested Interpretation of the Quantum Theory in Terms of 'Hidden' Variables. II," Phys. Rev. **85**, 180 (1952).

29. J. G. Cramer, "The Transactional Interpretation of Quantum Mechanics," Rev. Mod. Phys. **58**, 647 (1986).

30. L. de Broglie, *Nonlinear Wave Mechanics: A Causal Interpretation* (Elsevier, Amsterdam, 1960).

31. I. M. Besieris and A. M. Shaarawi, "A Linear Superposition Theory Based on Constrained Bilinear Invariants of a Factorized Embedded Operator," presented at the Joint IEEE AP-S / URSI Symposium, Blacksburg, VA June (1987).

32. R. W. Ziolkowski, "New Electromagnetic Directed Energy Pulses," Proc. SPIE Conference 873, Los Angeles, CA, January (1988).

33. T. T. Wu and H. M. Shen, "Radiation of an Electromagnetic Pulse from an Opening of a Circular Waveguide," Proc. SPIE Conference 873, Los Angeles, CA, January (1988).

34. H. E. Moses, "The Time-Dependent Inverse Source Problem for the Acoustic and Electromagnetic Equations in One- and Three-Dimensional Cases," J. Math. Phys. **25,** 1905 (1984).

35. H. E. Moses and R. T. Prosser, "Initial Conditions, Sources and Currents for Prescribed Time-Dependent Acoustic and Electromagnetic Fields in Three Dimensions, Part I: The Inverse Initial Value Problem. Acoustic and Electromagnetic 'Bullets,' Expanding Waves and Imploding Waves," IEEE Trans. Antennas Propagat. **AP-34,** 188 (1986).

36. E. Heyman and L. B. Felsen, "Propagating Pulsed Beam Solutions by Complex Source Parameter Substitution," IEEE Trans. Antennas Propagat. **AP-34,** 1062 (1986).

37. E. Heyman and B. Z. Steinberg, "Spectral Analysis of Complex-Source Pulsed Beams," J. Opt. Soc. Am. A **4,** 473 (1987).

38. P. D. Einziger and S. Raz, "Wave Solutions Under Complex Space-Time Shifts," J. Opt. Soc. Am. A **4,** 3 (1987).

39. E. Heyman and B. Z. Steinberg and L. B. Felsen, "Spectral Analysis of Focus Wave Modes (FWM)," J. Opt. Soc. Am. A **4,** 2081 (1987).

40. R. W. Ziolkowski, "Directed Transfer of Electromagnetic Energy in Space," presented at the Joint IEEE AP-S / URSI Symposium, Blacksburg, VA, June (1987).

41. L. Hormander, *The Analysis of Linear Partial Differential Operators Vol. III* (Springer-Verlag, New York, 1985).

42. L. Brillouin, *Wave Propagation and Group Velocity* (Academic Press, New York, 1960).

43. L. B. Felsen and N. Marcuvitz, *Radiation and Scattering of Waves* (Prentice Hall, Englewood Cliffs, NJ, 1973).

44. R. M. Lewis, "Asymptotic Theory of Wave Propagation," Arch. Ratl. Mech. Anal. **20,** 191 (1965).

45. L. B. Felsen, "Transient Electromagnetic Fields," in *Topics in Applied Physics Vol. 10,* edited by L. B. Felsen (Springer-Verlag, New York, 1976).

46. N. D. Hoc, I. M. Besieris and M. E. Sockell, "Phase-Space Asymptotic Analysis of Wave Propagation in Homogeneous Dispersive and Dissipative Media," IEEE Trans. Antennas Propagat. **AP-33,** 1237 (1985).

47. I. S. Gradshteyn and I. M. Ryzhik, *Tables of Integrals, Series and Products* (Academic Press, New York, 1965).

48. N. Bleistein and R. A. Handelsman, *Asymptotic Expansions of Integrals* (Dover, New York, 1986), chap. 8.

49. M. Abramowitz and I. A. Stegun, *Handbook of Mathematical Functions* (Dover, New York, 1972).

50. J. A. Stratton, *Electromagnetic Theory* (McGraw Hill, New York, 1941).

51. G. N. Watson, *A Treatise on the Theory of Bessel Functions* (Cambridge University Press, Cambridge, U.K., 1958).

52. P. M. Morse and H. Feshbach, *Methods of Theoretical Physics, Vol. I* (McGraw Hill, New York, 1953).

53. A. Aspect, P. Grangier and G. Roger, "Experimental Tests of Realistic Local Theories via Bell's Theorem," Phys. Rev. Lett. **47**, 460 (1981).

54. A. Aspect, P. Grangier and G. Roger, "Experimental Realization of Einstein-Podolsky-Rosen-Bohm *Gedankenexperiment:* A New Violation of Bell's Inequalities," Phys. Rev. Lett. **49**, 91 (1982).

55. A. Aspect, J. Dalibard and G. Roger, "Experimental Test of Bell's Inequalities Using Time-Varying Analyzers," Phys. Rev. Lett. **49**, 1804 (1982).

56. R. P. Feynman, R. B. Leighton and M. Sands, *The Feynman Lectures on Physics: Quantum Mechanics Vol. III* (Addison-Wesley, Reading, 1965).

57. A. B. Arons and M. B. Peppard, "Einstein's Proposal of the Photon Concept - A Translation of the 'Annalen Der Phyzik' Paper of 1905," Am. J. Phys. **33**, 367 (1965).

58. R. D. Prosser, "The Interpretation of Diffraction and Interference in Terms of Energy Flow," Int. J. Theor. Phys. **15**, 169 (1976).

59. R. D. Prosser, "The Quantum Theory and the Nature of Intrference," Int. J. Theor. Phys. **15**, 181 (1976).

60. A. O. Barut, *Electrodynamics and Classical Theory of Fields and Particles* (Dover, New York, 1980).

61. J. D. Jackson, *Classical Electrodynamics* (J. Wiley, New York, 1975).

62. R. Becker, *Electrodynamic Fields and Interactions* (Dover, New York, 1982).

63. C. Philippidis, C. Dewdney and B. J. Hiley, "Quantum Interference and the Quantum Potential," Nuovo Ciemento **52 B**, 15 (1979).

64. D. Bohm, B. J. Hiley and P. N. Kaloyerou, "An Ontological Basis for the Quantum Theory," Phys. Rep. **144**, 323 (1987).

65. C. Dewdney and B. J. Hiley, "A Quantum Potential Description of One-Dimensional Time-Independent Scattering from Square Barriers and Square Wells," Found. Phys. **12**, 27 (1982).

66. J. A. Wheeler and R. P. Feynman, "Interaction with the Absorber as the Mechanism of Radiation," Rev. Mod. Phys. **17**, 157 (1945).

67. J. A. Wheeler and R. P. Feynman, "Classical Electrodynamics in Terms of Direct Interparticle Action," Rev. Mod. Phys. **21**, 425 (1949).

68. J. G. Cramer, "Generalized Absorber Theory and Einstein-Podolsky-Rosen Paradox," Phys. Rev. D **22**, 362 (1980).

69. A. Einstein, B. Podolsky and N. Rosen, "Can Quantum-Mechanical Description of Physical Reality Be Considered Complete?," Phys. Rev. **47**, 777 (1935).

70. P. Agostini and G. Petite, "Photoelectric Effect Under Strong Irradiation," Contemp. Phys. **29,** 57 (1988).

71. P. Kruit, J. Kimmon, H. G. Muller and M. J. Van der Wiel, "Electron Spectra from Multiphoton Ionization of Xenon at 1064, 532 and 355 nm," Phys. Rev. A **28,** 248 (1983).

72. B. L. Dingus, C. Y. Yang, J. A. Goodman, S. K. Gupta, D. A. Krakauer, R. L. Talaga, G. B. Yodh, R. W. Ellsworth, R. L. Burman, K. B. Butterfield, R. Cady, R. D. Carlini, J. Lloyd-Evans, D. E. Nagle, V. D. Sandberg, C. A. Wilkinson, J. Linsely and R. C. Allen, "Search for Signals from Cygnus X-3 at Energies above 50 Tev," Phys. Rev. Lett. **60,** 1785 (1988).

73. L. K. Resvanis, A. Szentgyorgyi, J. Hudson, L. Kelley, J. G. Learned, S. Sinnis, V. Stenger, D. D. Weeks, J. Gaidos, M. Kertzman, F. Loeffler, T. Palfrey, G.Sembroski, C. Wilson, U. Camerini, J. P. Finley, W. Fry, J. Jennings, A. Kenter, M. Lomperski, R. Loveless, R. March, J. Matthews, R. Morse, D. Reeder and P. Slane, "VHE Gamma Rays from Hercules X-1," Astrophys. J. Lett. **328,** L9 (1988).

74. R. C. Lamb, M. F. Cawley, D. J. Fegan, K. G. Gibbs, P. W. Gorham, A. M. Hillas, D. A. Lewis, N. A. Porter, P. T. Reynolds and T. C. Weekes, "Tev Gamma Rays from Hercules X-1 Pulsed at an Anomalous Frequency," Astrophys. J. Lett. **328,** L13 (1988).

75. L. MacKinnon, "A Nondispersive de Broglie Wave Packet," Found. Phys. **8,** 157 (1978).

76. L. MacKinnon, "Particle Rest Mass and the de Broglie Wave Packet," Lett. Nuovo Cim. **31,** 37 (1981).

77. A. Einstein, "On the Quantum Theory of Radiation," in *Sources of Quantum Mechanics,* edited by B. L. Vann der Waerden (Dover, New York, 1967); originally published in Phyzik Z. **18,** 121 (1917).

78. L. de Broglie, *The Current Interpretation of Wave Mechanics* (Elsevier, Amsterdam, 1964).

79. G. Lochak, "de Broglie's Initial Conception of de Broglie Waves," in *The Wave-Particle Dualism* , edited by S. Diner, D. Fargue, G. Lochak and F. Selleri (Reidel, Dordrecht, 1984).

80. D. Bohm, "Proof that Probability Density Approaches $|\psi|^2$ in the Causal Interpretation of the Quantum Theory," Phys. Rev. **89,** 458 (1953).

81. D. Bohm and Vigier, "Model of the Causal Interpretation of Quantum Theory in Terms of a Fluid with Irregular Flactuations," Phys. Rev. **96,** 208 (1954).

82. D. Fargue, "Permanence of the Corpuscular Appearance and the Nonlinearity of the Wave Equation," in *The Wave-Particle Dualism* , edited by S. Diner, D. Fargue, G. Lochak and F. Selleri (Reidel, Dordrecht, 1984).

83. R. W. Ziolkowski, A. M. Shaarawi and I. M. Besieris, " A Space-Time Representation of a Massive, Relativistic, Spin Zero Particle," in the Proceedings of the International Symposium of Spacetime Symmetries, University of Maryland, College Park, MD, 1988 [Nucl. Phys. B (to be published)].

84. M. H. MacGregor, "Generalization of the Postulates of Special Relativity," Lett. Nuovo Cim. **43,** 49 (1985).

85. J. J. Sakurai, *Advanced Quantum Mechanics* (Benjamin/ Cummings, Menlo Park, 1984).

86. M. V. Berry and N. L. Balazs, "Nonspreading Wave Packets," Am. J. Phys. **47**, 264 (1979).

87. D. M. Greenberger, "Comment on 'Nonspreading Wave Packets'," Am. J. Phys. **48**, 256 (1980).

88. D. Han, Y. S. Kim and M. E. Noz, "Uncertainty Relations of Light Waves and the Concept of Photons," Phys. Rev. A **35**, 1682 (1987).

89. Y. S. Kim and E. P. Wigner, "Covariant Phase-Space Representation for Localized Light Waves," Phys. Rev. A **36**, 1293 (1987).

90. T. D. Newton and E. P. Wigner, "Localized States for Elementary Systems," Rev. Mod. Phys. **21**, 400 (1949).

91. H. Bacry, *Localizability and Space in Quantum Physics* (Springer-Verlag, Berlin, 1988).

The vita has been removed from the scanned document